

Comparison of Power-to-X-to-Power technologies for energy storage in 2030

By Senja Boom

Comparison of PtXtP technologies for energy storage in 2030

By

Senja Boom

to obtain the degree of Master of Science
Sustainable Energy Technology
at the Delft University of Technology,
to be defended publicly on Friday March 13, 2020 at 11:00 AM.

Student number: 4748611
Project duration: April 15, 2019 – March 13, 2020
Thesis committee: Prof.dr.ir. Andrea Ramirez Ramirez
Dr. Milos Cvetkovic
Prof.dr.ir. Wiebren de Jong

An electronic version of this thesis is available at <http://repository.tudelft.nl/>

Abstract

The energy transition is advancing rapidly, and the Dutch electricity grid is changing with it. Increasing shares of variable renewable energy sources create mismatches between electricity supply and demand. These mismatches create a need for large-scale energy storage. Existing large-scale energy storage technologies are pumped hydro energy storage and compressed air energy storage, but their storage potential in the Netherlands is limited. The alternative is to store energy in chemical bonds, for example by producing hydrogen, and regenerate the electricity later. This type of storage is called a Power-to-X-to-Power (PtXtP) system. Power-to-X technologies have existed for a long time. This report evaluates their potential in an energy storage application. First, PtXtP systems are compared to compressed air energy storage (CAES) and pumped hydro energy storage (PHES). The geographic potential of CAES and PHES in the Netherlands is limited for both technologies, proving large scale energy storage is a challenge to which PtXtP. Next, all PtXtP technologies are investigated and compared based on available literature. The three technologies with the most potential (hydrogen, ammonia and methane) are further investigated. This report gives a current and comprehensive overview of data on PtXtP system components, including amongst others their OPEX, CAPEX, efficiency and energy use. This data was used as input for several models of hydrogen, methane and ammonia storage systems, to determine system cost and performance in a dynamic system. Simulations are run with these PtXtP systems as energy storage technologies for a 1GW wind park.

The simulations are used to identify main system bottlenecks, investigate the impact of intermittent use on system performance, and evaluate the potential of a PtXtP storage system. The first important bottleneck is the size of the hydrogen buffer required for operation of the Haber-Bosch reactor and Sabatier reactor. It is as large as or larger than the storage capacity in a hydrogen storage system. The second bottleneck is the size of ammonia and hydrogen fuel cells. The required fuel cell power is 425 MW, which is larger than any current or expected fuel cells. Next the simulations were used to investigate the performance of a PtXtP system as energy storage medium in a VRES system. The first important finding is the tradeoff between system flexibility and system sizing. An ammonia system with 33%-100% flexibility can be 60% smaller than a 0%-100% system, while still processing the same annual amount of hydrogen. Intermittent system use increases the levelized cost of storage significantly, in these models by factor 2.2-4, due to the unchanged CAPEX which must be paid for a reduced system output. The first important finding related to the PtXtP system is that the cost and energy consumption of hydrogen transport and storage are relatively small compared to energy conversion steps. The electrolyser proved to be the system component with the highest cost and energy loss. Finally, the added value of the storage system is significant wind park size reduction. The 1GW wind park size could be reduced by 35% when connected to a hydrogen storage system, while still meeting the same demand. In addition, zero grid exchange can only be achieved when implementing a storage system. With lower shares of grid exchange, storage becomes increasingly more valuable.

The overall conclusion drawn is that hydrogen or methane systems seem to have the most potential for energy storage purposes. The report also shows energy storage is necessary, and no alternatives to PtXtP are available in the Netherlands. PtXtP will therefore have to play a large role in the future Dutch electricity grid. However, use of PtXtP storage will increase the price of electricity and several technological developments, mostly scale-ups, are necessary before a PtXtP system is feasible.

Acknowledgements

Since the age of seven, when I first learned about global warming and its devastating effects on nature and wildlife, I have felt driven to contribute to a solution that might relieve the pressure we put on our climate and ecological systems. My search for solutions led me to Eindhoven university of Technology, where I acquired a passion for sustainable energy. Years of study and activities followed, and I came to the conclusion that the real technological challenge of the energy transition is in energy storage, rather than renewable electricity generation. It was with this motivation that I started this thesis.

A little more than nine months later this thesis is completed, and I am incredibly grateful to everyone who has contributed (directly and indirectly) to this work. I want to thank Andrea Ramirez Ramirez for the countless ideas and suggestions that she contributed to this work. I would never have come this far without them. I also want to thank Andrea for helping me to grow as an independent, self-sufficient researcher. I want to thank Milos Cvetkovic for being my sounding board and sparring partner. He helped me make sense of a sometimes-chaotic and overwhelming project. Jonathan Moncada Botero helped me a lot as well, both with his scientific knowledge and his ability to ask the right questions. Finally, I want to thank Wiebren de Jong for joining my thesis committee and for the new insights he has given me in the courses I followed with him. In that he is not the only one. I had many great teachers, both in Eindhoven and Delft,

On a more personal note I want to thank my office mates, for providing me with the necessary moments of relaxation. I want to thank my boyfriend just for being there, and more importantly, I want to thank my family and close friends for their eternal support and faith in me. I would never have come as far as I have without them.

Table of Contents

Abstract	i
Acknowledgements	ii
Table of Contents	iii
List of figures	vii
1. List of tables.....	x
2. List of abbreviations	xii
3. Introduction.....	1
3.1. Demand-generation mismatch.....	1
3.2. Energy storage technologies	2
3.3. State of the art	3
3.4. Knowledge gaps.....	4
3.5. Research question	5
3.6. Thesis outline.....	5
4. Methodology	6
4.1. Thesis steps	6
4.2. KPI's	7
4.3. Simulation scenario	9
4.4. Scope	10
5. Large scale energy storage	12
5.1. Compressed air energy storage.....	12
5.2. Pumped hydro energy storage	12
5.3. Power to X to Power.....	13
5.4. Comparison	14
6. Power to X to Power technologies	16
6.1. Hydrogen as an energy carrier	16
6.2. Molecular hydrogen storage	17
6.3. Hydrogen in Chemical bonds.....	18
6.3.1. Methane	18
6.3.2. Methanol	18
6.3.3. Formic acid	18
6.3.4. Ammonia	19
6.3.5. LOHC's	19
6.3.6. Power to X	20
6.4. Hydrogen in metals (or hybrids).....	20

6.5.	Hydrogen adsorption.....	20
6.6.	Comparison and conclusion	21
7.	PtXtP system components.....	23
7.1.	Energy generation technology selection.....	23
7.1.1.	Generation.....	23
7.1.2.	E-Converters and transport.....	24
7.1.3.	Short term storage	25
7.2.	Hydrogen technology selection.....	25
7.2.1.	Production from water	25
7.2.2.	Transport and storage	27
7.2.3.	Regeneration of electricity	27
7.3.	Ammonia technology selection.....	28
7.3.1.	Nitrogen capture from air	28
7.3.2.	Ammonia production	29
7.3.3.	Ammonia storage and transport	31
7.3.4.	Regeneration	31
7.4.	Methane technology selection.....	32
7.4.1.	CO ₂ capture.....	32
7.4.2.	Methane production	32
7.4.3.	Storage and transport	32
7.4.4.	Regeneration	33
7.5.	Conclusion	33
8.	The model.....	34
8.1.	Assumptions	34
8.2.	Outputs.....	34
8.3.	Inputs.....	34
8.4.	Model structure.....	34
8.5.	Limitations	35
9.	Overview of model input values.....	36
9.1.	General assumptions.....	36
9.2.	Electricity input.....	36
9.3.	Carriers	37
9.4.	Generation.....	38
9.5.	Storage system	39
9.6.	Transport system.....	41
9.7.	Regeneration	42

10.	Scenarios	43
10.1.	System performance scenarios	43
10.1.1.	No storage	43
10.1.2.	H ₂	44
10.1.3.	H ₂ - full load	46
10.1.4.	Ammonia - Constant production	46
10.1.5.	Ammonia – Flexible production	48
10.1.6.	Ammonia – Full load	49
10.1.7.	Methane	49
10.1.8.	Methane – Full load	51
10.2.	Added value of storage	51
11.	Results	52
11.1.	Scenario results	52
11.1.1.	No storage	52
11.1.2.	Hydrogen	53
11.1.3.	H ₂ under full load	55
11.1.4.	Ammonia – constant	56
11.1.5.	Ammonia – flexible production	57
11.1.6.	Ammonia – full load	59
11.1.7.	Methane	61
11.1.8.	Methane – full load	63
11.2.	Added value of storage	64
11.3.	Comparison	65
11.3.1.	Bottlenecks	66
11.3.2.	VRES application	67
11.3.3.	System component comparison	68
12.	Sensitivity analysis	69
12.1.	Uncertainty of variables	69
12.2.	Use case scenarios	71
12.2.1.	Wind park owner	71
12.2.2.	H ₂ with battery	72
12.2.3.	Different year as input	75
13.	Conclusion	76
14.	Recommendations	78
15.	Bibliography	79
A.	Appendix I – The model	87

No storage	87
Hydrogen storage	88
Ammonia storage	90
Methane	92

List of figures

Figure 1: Electricity produced from variable renewable resources illustrates the "Dunkelflaute" (Energy Storage NL, 2019).	1
Figure 2: Graphic representation of solar and wind power generation against power consumption throughout the year (Energy Storage NL, 2019).	2
Figure 3: Comparison of storage technologies based on their discharge time and storage capacity (European Commission, 2017).	3
Figure 4: Developmental maturity of major electricity storage technologies according to T.M. Gür (Gür, 2018).	3
Figure 5: Comparison of storage technologies based on round trip efficiency, cost per kWh and discharge time as quoted by T.M. Gür (Gür, 2018), created by Yang et al. (Yang, et al., 2011). ReSOC stands for Reversible Solid Oxide Cell, CAES is Compressed Air Energy Storage, Ni-Cd is Nickel-Cadmium batteries.	4
Figure 6: Diagram of the methodology for this thesis.	6
Figure 7: Definitions of Technology Readiness Levels (Blanc, et al., 2017).....	9
Figure 8: Map of all existing, planned, and potential wind parks in the Dutch North Sea. Red represents existing wind parks (1 GW), blue represents wind parks planned for 2023 (3.5 GW) , green represents wind parks planned for 2030 (6.1 GW), yellow represents area's designated for wind parks in the future (0.9 GW) (Wiebes, 2018).	11
Figure 9: PHES potential in Europe according to eStorage (eStorage, 2015).....	13
Figure 10: Overview of different pathways for hydrogen storage and their hydrogen density (kg of H ₂ /m ³) (Andersson & Grönkvist, 2019)	16
Figure 11: Overview of underground salt (purple), gas (green) and oil (red) fields suitable for hydrogen storage in the Netherlands. The pictures on the right show suitability; Green are the most suitable caverns, yellow are usable caverns, red are not usable (Van Gessel, Breunese, Juez Larré, Huijskes, & Remmelts, 2018).	17
Figure 12: Energy storage density (kWh/m ³) of LOHC's compared to conventional storage technologies, including power generation losses. (Teichmann, Arlt, Wasserscheid, & Freymann, 2011).....	19
Figure 13: Hourly generated power from off shore wind plants in the Netherlands, week 1 (Open Power System Data, 2019)	23
Figure 14: Cumulative mismatch between wind generation and electricity demand in MWh in the year 2018, generated from data from the Open Power Systems Data (Open Power System Data, 2019). .	24
Figure 15: Properties of selected chemistries of lithium-ion battery electricity storage systems, 2016 and 2030 (IRENA, 2017).....	25
Figure 16: System fluid schematic as designed by Nuttall (Nuttall, 1977).....	26
Figure 17: Schematic depiction of alkaline electrolysis (AEC), proton exchange membrane electrolysis (PEMEC) and solid oxide electrolysis cells (SOEC) (Schmidt, et al., 2017).....	26
Figure 18: System steps in a PSA nitrogen separation plant (Ivanova & Lewis, 2012)	28
Figure 19: Tool for selection of the right nitrogen separation type based on purity and flowrate (Ivanova & Lewis, 2012)	29
Figure 20: Schematic representation of a simplified Haber-Bosch system (Goetheer, 2018).....	30
Figure 21: Schematic representation of electrochemical ammonia production (Amar, Lan, Petit, & Tao, 2011).....	30
Figure 22: Schematic illustration of a simplified ammonia storage loop (Morgan, Manwell, & MacGowan, 2014)	31

Figure 23: Map of the natural gas grid as owned by GasUnie, the feed-in stations are marked by a black circle with a white triangle inside (Gielisse, Dröge, & Kuik, 2018).....	33
Figure 24: Simplified schematic of the intended model structure. Each arrow represents a process step.	35
Figure 25: Simplified diagram of the model for a no-storage scenario.....	43
Figure 26: Image of the model in Simulink for illustration of the type of model that was used. This figure shows the no storage scenario. P_gen30 is the hourly electricity generation from the wind park, P_load30 is the hourly demand. After correction for losses, the mismatch is monitored as curtailment when it is >0, and as grid demand when it is <0. The cumulative mismatch at the end of the year is zero.....	44
Figure 27: Simplified schematic representation of the model for the hydrogen scenario	45
Figure 28: Map illustrating the hydrogen scenario. Yellow is one of the designated areas for future wind parks. Black is the DC cable connecting the wind park to the shore. Red is the grid connection point, where the fuel cell and electrolyser are located. Blue is the salt cavern location and green is the hydrogen pipeline connecting them.	45
Figure 29: Zoomed in image of Figure 28.....	46
Figure 30: Simplified schematic view of the constant Haber-Bosch scenario	47
Figure 31: Hydrogen buffer content and size.....	47
Figure 32: Map of the ammonia system. Yellow is one of the designated areas for future wind parks. Black is the DC cable connecting the wind park to the shore. Red is the storage site containing the grid connection point, ammonia tank, Haber-Bosch reactor and Fuel cell.....	48
Figure 33: Zoomed in image of Figure 32.....	48
Figure 34: schematic representation of the methane storage system	50
Figure 35: Map of the methane scenario, yellow represents the designated area for future wind parks. Black is the DC cable connecting the wind park to the shore. Red is the grid connection point, where the fuel cell and Sabatier reactor are located. Orange is the gas injection station, the hydrogen pipeline connecting them is marked green. The gas turbine can be any gas turbine already connected to the gas and electricity grid.....	50
Figure 36: Zoomed-in image of Figure 35.	51
Figure 37: Hourly mismatch of week 1 for 2018	52
Figure 38: Cumulative mismatch between wind generation and electricity demand in MWh in the year 2018, generated from data from the Open Power Systems Data (Open Power System Data, 2019). .	52
Figure 39: Relation between system size, system cost and grid interaction	54
Figure 40: Contribution of system components to storage system costs (CAPEX and OPEX). Storage system cost is 97.7 M€.	54
Figure 41: Contribution of system components to storage system energy use. The total energy loss in the storage system is 686 GWh per year (65% of 1.06 TWh).	55
Figure 42: Ammonia and hydrogen content of the salt cavern, hydrogen buffer and ammonia tank.	56
Figure 43: H ₂ storage in hydrogen buffers with hydrogen storage in salt cavern as a reference.....	59
Figure 44: The impact of flexible system use on system size.....	59
Figure 45: Breakdown of system electricity use.....	60
Figure 46: Contribution of system components to total system energy use. Total system energy use is 979 GWh, not included is the Sabatier reactor that adds 244 GWh of energy per year.	62
Figure 47: Contribution of system components to storage system cost. Total system energy cost is 95 M€.	62
Figure 48: Breakdown of costs for a methane PtXtP system under constant maximum load.	63
Figure 49: Tradeoff between system oversizing and grid demand for a system with hydrogen storage, in case of a yearly demand of 3.28 TWh.	64

Figure 50: Tradeoff between system oversizing and grid demand for a system without storage, in case of a yearly demand of 3.28 TWh.	65
Figure 51: Numbers of caverns suitable for hydrogen storage per size and location. The y-axis shows the number of fields. (Van Gessel, Breunese, Juez Larré, Huijskes, & Remmelts, 2018).....	67
Figure 52: Overview of system component contributions to cost and energy use for the hydrogen, ammonia and methane storage system in a VRES scenario.	68
Figure 53: Relative impact of different parameters on the storage system cost and roundtrip efficiency. All axes are expressed in percentages. Cost dependencies are linear, efficiency dependencies contain a slight curvature.....	70
Figure 55: Illustration of the potential advantage of the use of a primary battery system (discrete steps), in this case the battery capacity is limited to 1 MWh.....	73
Figure 56: Illustration of potential advantages of a secondary battery storage system (discrete steps), in this case the electrolyser power is limited to 1 MW.....	73
Figure 57: Performance of a storage system containing a hydrogen storage system and primary batteries. Continuous lines indicate the hydrogen system without batteries, dotted lines indicate the mixed system.....	74
Figure 58: Performance of a storage system containing a hydrogen storage system and secondary batteries. Continuous lines indicate the hydrogen system without batteries, dotted lines indicate the mixed system.....	75

1. List of tables

Table 1: Overview of levelized cost of storage, potential capacity and roundtrip efficiency of CAES, PHES and PtXtP	15
Table 2: Definitions of the scores awarded to system components for determination of technological feasibility of each PtXtP storage system component.....	21
Table 3: Overview and comparison of different hydrogen storage technologies based on TRL and technological complications. Roundtrip efficiency is used as a deciding factor when scores are too close too call. ++=3, +=2,-=1,- -=0.....	22
Table 4: Comparison of fuel cell types as done by IEA (IEA, 2015). FC stands for fuel cell, PEM stands for polymer electric membrane, SO stands for solid oxide, PA stands for phosphoric acid fuel cell, MC stands for molten carbonate fuel cell.	27
Table 5: Output of simulations for the scenario of a 1 GW wind plant generating electricity for the Dutch energy grid, without storage.	53
Table 6: Output of simulations for the scenario of a 1 GW wind plant generating electricity for the Dutch energy grid, connected to a hydrogen storage system	53
Table 7: Output of simulations for the scenario of a hydrogen storage system containing a 425 MW electrolyser and 425 MW fuel cell running at full capacity for one year. Compared to the same hydrogen storage system connected to a 1 GW wind plant and a Dutch demand cycle.	55
Table 8: Output of simulations for the scenario of a 1 GW wind plant generating electricity for the Dutch energy grid, connected to an ammonia storage system with a HB reactor running constantly.....	57
Table 9: Output of simulations for the scenario of a 1 GW wind plant generating electricity for the Dutch energy grid, connected to an ammonia storage system with a HB reactor with flexible operation between 33% and 100% of full capacity.	57
Table 10: Output of simulations for the scenario of an ammonia storage system containing a 425 MW electrolyser and 425 MW ammonia fuel cell running at full capacity for one year, connected to a HB reactor. Compared to the same ammonia storage system connected to a 1 GW wind plant and a Dutch demand cycle, where the HB reactor has a minimum load of 33%.	60
Table 11: Output of simulations for the scenario of a 1 GW wind plant generating electricity for the Dutch energy grid, connected to a methane storage system with a Sabatier reactor with flexible operation between 40% and 100% of full capacity.....	61
Table 12: Output of simulations for the scenario of an ammonia storage system containing a 425 MW electrolyser and 425 MW gas turbine running at full capacity for one year, connected to a Sabatier reactor. Compared to the same methane storage system connected to a 1 GW wind plant and a Dutch demand cycle, where the Sabatier reactor has a minimum load of 40%.	63
Table 13: Gathered results of all PtXtP technologies in VRES systems. The no storage scenario consists of a 1 GW wind park and matching average Dutch electricity use. The H ₂ scenario contains a 425 MW electrolyser and fuel cell. The NH ₃ scenario contains an electrolyser, ammonia fuel cell and HB reactor with a minimum load of 33%. The CH ₄ scenario contains an electrolyser, gas turbine and Sabatier reactor with a minimum load of 40%. PHES and CAES information given for frame of reference.....	65
Table 14: Representation of technological bottlenecks as identified in literature. The system components are feedstocks used for energy storage ('carrier', e.g. purified water to produce H ₂ , CO ₂ for creation of methane), the absorption of hydrogen or electricity ('production'), transport, storage and electricity or hydrogen regeneration.	66
Table 15: Gathered results of system performance when connected to the 1 GW wind park and Dutch electricity demand, compared to system performance under full load (425 MW in and 425 MW out for one year)	67

Table 16: Uncertainty ranges of model output for storage system cost for the range of data found in chapter 10.	71
Table 17: Uncertainty ranges of model output for roundtrip efficiency based on uncertainty in parameters from chapter 10.	71
Table 18: Results of simulation of a hydrogen storage system serving Dutch electricity demand, compared to the simulation output of a hydrogen storage system serving a constant output.....	72
Table 19: Output of simulations for the scenario of a 1 GW wind plant generating electricity for the Dutch energy grid, connected to a hydrogen storage system, without batteries, compared to a system with primary or secondary batteries.....	74
Table 20: Comparison of simulation outcomes of a hydrogen storage system when connected to a 1 GW wind generation profile based on the year 2017 and 2018 for comparison and validation of the model's assumptions. Table shows there is no significant difference in system performance due to the wind profile.	75
Table 21: Repetition of Table 3.	76
Table 22: Table containing the output of the most important scenarios, hydrogen in a VRES system, flexible ammonia production in a VRES system and flexible methane production in a VRES system..	77

2. List of abbreviations

AEC	Alkaline electrolysis cell
ASU	Air separation unit
bcm	Billion cubic meters of natural gas
CAES	Compressed air energy storage
CH ₄	Methane
CH ₃ OH	Methanol
DAC	Direct air capture
DAFC	Direct ammonia fuel cell
FC	Fuel cell
H ₂	Hydrogen
HB	Haber-Bosch
HCOOH	Formic Acid
IPHES	Inversed pumped hydro energy storage
KPI	Key performance indicator
LCOE	Levelized cost of energy
LCOS	Levelized cost of storage
LHV	Lower heating value
LOHC	Liquid organic hydrogen carrier
LTO	Lithium titanate oxide
MCH	Methylcyclohexane
NH ₃	ammonia
PEM	Proton exchange membrane
PEMEC	Proton exchange membrane electrolysis cell
PHES	Pumped Hydro Energy Storage
PtX	Power-to-X
PtXtP	Power-to-X-to-Power
PSA	Pressure swing absorption
SOEC	Solid oxide electrolysis cell
SOFC	Solid oxide fuel cell
SPE	Solid polymer electrolyte
SSPHS	Subsurface pumped hydro storage
t	Tonne
TRL	Technology readiness level
VRES	Variable renewable energy source

3. Introduction

The energy transition is advancing and gaining momentum, as a result the share of renewable energy sources increases. In 2018 the share of renewables in the Dutch electricity market was 15% (CBS, 2019), by 2023 this is expected to have increased to 41% (Ministerie van Economische Zaken, 2016). The Dutch climate agreement states that 70% of all electricity is generated by renewable resources in 2030 and by 2050 the electricity grid will have to be 100% renewable (Rijksoverheid, 2019). The biggest contributing renewable energy source is offshore wind energy. Wind energy is a variable renewable energy source (VRES), and while it is necessary for the reduction of CO2 emissions and prevention of climate change, its variability poses serious threats to grid stability and security of supply of electricity. The energy transition, therefore, goes hand in hand with a necessity for energy storage, as was illustrated by the Energiewende, the German energy transition. Germany is the first country in Europe to achieve high shares (up to 38%) of electricity from VRES and unwanted consequences have occurred. Black outs, negative electricity prices in the intraday electricity market and high electricity prices for consumers have afflicted the German electricity grid (Boemer, et al., 2011). Therefore, Germany is the first country to encounter the corresponding need for energy storage, grid balancing and power quality control. To complete the Dutch energy transition without these negative side effects, large-scale energy storage is necessary.

3.1. Demand-generation mismatch

The demand for energy storage varies from short term (seconds, minutes, hours) to long term (days, weeks, months). A good example of the necessity for large capacity, long duration energy storage in Germany is the “Dunkelflaute”. The Dunkelflaute is a period of up to 2 weeks where both solar and wind energy are produced in small quantities. Figure 1 shows the Dunkelflaute based on data from Fraunhofer ISE and illustrated by Energy Storage NL (Energy Storage NL, 2019).

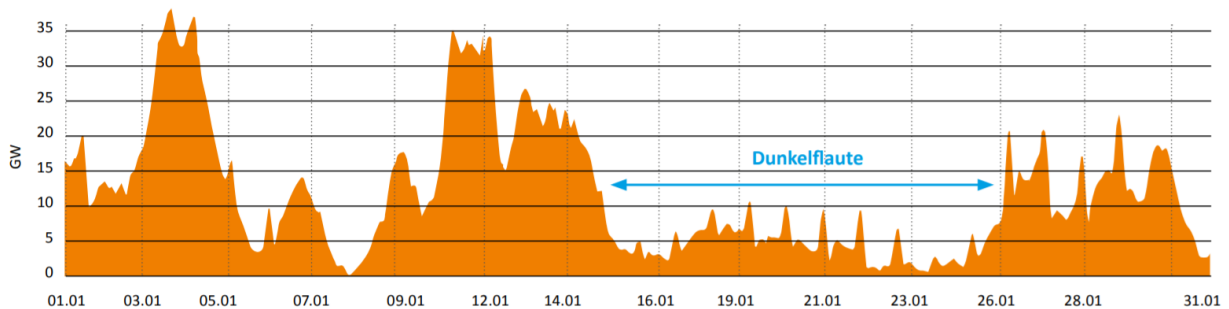


Figure 1: Electricity produced from variable renewable resources illustrates the "Dunkelflaute" (Energy Storage NL, 2019).

Also illustrated by Energy Storage NL in the same report is the difference between production and consumption of electricity in summer and winter (Energy Storage NL, 2019). Solar energy is more available in summer, wind energy is more available in winter, but the two sources combined do not result in a steady generation. The result is a net surplus of electricity in summer and a net shortage of electricity in winter. Figure 2 illustrates this mismatch. The blue line illustrates the electricity produced from solar and wind, the orange line shows the consumption of electricity. To balance these demand and production gaps renewables must be either be curtailed or stored. Curtailment leads to oversizing of the system and does not provide a solution for electricity deficits, which is why the solution must come from energy storage. While this sounds simple, energy storage is one of the largest techno-

economic challenges today. Many energy storage technologies have been developed, but not all of these are suitable for storage of VRES in The Netherlands. The next chapter discusses some of these.

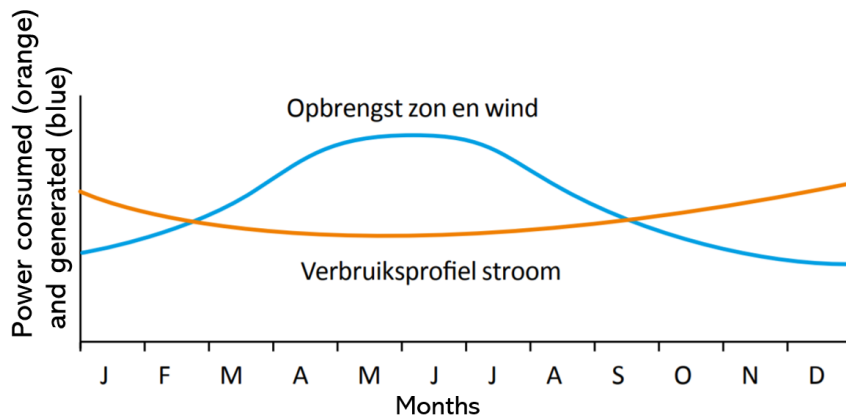


Figure 2: Graphic representation of solar and wind power generation against power consumption throughout the year (Energy Storage NL, 2019).

3.2. Energy storage technologies

Some well-known storage technologies are batteries, flywheels, compressed air energy storage, pumped hydro storage and energy storage in molecules. An overview of these technologies is given in the Ragone plot in Figure 3. The vertical and horizontal axis show the discharge time and storage capacity respectively. This allows an easy, visual comparison between storage technologies. Short term, small scale energy storage media are found in the bottom left area of the plot, large-scale, long term storage is shown in the top right corner. Short term, small scale energy storage is already used in many technological applications (mobile phones, laptops, cameras, vehicles). Most of these devices use batteries, while others use capacitors or flywheels for energy storage. Apart from this short term, small scale energy storage the increase of VRES in the grid also demands long term and large-scale storage solutions. The technologies that are currently showing potential for large scale energy storage are pumped hydroelectric storage (PHES), compressed air energy storage (CAES) and PtXtP (Gür, 2018). PHES is one of the oldest storage technologies and currently represents 90% of the storage capacity worldwide (European Commission, 2017). CAES is newer but has also been deployed. PtXtP, however, is new and is still in development.

A convenient overview of storage media and their level of maturity was created by Gür and is shown in Figure 4. Dutch and European policy makers have placed their hopes on energy storage in molecules (Energy Storage NL, 2019) (European Commission, 2017). Electricity is generated and used to produce a certain molecule, the energy carrier. The energy carrier is stored until an energy deficit occurs and the energy carrier is used to regenerate electricity. Examples of these energy carriers are hydrogen and methane, as is shown in the comparison in Figure 3. Other energy carriers can also be used, which explains the broader and more commonly used term: power-to-x-to-power (PtXtP). The relevance of PtXtP as an addition to the currently available large-scale energy storage technologies is further discussed in chapter 5.

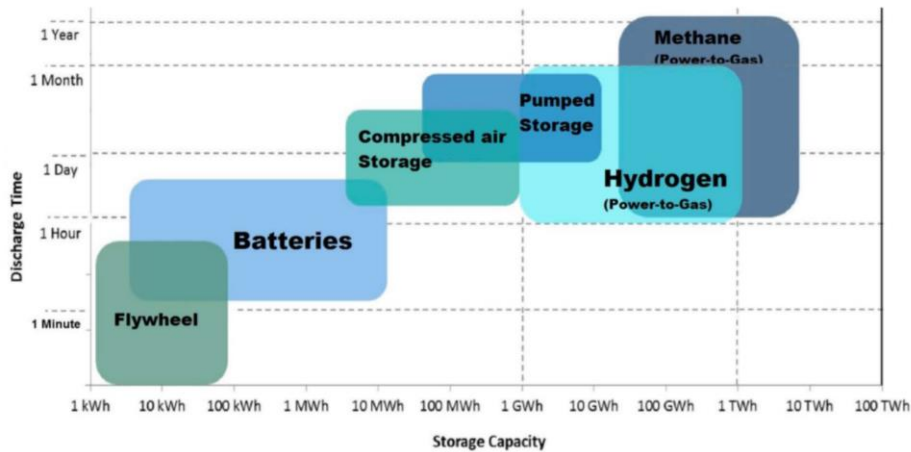


Figure 3: Comparison of storage technologies based on their discharge time and storage capacity (European Commission, 2017).

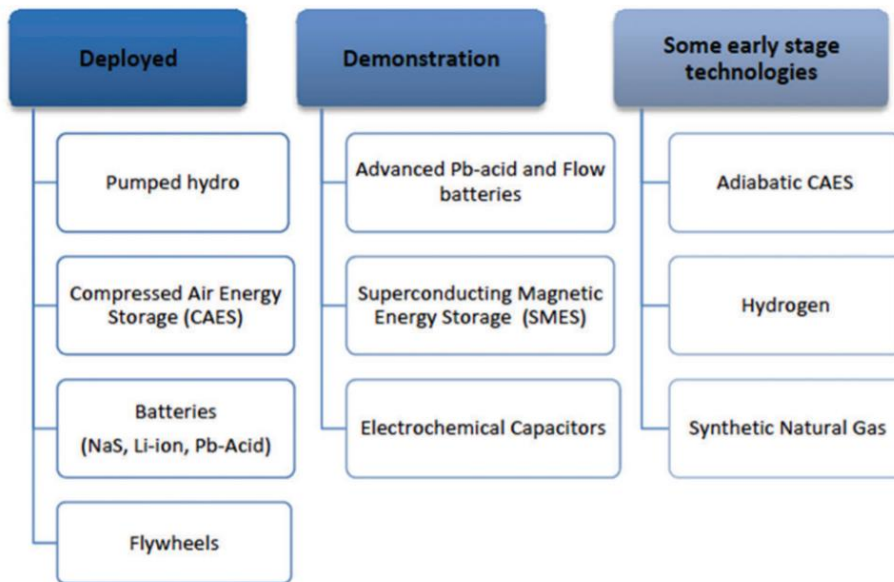


Figure 4: Developmental maturity of major electricity storage technologies according to T.M. Gür (Gür, 2018)

3.3. State of the art

Many studies have compared energy storage technologies. One of the most recent and comprehensive overviews was written by Tim Gür (2018). Energy storage in chemicals is included in his study. Interesting is the differentiation between short term, high power technologies and long term, high capacity technologies. Capacitors and fly wheels are deemed most suitable for energy storage for the duration of seconds. Energy storage in chemicals, like hydrogen or methane, is deemed more suitable for long term storage of large capacities. Figure 5 shows a comparison of different storage technologies. Typical large scale energy storage technologies have a low cost per kWh and are capable of long periods of charge or discharge (top left corner of Figure 5). Short term energy storage solutions can be more expensive per kWh of capacity, but typically have a large charge and discharge power capacity (bottom right corner of Figure 5).

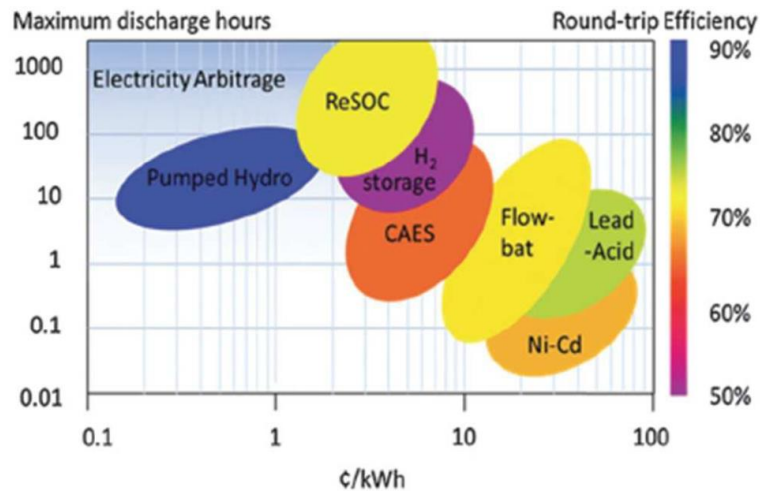


Figure 5: Comparison of storage technologies based on round trip efficiency, cost per kWh and discharge time as quoted by T.M. Gür (Gür, 2018), created by Yang et al. (Yang, et al., 2011). ReSOC stands for Reversible Solid Oxide Cell, CAES is Compressed Air Energy Storage, Ni-Cd is Nickel-Cadmium batteries.

While this comparison uses different characteristics to compare the technologies than the one in Figure 3, they both show PtXtP technologies as suitable for long term, large capacity storage systems. Figure 3 and Figure 5 show that PtXtP is relatively cheap for storage capacity, which makes it interesting for large amounts of energy storage. Figure 5 shows that the efficiency of hydrogen storage is comparatively low, a lot of energy is lost in the conversion of electricity to hydrogen and the regeneration, which encourages energy storage over long periods of time. It's because of these two qualities that PtXtP is considered a large scale, long term energy storage solution. Other technologies, like batteries and flow-batteries, are shown as short-term storage solutions. For a balanced energy grid short term as well as long term storage technologies are required. Battery and flow battery storage are therefore complementary to PtXtP.

3.4. Knowledge gaps

Most Dutch policy makers are in consensus that PtXtP systems are going to be necessary in the Dutch electricity system when large shares of VRES are introduced. This consensus rests on estimations of cost and efficiency of hydrogen technologies. However, not a lot of research is done yet toward the costs and performance of PtXtP systems as energy storage technology. The effect of variable electricity production on efficiency and cost is not accounted for. More importantly, the performance of PtXtP technologies in an integrated system for VRES storage in the Netherlands has not been evaluated yet. The goal of this thesis is to provide a system analysis of PtXtP storage systems, with the purpose of addressing the following knowledge gaps:

- Main system bottlenecks, as well as techno-economic challenges and opportunities that occur when combining system components of a PtXtP system for the use of large-scale energy storage.
- The effect of intermittent use due to VRES electricity input on cost and efficiency of PtXtP systems.
- A current and reliable overview of data regarding the cost, efficiency and energy use of PtXtP systems.

3.5. Research question

This study aims to evaluate the performance of PtXtP systems as large-scale energy storage technology. In order to do so the relevant context and competing technologies are explored. In addition, different PtXtP technologies must be compared to identify the technologies with the most potential for use as energy storage system. Based on available input this study will then identify the bottlenecks in PtXtP storage systems that will occur when the system is implemented in the Dutch electricity grid in 2030. The aim is captured in the following research questions.

What is the techno-economic potential of power to x to power technologies for energy storage of variable renewable electricity in the Netherlands in 2030?

In order to answer this question several sub-questions are posed:

1. How do PtXtP technologies compare to existing energy storage technologies and to each other?
2. Which PtXtP technologies show the most potential for use as an energy storage technology in 2030?
3. What are the technical limitations to the use of PtXtP technologies as energy storage medium?

3.6. Thesis outline

The first step towards answering the research questions is to create a methodology. The methodology is given in chapter 4. Research sub-question 1 requires a broad view and comparison of different large-scale energy storage technologies. The initial comparison is in chapter 5; this will give the reader a context of large-scale energy storage technologies to PtXtP technologies in perspective. Chapter 8 will describe a model that will be used for simulation of PtXtP technologies as large-scale energy storage technology. Unfortunately, not all PtXtP technologies can be included in the simulations. Chapter 6 describes and compares existing PtXtP technologies, in order to select the three most promising ones. Those three are further investigated in chapter 7, for the purpose of selecting the specific technologies that are used in the simulated PtXtP systems. Chapter 9 gives an overview of the performance indicators of each of these technologies. These are used as input for the simulation model. After creation of the model, several scenarios will be created to test the PtXtP systems under different circumstances. The scenarios are described in chapter 10. Chapter 12 contains the sensitivity analysis, chapter 11 discusses the results of the simulations. Chapter 13 and 14 contain the conclusion and recommendations.

4. Methodology

The goal of this thesis is to evaluate and compare the potential of PtXtP systems as energy storage technologies for electricity systems with large shares of VRES. Given the low technology readiness level (TRL) of PtXtP, the comparisons must be done based on literature research and model simulations. The literature studies are done to narrow down the scope and provide model input. Afterwards the model is created in order to identify system bottlenecks and evaluate the dynamic performance of PtXtP systems when connected to VRESs.

4.1. Thesis steps

The model simulates the use case of a storage facility to balance the intermittent production of a 100% renewable source, which should give insight into system bottle necks. Additionally, the output of the model can be used to compare the performance of different PtXtP technologies as an energy storage application. The steps taken to create a realistic model are given in

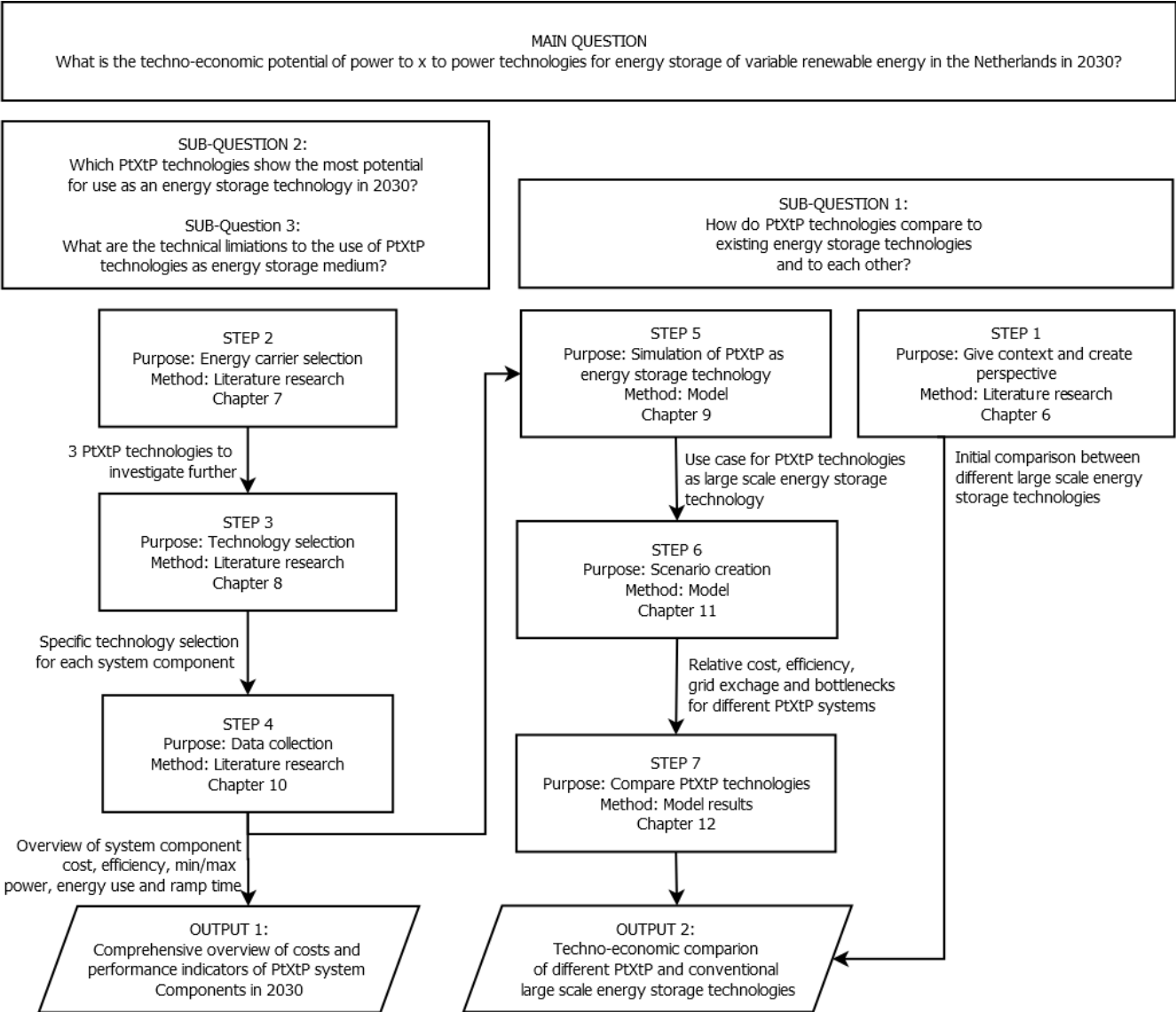


Figure 6.

Figure 6: Diagram of the methodology for this thesis.

Step 1 is to give an overview of currently deployed large-scale energy storage technologies. The overview is presented in chapter 6. The purpose of this chapter is to create a baseline, illustrate the demand for new large-scale energy storage technologies and give an initial comparison with the technologies to beat.

Step 2 is to reduce the scope of the comparison. There are many types of energy carriers to which the “X” in PtXtP systems can refer, not all of them can be modelled. Instead, the top three energy carriers are selected that show the most potential as energy storage system. The selection is done based on literature research and the KPI’s identified in subchapter 4.2. Chapter 7 reviews the different energy carriers and gives the top three after comparison.

Once the energy carriers are selected, many technologies are still an option. Hydrogen, for example, is generated in either an alkaline electrolysis cell (AEC), proton exchange membrane electrolysis cell (PEMEC) or a solid oxide electrolysis cells (SOEC). Step 3 is therefore to compare the specific technologies to decide which technology is most likely to be implemented in a VRES storage system in 2030. This is done in chapter 8.

Once all the technologies are selected, data needs to be gathered to serve as input for the model. This is step 4. A comprehensive literature study, along with expert opinions results in a big table containing the most current technology performance predictions for 2030. This part of the thesis also allows for identification of uncertainties and knowledge gaps. The table can be found in chapter 10.

Step 5 is to create the models that will be used to simulate the PtXtP systems. The preferred software is Simulink, because of its affinity with timeseries simulations. To test the PtXtP systems in the virtual environment scenarios are created, testing different system configurations and circumstances. This is Step 6 and is done in chapter 9.

Step 7 is the sensitivity analysis, which consists of two parts. The first is an analysis of uncertainty of the most input variables. The second is an analysis of the model’s sensitivity to different use cases. The purpose of these analysis is to find accuracy intervals and to validate the conclusions for many different use cases. The final step is step 8: the results, followed by the conclusions and recommendations.

4.2. KPI’s

In order to design the right model for the comparison certain key performance indicators (KPI’s) must be identified. As stated before, this thesis aims to evaluate the techno-economic potential of PtXtP as energy storage. KPI’s are selected that help identify the technological feasibility of the system and the economics of the system. Technological KPI’s are deducted from the purpose of the storage system. The purpose of the storage system is to reduce the pressure on the grid from VRES and to optimize the use of generated wind energy. The pressure on the grid is determined by the system capacity and power, these are design choices and will be optimized in the simulations. However, the capacity can be limited by geographic availability in the Netherlands, which is why the potential capacity in the Netherlands is an important KPI. The amount of useful energy from the wind park is determined by the energy consumption or losses in the storage system. Energy lost in the storage system must be compensated by oversizing of the wind park, or by demanding electricity from the grid. Both options go directly against the purpose of the storage system, which is why the roundtrip efficiency is an important KPI.

An important factor in decision making for the Dutch electricity grid is the cost. The cost can be expressed as the storage system cost, or as cost per MWh stored. If the storage system is much more expensive than system oversizing the storage system will most likely not considered a good solution.

The same is true when the added cost of storage create electricity prices that are not affordable for Dutch consumers. For that reason, the storage system costs and the Levelized cost of storage are included in the list of KPI's.

Finally, the technology readiness level (TRL) is included. Only technologies that are expected to be sold and used on a large scale by 2030 are included in the comparison. Not enough data is available for technologies that are currently functioning only at lab scale. In addition, the storage system size will most likely be several hundreds of MWs, scale up from lab-scale to hundreds of MW in 10 years is considered unrealistic.

An important consideration in the selection of a storage system is the CO₂ footprint of the system. The purpose of implementing VRES in the Dutch grid is to reduce CO₂ emissions and use of fossil fuels. However, data on the CO₂ footprint of different system components is difficult to find. For that reason, the CO₂ footprint is not included in the KPI's. However, storage technologies that use fossil fuels or create a net production of CO₂ are not considered in this thesis. Other KPI's that are often mentioned are durability and energy or power density. These are included in the research, but are not in the final KPI's, instead they are used as intermediate variables. The required storage space and system sizing is evaluated after modelling. Durability is used as intermediate variable for the determination of the annualized CAPEX. Similarly, self-discharge rates are used as intermediate variables for determination of the roundtrip efficiency.

The list of relevant KPI's was validated by a review of several energy storage comparisons and is given below (Gür, 2018), (Del Peroa, et al., 2018), (RVO, 2006):

- Storage system cost (€)
- Levelized cost of storage per MWh (€/MWh)
- Roundtrip efficiency (%)
- Potential capacity in NL (MWh)
- TRL

The *storage system cost* (euros) is the sum of the annualized CAPEX, fixed OPEX and variable OPEX of each component in the storage system. The fixed OPEX includes all costs that are made per year, like parcel rent and labor cost. Variable OPEX costs are the costs that vary per MWh produced, like the cost of water for production of hydrogen. The cost for electricity is not included, because electricity prices fluctuate strongly. Instead, the system is seen as a closed system. Energy is exchanged between the system components, while only the electricity input and output of the entire system are measured. The annualized CAPEX is calculated as indicated below, where *i* is the interest rate, and *T* is the lifetime in years. This definition is used in many other reports, including the HyChain report (ISPT, 2019).

$$\text{Annualized CAPEX} = \text{CAPEX} \cdot \frac{i}{1 - \frac{1}{(1+i)^T}}$$

Levelized cost of storage per MWh is calculated as the annual system cost divided by the number of MWh's delivered back to the grid. This translates into the cost added to the electricity price for consumers by the system. The calculation of the levelized cost of storage (LCOS) is given in the formula below.

$$\text{LCOS} = \frac{\text{Storage system cost (€)}}{\text{Energy output (MWh)}}$$

Roundtrip efficiency is a measure for the ability of the system to deliver back energy that was stored before. An ideal system delivers back everything, in reality some energy is always lost. The roundtrip

efficiency is defined as the total energy that is delivered to meet demand, divided by the total energy that goes into the system.

The *potential capacity in the Netherlands* determines how much energy can be stored. Some types of energy storage, like PHES, require geological features that the Netherlands might not possess. This thesis focuses on the Netherlands and the energy storage is assumed to be completely in Dutch borders, to prevent dependencies and double counting from different countries.

The *TRL* is an indicator for the state of development of the technology, the defined levels are given in Figure 7. Developments are moving fast, and many technologies show a lot of potential on lab scale. However, the storage system must be implemented in 2030, and is large scale, which means the TRL must be at 7 or higher for large scale applications of a technology, higher TRL levels are preferred.

Phase TRL		Hardware	Software
Research	1	Basic principles	
	2	Concept and application formulation	
	3	Concept validation	
Development	4	Experimental pilot	
	5	Demonstration pilot	
	6	Industrial pilot	
Deployment	7	First implementation	Industrialization detailed scope
	8	A few records of implementation	Release version
	9	Extensive implementation	

Figure 7: Definitions of Technology Readiness Levels (Blanc, et al., 2017)

4.3. Simulation scenario

The model will simulate a use case of VRES generation and Dutch demand for large scale energy storage technologies. Offshore wind was selected because the Dutch electricity mix will contain large shares of wind energy (Ministerie van Economische Zaken, 2016). In addition, wind energy is most likely to be generated in a centralized hub, requiring centralized, large scale storage. Finally, the wind generation profile is very intermittent, which makes a good test case for the energy storage system.

The Dutch government has created a roadmap for offshore wind projects up to 2030. The total rated power of wind parks in the North Sea is planned to be 11.5 GW. Approximately 1 GW already exists, 3.5 GW is planned in the roadmap for offshore wind upto 2023, and an additional 6.1 GW is planned in the roadmap to 2030 (Wiebes, 2018). The location for the remaining 0.9 GW is yet to be determined and will be constructed in one of the designated areas, indicated with yellow in in Figure 8 (next page). For existing and planned wind parks connection issues are currently being solved and tenders are already closing. For the 0.9 GW parks that are still to be determined, the options are still open. The overview of current and future wind parks in the North Sea is given in Figure 8 (next page). The scenario in this study is to use a PtXtP system as energy storage for these final parks. For easy reapplication and

scaling the wind power source is assumed to be 1 GW. This scale is close to the size of future wind projects and it is an easy figure to scale out. Produced electricity is transported to shore to meet the demand on the Dutch electricity grid. Conditions between the wind park and the storage system, like offshore distance and cable types, are assumed to be equal to the 4 GW wind park of IJmuiden Ver. Electricity surplus is stored by the PtXtP system, in times of deficit the PtXtP system delivers electricity. To prevent large adaptations to the electricity transmission grid a good location for the grid connection and storage system must be selected. This is done after more thorough research of the generation and demand in chapter 8.

Important to know is that the energy storage demand is heavily dependent of the import and export of electricity to neighboring countries. At times of simultaneous strong winds in Germany and the Netherlands peak production might be increased by excess electricity flowing from Germany to the Netherlands. At other times peak production may be exported to neighboring systems, reducing the storage requirement. Also important are limitations to the scaling of the system. The system is scaled to exactly meet the generation and demand of 2018. In reality some oversizing would be required because of uncertainties and to provide a level of grid security. These limitations, amongst other simplifications, are okay for a comparison between the technologies, but the results are not conclusive on the absolute cost and efficiency of the system.

4.4. Scope

This study focusses on PtXtP technologies as energy storage technology for daily, weekly and seasonal energy storage, as for smaller timescales several other energy storage technologies are available as was illustrated in Figure 3. The final GW of wind power capacity will be completed in 2030, which means the large-scale energy storage facility will also be modelled for that year. The considered timeframe is therefore in 2030, simulations will simulate one year with timesteps of one hour. The geographical scope of this study is the Netherlands. The electricity generation and storage technologies are initially evaluated from the perspective of the balancing responsible party, in this case TenneT, meaning the system is in the end considered a black box, where electricity is absorbed in times of electricity surplus and electricity is regenerated in times of electricity deficit. In reality, TenneT is legally not allowed to store energy and deliver energy back to the grid. This means different storage system components might be owned by different owners. Exchanges of electricity, hydrogen or money between owners of different storage system components are not considered, only system input and output are considered.

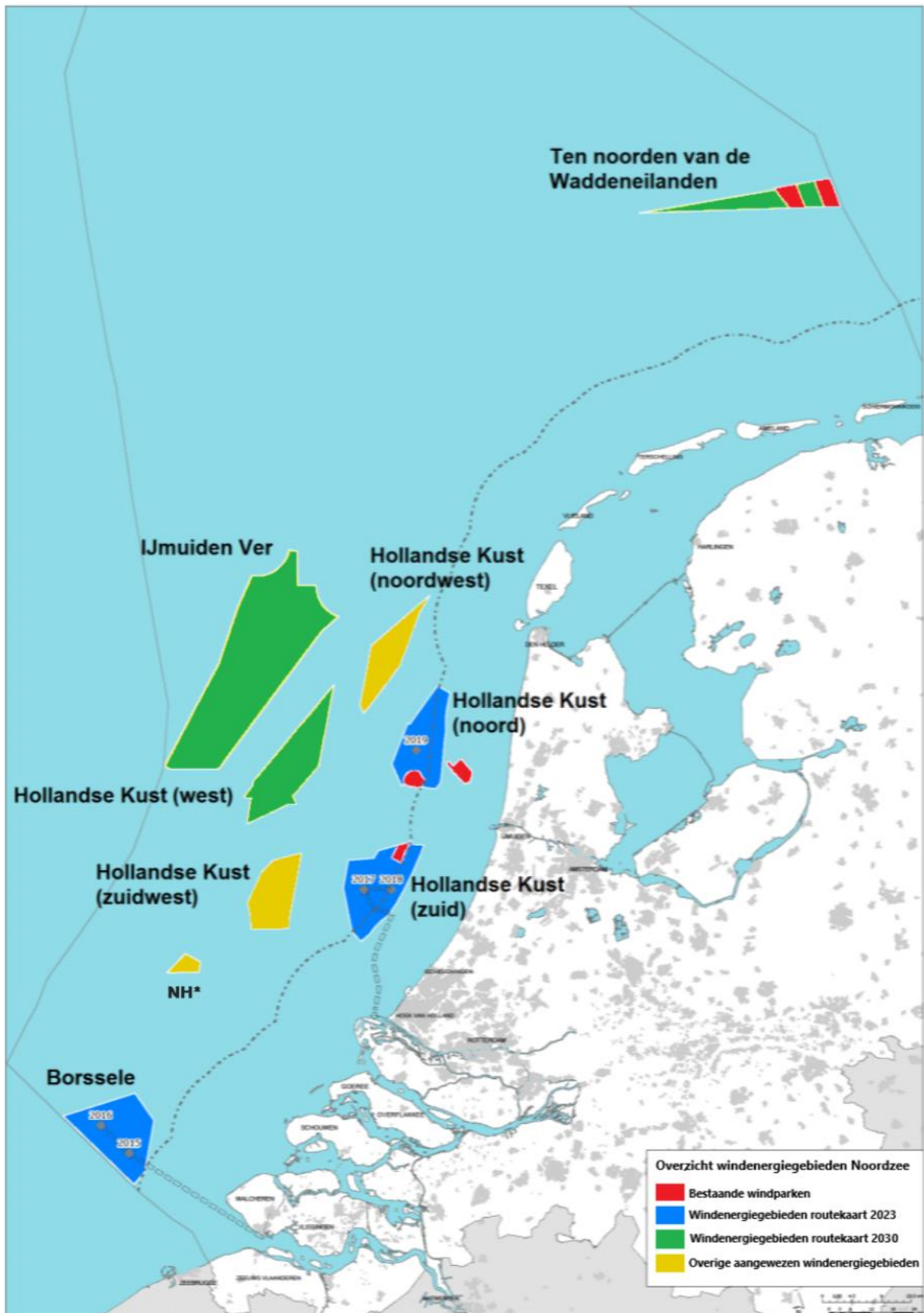


Figure 8: Map of all existing, planned, and potential wind parks in the Dutch North Sea. Red represents existing wind parks (1 GW), blue represents wind parks planned for 2023 (3.5 GW), green represents wind parks planned for 2030 (6.1 GW), yellow represents areas designated for wind parks in the future (0.9 GW) (Wiebes, 2018).

5. Large scale energy storage

The need for energy storage is growing and there are many technologies that might provide the necessary energy storage capacity to increase the share of renewables. In order to evaluate the potential of PtXtP technologies an overview of current large-scale energy storage systems is given to create an image of the market and to give the PtXtP results the proper perspective. The two currently deployed large-scale energy storage technologies are CAES and PHES. The KPI's of the comparison were identified in the methodology, however, the system cost is strongly dependent on system scaling. For that reason, the KPI's included here are storage system cost per MWh output, round-trip efficiency and the available potential in the Netherlands.

5.1. Compressed air energy storage

Compressed air energy storage (CAES) is a type of mechanical storage. Air is compressed and stored in underground caverns during times of electricity surplus, in times of electricity deficit the air is released through a turbine to regenerate electricity. These compression and release steps result in heat creation and heat loss. To reduce the temperature at compression cooling is required, to increase the temperature at release natural gas is mixed in with the air and combusted (Gür, 2018). Future CAES developments are aimed at adiabatic CAES, meaning the heat from compression is stored and re-used during air release, eliminating the use of fossil fuels.

The next important challenge is the availability of underground storage reservoirs that are suitable for CAES. TNO evaluated the potential of underground storage reservoirs in the Netherlands for CAES, hydrogen and methane (Van Gessel, Breunese, Juez Larré, Huijskes, & Remmelts, 2018). For CAES salt caverns are required. In the Netherlands caverns with a total potential of 1.98 PJ (550 GWh) storage capacity are available. De Boer et al. modelled a Dutch electricity system based on three large scale storage capacities (De Boer, Grond, Moll, & Benders, 2014). They conclude different potentials for CAES storage, their analysis predicts a potential of 0.069 TWh (69 GWh) for CAES technology. The difference between their predictions can be explained by their selection of caverns. Van Gessel et al. identify a total of 8 areas with suitable salt caverns, while De Boer et al. only select the three areas of salt domes with the most potential.

The expected demand for seasonal energy storage in 2030 is in the order of 50,000 GWh for 2030 (Mulder, Postma, Klop, & Visser, 2015), which means even the max of 550 GWh CAES capacity will not be sufficient for a large share VRES electricity system.

- Cost per MWh: 27-49 €/MWh (European Commission, 2017)
- Roundtrip efficiency: currently 50-60%, expected to raise to 86% (Gür, 2018)
- Potential capacity in NL: 69-550 GWh (Van Gessel, Breunese, Juez Larré, Huijskes, & Remmelts, 2018), (De Boer, Grond, Moll, & Benders, 2014)
- TRL: 8 for conventional, 6 for adiabatic operation (EASAC, 2017)

5.2. Pumped hydro energy storage

PHES, like CAES, is a type of mechanical storage. In times of electricity surplus water is pumped up and stored in a natural reservoir. In times of electricity deficit water is released through turbines that convert potential and kinetic energy into electric energy. This technology is the most efficient and affordable technology for large-scale energy storage at this moment. PHES requires enough water and a storage basin with a significant height difference. While the waterflow is available in the Netherlands, the natural height differences are not.

In the Netherlands PHES does not have much potential, De Boer et al. therefore assumed the availability of 85 TWh of PHES in Norway (De Boer, Grond, Moll, & Benders, 2014). In 2015 eStorage created an inventory of PHES potential in western Europe, it shows the Netherlands does not have any natural potential for PHES. Figure 9 shows the map with the potentials for different countries. Other researchers involve artificial PHES or Inversed PHES (IPHES). IPHES involves the creation of an artificial lake, which is used as a reservoir to pump sea water up and regenerate power when water flows down. This can be done offshore. The first experiment is planned for 2021, when the iLand of the coast of Belgium is expected to be ready for operation (Entso-e, 2018). This artificial island occupying an area of 2x4 km will have a storage capacity of 2 GWh and 550 MW power. The capacity will be available for use to Belgium, the Netherlands, UK and Germany. Other options are seawater pumped hydro storage (SPHS) and sub-surface pumped hydro storage (SSPHS). While the iLand is an interesting new development, the storage capacity of 2 GWh per artificial island is not considered large enough to provide the energy storage for a fully renewable electricity system.

- Cost per MWh of capacity: 21 €/MWh for artificial reservoirs (Kibrit, 2013), 7-14 \$/MWh (Yang, et al., 2011) or 18-24 €/MWh for natural reservoirs (European Commission, 2017)
- Roundtrip efficiency: 75-85%
- Potential capacity in NL: 0 for natural reservoirs, unknown for SPHS and SSPHS (eStorage, 2015)
- TRL: 9 (eStorage, 2015)

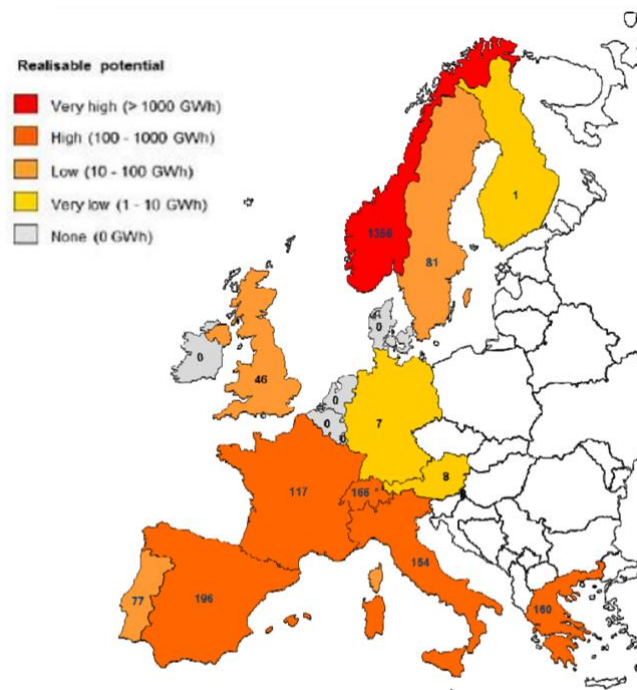


Figure 9: PHES potential in Europe according to eStorage (eStorage, 2015)

5.3. Power to X to Power

The technology that is considered to complement CAES and PHES is PtXtP, or energy storage in chemicals. The important difference is that energy is not stored mechanically, but chemically. Some of these PtXtP technologies are quite mature. The Haber-Bosch process for example, which is used to produce ammonia out of nitrogen and hydrogen, was developed in 1909. Other system components,

like PEM fuel cells, are relatively new. The application of these known processes for energy storage is also relatively new, but many organizations have already expressed their confidence in the technology. Netbeheer Nederland (the sector organization for the Dutch electricity grid) has issued a report where the role of PtXtP (hydrogen) in energy storage is described as follows:

“..., for long term storage (storage over a couple of months) hydrogen will be used. Hydrogen from electrolysis is therefore an important new energy carrier. The hydrogen electrolysis will be realized on several voltage levels.” (Afman & Rooijers, 2017)

Netbeheer Nederland is expressing its confidence in hydrogen specifically, while the European Commission mentions hydrogen and methane (European Commission, 2017). The Dutch government also adds ammonia to the list of options (Energy Storage NL, 2019). Most major stakeholders are counting on PtXtP as an energy storage medium in the future. However, PtXtP plants have not been used as storage systems before. Policy makers base their decision on knowledge of subsystems in PtXtP technologies. Production of hydrogen from water through electrolysis has been done since before the 1800's. Conversion of hydrogen and nitrogen into ammonia using the Haber-Bosch process has been done since the early 1900's. The technologies are therefore not new, the application is. The question to be answered now is how well different PtXtP technologies perform in this new application.

In order to make a first comparison to PHES and CAES similar values for PtXtP were found. The values below come from a number of these studies and give an order of magnitude, rather than precise values. These estimations are based on lab scale results and thermodynamic principles, rather than observed values. The available energy storage capacity is based on hydrogen storage in underground caverns, which is estimated to be around 1800 PJ (Van Gessel, Breunese, Juez Larré, Huijskes, & Remmelts, 2018).

- Cost per MWh: 50-150 €/MWh strongly dependent of storage technology and electricity price. (HyUnder, 2014) (Hydrogen Europe, 2018), (Fuel cells and hydrogen joint undertaking, 2015).
- Roundtrip efficiency: currently ~30% (De Boer, Grond, Moll, & Benders, 2014)
- Potential capacity in NL: 500-556 TWh (Van Gessel, Breunese, Juez Larré, Huijskes, & Remmelts, 2018), (De Boer, Grond, Moll, & Benders, 2014)

5.4. Comparison

After review PHES seems to be the cheapest and most efficient large-scale energy storage technology, which explains why it currently makes up the largest share of energy storage capacity in the world. Each technology was briefly discussed, Table 1 gives an overview of the values mentioned. While CAES and PHES are more efficient, significantly cheaper and have a higher TRL than PtXtP technologies, they are limited by available geological capacity (Hadjipaschalis, Poullikkas, & Efthimiou, 2009). Their capacity in the Netherlands was evaluated by TNO and by De Boer et al. (De Boer, Grond, Moll, & Benders, 2014), (Van Gessel, Breunese, Juez Larré, Huijskes, & Remmelts, 2018). Van Gessel at all have analyzed the future electricity grid and predict a storage necessity of 10 bcm of green gas or an equivalent of that for hydrogen, which is equal to roughly 100 TWh. This first, preliminary analysis shows PtXtP storage systems can therefore still prove valuable or even necessary in a 100% VRES system.

Table 1: Overview of levelized cost of storage, potential capacity and roundtrip efficiency of CAES, PHES and PtXtP

	PHES	CAES	PtXtP
Levelized cost of storage	6.3-24 €/MWh	27-49	50-150 €/MWh
Roundtrip efficiency	75-85%	60%	30%
Potential capacity in the Netherlands	0 (85 TWh in Norway)	0-0.55 TWh	500-556 TWh

The conclusion is that the energy storage demand cannot be met by PHES and CAES alone. PtXtP technologies are considered the next solution, they could provide enough storage capacity, but at high monetary and energy cost. In addition, the PtXtP solution comes with a lot of uncertainty. So far, PtXtP plants have not been deployed on a large scale and many types of PtXtP are still under development. The next chapter will further exploit these different types, in order to select the three most likely to be implemented as a large-scale energy storage system.

6. Power to X to Power technologies

The review of CAES and PHS technologies has illustrated the potential relevance of PtXtP technologies. This thesis will compare several PtXtP technologies on their performance as a large-scale energy storage technology. However, the spectrum of PtXtP technologies is wide, and differences can be great, which is why institutions have a divided focus. The European Commission focuses on hydrogen and methane in reports on future energy storage systems (European Commission, 2017). The Dutch government has created scenarios where hydrogen, methane and ammonia are used for energy storage in the “National plan of action for Energy storage and conversion 2019” [translated] (Energy Storage NL, 2019). The Japanese government is running pilots with liquid hydrogen and organic hydrides (toluene or methylcyclohexane, MCH) (Nagashima, 2018). This chapter will review all available PtXtP technologies in order to select the three most promising technologies for further comparison in simulations. An overview of the comparison is given in Table 3.

6.1. Hydrogen as an energy carrier

The one consensus about PtXtP is that atomic hydrogen (H) is the best element to use in energy carriers, it forms energy rich bonds and is the lightest atom. In addition, hydrogen is one of the most abundant atoms on earth and H₂ is easily formed by electrolysis of water. The form in which hydrogen is best stored and transported is still under debate. Atomic hydrogen can be bonded to metals or stored in chemical bonds. Molecular hydrogen can be adsorbed or stored under pressure and cold temperatures. Andersson and Grönkvist use the same categorization and have created the overview shown in Figure 10 (Andersson & Grönkvist, 2019). Their report gives an overview of hydrogen storage technologies and the current state of the art (May 2019).

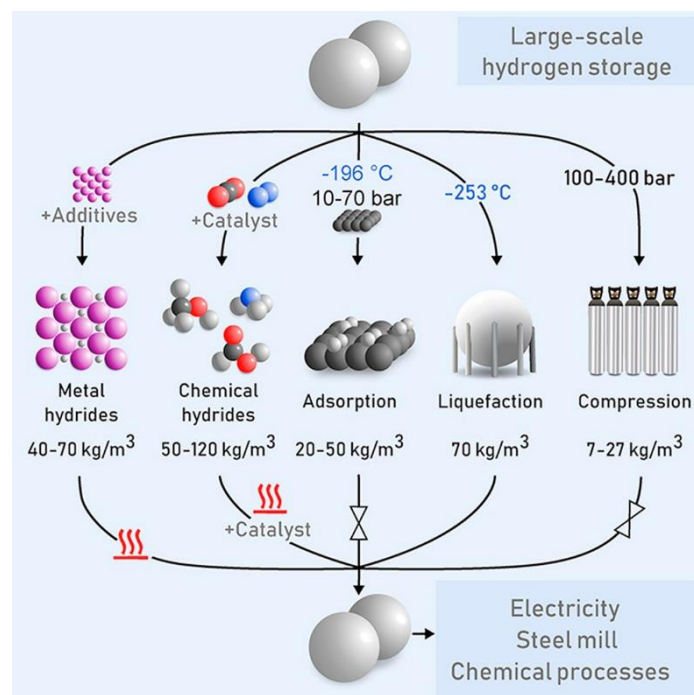


Figure 10: Overview of different pathways for hydrogen storage and their hydrogen density (kg of H₂/m³) (Andersson & Grönkvist, 2019)

6.2. Molecular hydrogen storage

The most straightforward form of hydrogen storage is to store hydrogen (H₂) as a liquid or gas in tanks. Transport can be done either through pipelines or with tankers. Pressurized hydrogen is used as energy carrier in passenger cars, where hydrogen is pressurized and stored in a heavy tank at 350 or even 700 Bar. However, the maximum pressure storage of large quantities of hydrogen (several GWh and up) for above ground is lower at 100 bar (Andersson & Grönkvist, 2019). The advantage of hydrogen storage under pressure are the high storage efficiency (5-20% compressor losses) and high charge/discharge rates (Zheng, et al., 2012). Downsides to transport of gaseous hydrogen are the low energy density, self-discharge, and risk of explosion. In addition, hydrogen storage at room temperature under high pressure causes embrittlement of the storage tank metal. Embrittlement occurs when hydrogen penetrates the atomic metal structure and causes cracking.

To prevent the use of hydrogen tanks, hydrogen can also be stored in natural underground gas reservoirs. TNO has identified suitable locations and has found a total of 277 TWh on shore storage potential and 179 TWh off shore storage potential (Van Gessel, Breunese, Juez Larré, Huijskes, & Remmelts, 2018). Figure 11 shows the locations of caverns available for underground hydrogen storage. Andersson and Grönkvist state that when hydrogen is stored in sub-ground reservoirs, the pressure of storage will not exceed 200 bar when dealing with large quantities of hydrogen. The advantage to using caverns is the elimination of large tanks. The downside is the requirement of cushion gas. Cushion gas is a portion of the stored gas that must stay in the cavern to prevent collapsing and to provide the necessary pressure for operation, which renders is useless (Andersson & Grönkvist, 2019).

Molecular hydrogen can also be stored as a liquid. Liquid hydrogen is produced by cooling the hydrogen down to -253 °C (Office of energy efficiency and renewable energy, n.a.). This allows a large amount of hydrogen to be stored in a small volume. Down sides to liquid hydrogen are the energy losses in cooling and the hydrogen losses due to evaporation. Up to 30% of the LHV of hydrogen is consumed when cooling the hydrogen down to -253 °C (Zheng, et al., 2012).

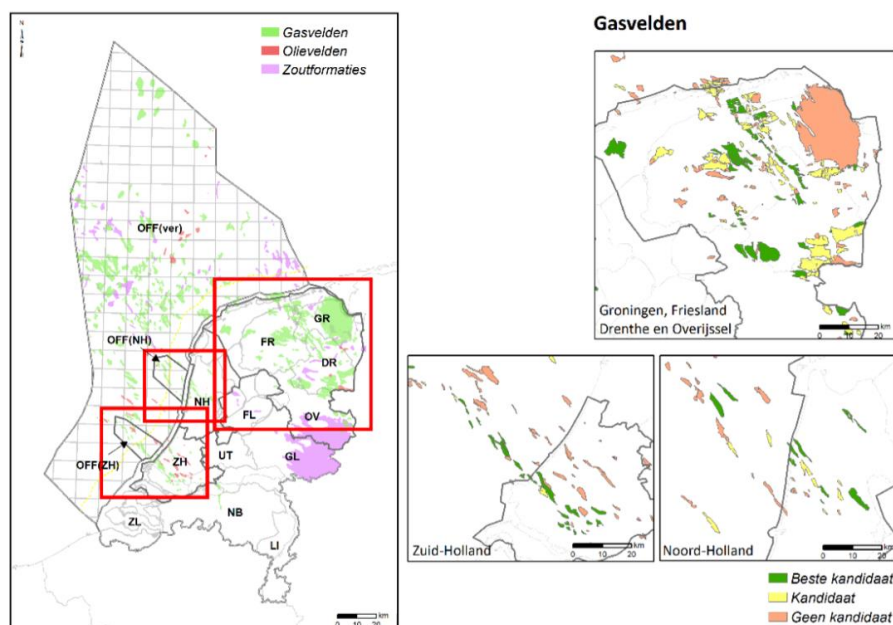


Figure 11: Overview of underground salt (purple), gas (green) and oil (red) fields suitable for hydrogen storage in the Netherlands. The pictures on the right show suitability; Green are the most suitable caverns, yellow are usable caverns, red are not usable (Van Gessel, Breunese, Juez Larré, Huijskes, & Remmelts, 2018).

6.3. Hydrogen in Chemical bonds

Hydrogen can be bonded to other atoms before storage to create molecules that are easier to handle. Molecules that are currently considered as carriers are methane, methanol, ammonia, formic acid and liquid organic hydrogen carriers (LOHC's).

6.3.1. Methane

Methane is gaseous under standard conditions and is the main component in natural gas. It is most commonly produced by reacting CO with H₂ (syngas), to produce CH₄ and H₂O. Hydrogen and carbon monoxide are created from water and CO₂ using renewable energy. Methanation occurs in the Sabatier reaction (Van Leeuwen, 2018), (Duong Dang & Steinberg, 1977). For regeneration of electricity methane can first be dehydrogenated or combusted.

Methane storage is very easy, it is compatible with the current natural gas system, which means the current infrastructure and technology can be used (Van Leeuwen, 2018). Methane can also be stored in former natural gas reservoirs underground. TNO has identified suitable reservoirs with a total of 1178 TWh on shore and 761 TWh offshore capacity (Van Gessel, Breunese, Juez Larré, Huijskes, & Remmelts, 2018). De Boer et al. identify 552 TWh available for methane storage (De Boer, Grond, Moll, & Benders, 2014). Other advantages of methane storage over hydrogen storage are the higher volumetric energy density and lower risk of leaking. A big disadvantage of renewable methane production is the requirement of CO₂ (Gür, 2018). CO₂ capture from air is difficult and energy consuming, while CO₂ capture from flue gases only delays CO₂ emission, instead of preventing it. Another disadvantage compared to direct hydrogen storage is the energy efficiency of conversion. The roundtrip efficiency of power-methane-power storage is estimated to be 40% at most but is currently estimated at 28% (Afman & Rooijers, 2017). Finally, the gravimetric energy density of methane is lower than that of hydrogen.

6.3.2. Methanol

A comparable chemical that can be used as hydrogen carrier is methanol (Onishi, Laurency, Beller, & Himeda, 2018). Methanol is liquid at room temperature and is used extensively in industry, which makes it easy to handle. It is typically produced by reacting CO₂ with H₂ to produce methanol (CH₃OH) and H₂O, although alternative pathways have also emerged (Gür, 2018). For regeneration, methanol can be used as fuel in turbines (Methanol institute, 2016).

Methanol storage is done in above ground tankers, made specially for methanol storage. These storage tanks are designed specifically for dealing with the high flammability, corrosion and vaporization (Methanol institute, 2016). The advantage of methanol over hydrogen is the fact that it is fluid at room temperature. A disadvantage is that it has a lower energy density than hydrogen and methane. Like the production of methane, this process is also dependent of CO₂ capture. The round-trip efficiency is approximately 28%, the same as that of methane (ISPT, 2017).

6.3.3. Formic acid

Formic acid is another carbonyl compound, it is also produced by bonding of CO₂ and H₂ to form CH₂O₂ (HCOOH). Formic acid is the easiest molecule to form out of hydrogen and CO₂, which is why it can be produced without producing any unwanted side products (Moret, Dyson, & Laurency, 2014). Formic acid, like methanol is liquid at room temperature. The energy in formic acid can be regenerated by dehydrogenation or by use of a direct formic acid fuel cell (Van Haperen, 2016). Storage of formic acid is done in non-metal tanks, specifically designed to withstand the corrosion, flammability and pressure

built up by decomposition of formic acid into CO_2 and H_2 . This decomposition mainly takes place at higher temperatures, which is why formic acid storage containers are advised to be cooled below $4\text{ }^\circ\text{C}$ (Fischer Scientific, 2007). An advantage of formic acid over hydrogen and methane is the high volumetric density and ease of handling due to its liquid nature. The second advantage is the ease with which the hydrogen is recovered (Andersson & Grönkvist, 2019). Large disadvantages are the low gravimetric energy density and acidity.

6.3.4. Ammonia

Ammonia (NH_3) or Ammonium (NH_4^+) is a nitrogen-based energy carrier. Ammonia is formed out of N_2 and renewable H_2 in the Haber-Bosch process (Gür, 2018). N_2 can be taken from air as it represents 79% of the atmosphere near the surface. Production of ammonia, like formic acid, can be done without hardly any production of side products due to the nature of the nitrogen atoms (Van Haperen, 2016). Ammonia does easily react with water to NH_4^+ , which is a strong base, making it incompatible with some metals, like copper (Halpern, 1953). Regeneration of ammonia back to electricity can be done by cracking it back to hydrogen, combustion in specific turbines or by feeding into a Solid Oxide Fuel Cell (Hans Vrijenhoef, personal communication, 2020).

While the ammonia infrastructure is not as readily available as the methane infrastructure, ammonia is a widely used industrial substance, and the technology necessary for handling is therefore readily available. The advantage of ammonia over methane is the use of N_2 instead of CO_2 , and the higher roundtrip efficiency (Van Haperen, 2016). Disadvantages of ammonia over methane are the lower energy density and the potential exhaust of NO_x when burning ammonia as a fuel.

6.3.5. LOHC's

A different category of hydrogen carriers is the more complex Liquid Organic Hydrogen Carriers (LOHC's), which often have a cyclic molecule structure. Toluene (MCH, C_7H_{14}) is one of the most common LOHC's. Other complex LOHC examples are methylcyclohexane (Chiyodacorp, 2017), decaline, cyclohexane and bicyclohexane (Van Eldik & Hubbard, 2017). Teichmann et al. consider these LOHC's as energy storage media in the built environment (Teichmann, et al., 2012). They also look at the whole group of LOHC's and design a future electricity system based on N-ethyl carbazole. They compare the energy density of different large-scale technologies in Figure 12 (Teichmann, Arlt, Wasserscheid, & Freymann, 2011).

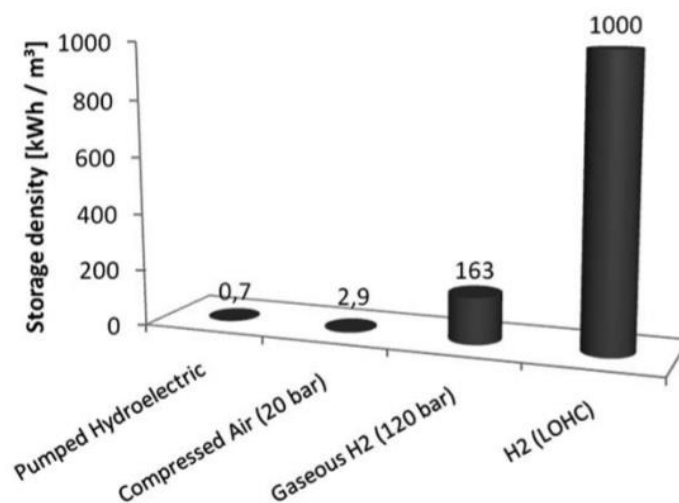


Figure 12: Energy storage density (kWh/m^3) of LOHC's compared to conventional storage technologies, including power generation losses. (Teichmann, Arlt, Wasserscheid, & Freymann, 2011)

Important to notice is that they compare the energy density of LOHC's to gaseous hydrogen at 120 bar, which is a relatively low pressure. Hydrogen at 700 Bar would have a storage density of approximately 950 kWh/m³, which is close to the 1000 kWh/m³ of LOHC's.

An advantage of LOHC's is the fact that they are liquid, which allows for easy handling and causes a high volumetric energy density. The downside to LOHC's is the energy consumed in binding and releasing hydrogen (Teichmann et al. state hydrogen is released at a temperature of 100 degrees Celsius), and the fact that the dehydrogenated LOHC's must be replaced after a number of cycles and recollected after each cycle, which requires two-way transport systems.

6.3.6. Power to X

Other hydrogen containing molecules that can be produced using (renewable) electricity are e.g. ethylene (C₂H₄) and DME (dimethyl ether, C₂H₆O) (Álvarez, et al., 2018). These molecules are more complex to produce (one of the intermediate stages of DME production is the production of methanol) and have a higher value than most of the hydrogen carriers discussed before. For this reason, they are not used for regeneration of hydrogen or electricity. Ethylene is usually produced for use as a platform chemical, while DME is considered a potential automotive fuel. For energy storage in the electricity grid the energy must be stored and regenerated, which is why these products are not included in the comparison of this report.

6.4. Hydrogen in metals (or hybrids)

Like molecules, metals can also be hydrated. Metals absorb the hydrogen to form a solid that contains hydrogen. After storage and transport the hydrogen is desorbed. The storage and release are usually created with pressure or temperature swings. The number of materials used for hydrogen adsorption is immense. Shin-ichi et al. identify several materials as complex hydrides (Shin-ichi, Nakamori, Eliseo, Züttel, & Craig, 2007). Metal hydrides, activated charcoal and advanced carbons are mentioned by Shin-ichi et al. as the predecessor of complex hydrides, e.g. [AlH₄]⁻, [NH₂]⁻ and [BH₄]⁻. Downside to storage of hydrogen in solids is the low TRL, poor heat management, low weight percentage of hydrogen, resulting in low gravimetric energy density, and its solid state, which makes it difficult to transport. In addition, individual metal hydride technologies are dealing with different limitations, like slow kinetics (slow charging/discharging), undesirable side reactions and a limited number of cycles (Shin-ichi, Nakamori, Eliseo, Züttel, & Craig, 2007).

6.5. Hydrogen adsorption

In addition to hydrogen storage in chemicals and metal, where hydrogen is reacted or absorbed, hydrogen can also be stored by use of adsorption. The most important difference is between hydrogen bonding and hydrogen adsorption is the type of bonds. Adsorption uses Van Der Waals forces, while metals use metal bonds, organic compounds use chemical bonds. Roszak et al. evaluate the technological feasibility of hydrogen storage in graphene based nanoporous material (Roszak, Firley, Roszak, Pfeifer, & Kuchta, 2016). Their conclusion is that hydrogen adsorption should technologically be feasible. They all mention years of research failing to find a practical application of the technology. Should a practical application be found, the advantage of hydrogen adsorption over hydrogen carriers is the low amount of energy required for regeneration of hydrogen. Given the poor outlook of hydrogen storage in adsorbing materials the technology will not be considered in this report.

6.6. Comparison and conclusion

The basic working principles of hydrogen storage technologies have been explained and their advantages and disadvantages have been discussed. Based on this preliminary comparison the three PtXtP technologies with the most potential are selected for further modeling. In addition, the comparison is a first indication of bottlenecks in technological development. The three technologies that will be modelled are the ones that are most likely to be completed and scaled up to meet large-scale storage demands by 2030.

The first conclusion is that many PtXtP system components are at present only available on a small scale and in early stages of market entry, which means there is a large gap between the current state of technology and the required state of technology. Based on this conclusion the main selection criterion of comparison is whether the entire large-scale system can be realized by 2030. This is dependent on the current state of technology and foreseeable complications in development. When the technological feasibility comparison is too close to call, the KPI's as identified in the methodology can be deciding factors. However, the cost per MWh and system cost are not available in literature, and the potential capacity in the Netherlands is not a limiting factor for any of the PtXtP technologies, which leaves the roundtrip efficiency as the deciding factor. The roundtrip efficiency is defined as the electricity input over the electricity regenerated after storage (Andersson & Grönkvist, 2019).

To achieve a functioning storage system by 2030 each link in the chain, from Power to X to Power, must be realizable on a large scale. Therefore, each of the system components is evaluated: the feedstocks going in ('carrier', e.g. purified water to produce H₂), the absorption of hydrogen or electricity ('production'), transport, storage and electricity or hydrogen regeneration. To facilitate the comparison a uniform notation is used. Four categories are created, the categories are '++', '+', '-', '- -'. The most important factor is TRL, if it is not possible to scale up a technology to several hundreds of MW's before 2030, the PtXtP system is not feasible at all. The second point of evaluation is whether there are foreseeable complications in technological development. Examples of complications are safety issues, use of rare materials, system complexity and others. The complications have been discussed in the previous sub-chapters. To enable a direct comparison and selection the colors were assigned a number: red is 0, orange is 1, yellow is 2 and green is 3. Table 2 shows the definitions of the scores, an overview of the comparison is given in Table 3.

Table 2: Definitions of the scores awarded to system components for determination of technological feasibility of each PtXtP storage system component.

Notation	Description	Score
++	Commercially available (TRL 9) and straight forward development	3
+	Commercially available (TRL 9) but technology is complex or challenging	2
-	Not commercially available but development is straight forward	1
- -	Not commercially available and development may be complicated	0

Table 3: Overview and comparison of different hydrogen storage technologies based on TRL and technological complications. Roundtrip efficiency is used as a deciding factor when scores are too close to call. +++=3, +=2, -=1, --=0.

	Hydrogen (g)	Hydrogen (l)	Methane	Methanol	Ammonia	Formic Acid	LOHC	Metal
Carrier	++	++	--	--	++	--	--	--
Production/ 'charging'	+	+	+	-	+	-	-	-
Transport	+	-	++	-	+	-	+	--
Storage	-	--	++	++	+	+	++	++
Regeneration/ 'discharging'	+	+	++	+	+	-	-	+
Roundtrip efficiency	38% ¹	34% ¹	28% ¹	27% ¹	30% ¹	25% ²	24% ¹	28% ¹
Points	10	8	11	7	11	9	7	5

¹ Numbers retrieved from the Power to Ammonia report by ISPT (ISPT, 2017) The efficiency was taken from a source that included most technologies. This was done to create a fair, uniform comparison.

² Round-trip efficiency according to Van Haperen (Van Haperen, 2016). This value was not included in Andersson and Grönkvist's report.

Based on this comparison the top three PtXtP technologies are selected for the next step of the comparison, simulation through models. Gaseous hydrogen, methane and ammonia are selected as the PtXtP technologies with the most potential. These technologies will be interesting to compare because their advantages lie in different areas; hydrogen is easy to produce, methane has the advantage of an existing infrastructure, and ammonia is easily compressed and stored to liquid form. The disadvantages are also complementary; hydrogen is difficult to transport and store, methane uses CO₂, which can be difficult to gather, and ammonia is currently not as easily regenerated. A more detailed comparison will be given after simulation, but first the three selected technologies are investigated further to determine for each system component which specific technology is selected for further modeling.

7. PtXtP system components

After selection of the three most promising technologies this chapter describes the selected technologies in a storage system context, from power to x to power. It gives an overview of different system components and selects the expected dominant technology types for large scale energy storage of the 1 GW win plant. The wind plant is planned to be operating in 2030, which means the expected dominant storage technologies for that year must be selected. The system components of a PtXtP system are production, conversion, transport, storage and regeneration. Technological descriptions and context are given to create a better understanding of opportunities and limitations.

7.1. Energy generation technology selection

The full cycle, from power to X to power, will be included in simulations. The first step is therefore the generation of electricity. In order to create a realistic use case of the PtXtP technologies a VRES is simulated, in this case wind.

7.1.1. Generation

The installed power capacity of the windfarm is 1 GW. However, the actual power output fluctuates with wind speed. The output can be predicted roughly, with the prediction of wind power, but cannot be known exactly. In this model data from 2018 is used and adapted to fit the scenario. In total 3.5 TWh of wind energy was generated in 2018, the total installed offshore capacity in 2018 was 957 MW (CBS, 2019). To model the hourly fluctuations, generated power and load in 2018 were taken from Open power system data and ENTSO-E (Open Power System Data, 2019). Figure 13 shows the hourly generated wind power in week 1 of 2018. This figure demonstrates the intermittency of the generated wind power. The data was then linearly scaled from 957 MW to 1 GW. This approach implies several assumptions; The wind speed in 2030 is assumed to follow the same path as the wind speed 2018. The performance of a wind turbine relative to its rated power is assumed to be similar in 2018 and 2030. The incorporation of switchable gears into wind turbine design might result in a more stable output of power, but details regarding this development are not in the scope of this research.

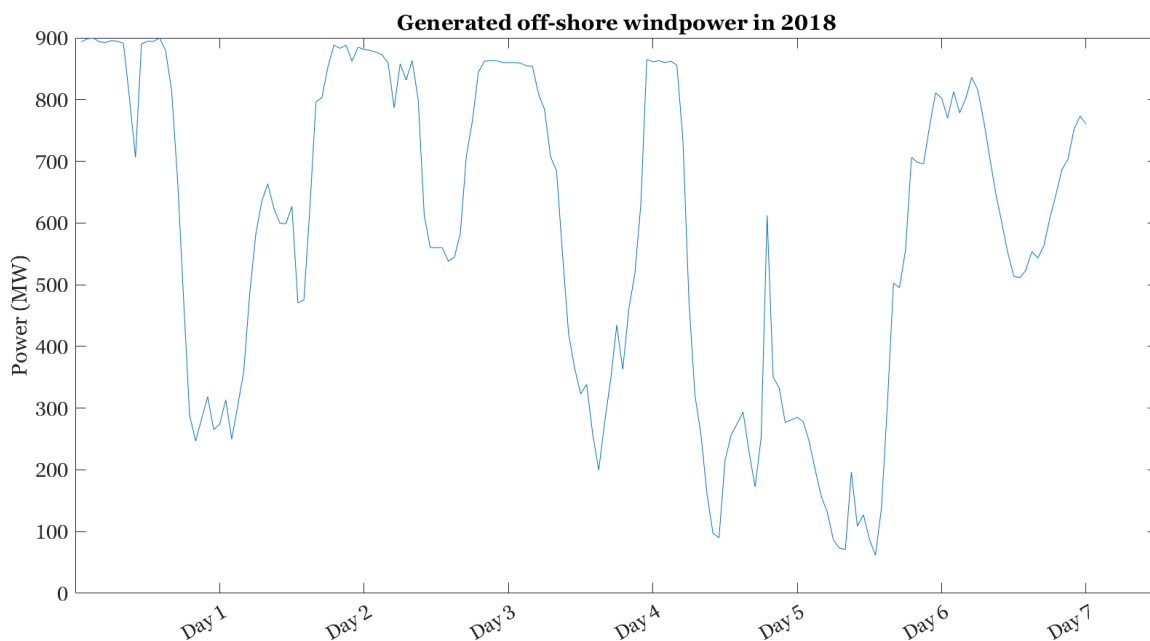


Figure 13: Hourly generated power from off shore wind plants in the Netherlands, week 1 (Open Power System Data, 2019)

Demand data

The electricity demand data is also created from 2018 data from Open Power System Data and scaled up to match the expected demand in 2030. The total demand in 2018 was 116.5 TWh, the demand in 2030 is expected to be 135 TWh according to Netbeheer Nederland (Netbeheer Nederland, n.a.). The demand is therefore scaled with a factor 1.158 to approach the total Dutch demand in 2030. As the 1 GW wind park will not generate enough electricity to provide for the whole of the Netherlands, the data is scaled down again to a percentage of the Dutch electricity consumption that matches the generation. This is done in such a way that the yearly demand is equal to yearly generation. The net mismatch at the end of the year is zero. This is illustrated by a graph of the cumulative mismatch, as given in Figure 14. This approach implies an average Dutch electricity use, including industry, households and all other electricity users. It also assumed demand patterns in 2030 are the same as in 2018. Electrification of industry may increase the share of relatively stable electricity consumption, but these developments are outside the scope of this report.

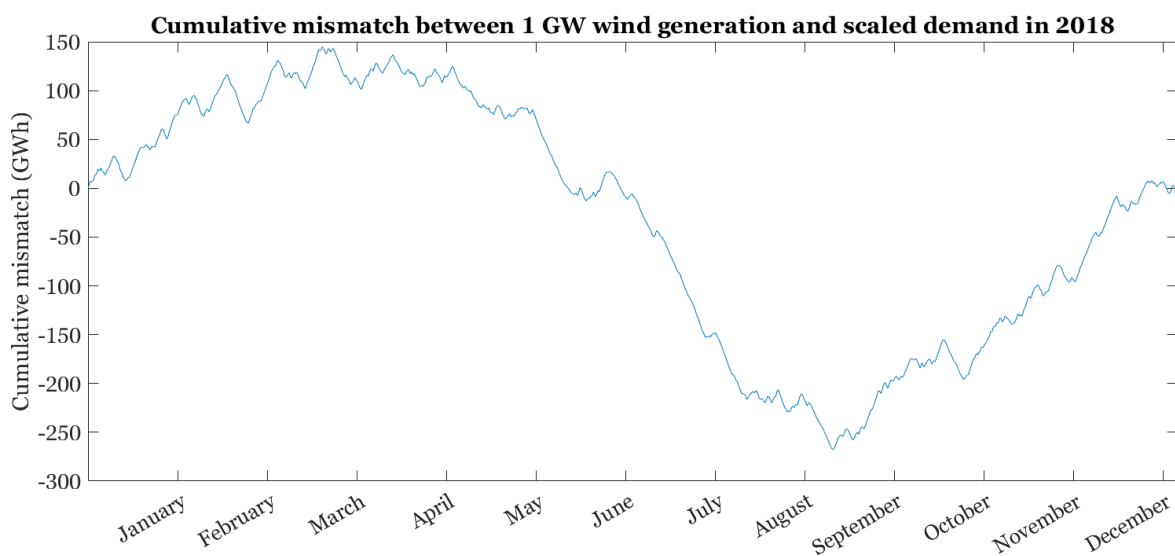


Figure 14: Cumulative mismatch between wind generation and electricity demand in MWh in the year 2018, generated from data from the Open Power Systems Data (Open Power System Data, 2019).

7.1.2. E-Converters and transport

For this report the storage facilities are assumed to be onshore, where the wind power is connected to the grid. The most obvious connection point for IJmuiden Ver is in the harbor of Rotterdam, but this point might be overloaded (TenneT TSO B.V., 2019). For that reason, TenneT is considering Geertruidenberg in Noord-Brabant as an alternative connection point further inland, along with several options in Zeeland (TenneT TSO B.V., 2019). The connection in Geertruidenberg is currently used by a coal fired power plant that will be closed by 2024. This replacement of coal energy by wind energy prevents large grid adaptations. To prevent unnecessary losses, wind energy is distributed to meet demand primarily, only electricity mismatches are converted in the storage facility. The regenerated power must be transported from the wind turbines to the distribution and storage facility and from there to the end users.

The power generated in the wind park can be transported back to shore as AC power or as DC power. The most important advantage of DC power transmission is the lower power loss compared to AC power. When electricity is transported over small distances the conversion losses of AC-DC and back are too high to compensate for the lower cable losses of transport. However, when the distance is long, or when conversion is unavoidable, power is better transported through DC cables. TenneT, the

Dutch grid operator, has decided to use AC power cables for wind parks up to 23 km of the coast but is planning to use DC cables for future wind parks that are 50 km off the coast (Wiebes, 2018). The conversion of AC to DC, back to AC, and voltage conversion is done by rectifiers, converters and transformers. The next step is distribution from the storage facility to the electricity consumer. During this distribution stage grid losses occur as well. Energy losses in the DC transportation and distribution grid are included in the model, exact values and their references are given in chapter 9.

7.1.3. Short term storage

Energy storage in hydrogen and hydrogen carriers is more suitable for long term energy storage. Wind power generation is intermittent on an hourly time scale too, meaning short term energy storage technologies is also necessary in a well-balanced electricity system. Hourly demand-generation mismatches can be compensated by energy storage in batteries. A model must therefore be constructed with a combination of batteries and PtXtP to create the most realistic scenario. The selected battery type is LTO (Lithium Titanate Oxide), based on the comparison done by IRENA. The selection was based on cost, cycle life, and efficiency. The overview as created by IRENA is given in Figure 15. The batteries will be sized to meet the average daily mismatch.

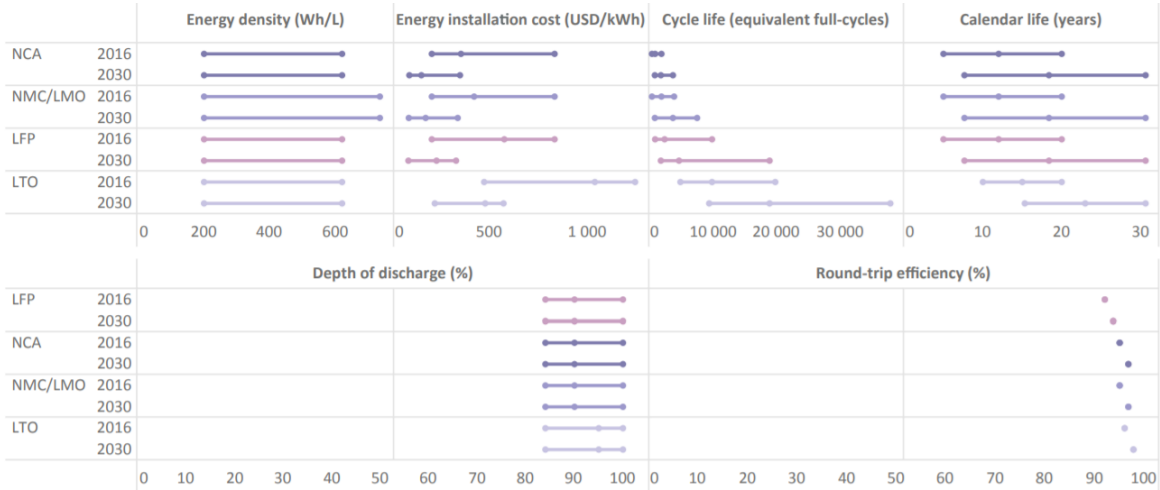


Figure 15: Properties of selected chemistries of lithium-ion battery electricity storage systems, 2016 and 2030 (IRENA, 2017)

7.2. Hydrogen technology selection

The three selected energy carriers are hydrogen, ammonia and methane. The first step for each is of these is the production of hydrogen. This subchapter will discuss the components for the power-to-hydrogen-to-power storage system and will select the technologies most likely to be dominant in 2030. The components include production, transport, storage and regeneration to energy.

7.2.1. Production from water

The formation of hydrogen from water through electrolysis is one of the oldest industrial processes and was discovered in 1800 by William Nicholson and Anthony Carlisle (Cox & Williamson, 1997). It was first industrialized by Dmitry Lachinov in 1888. Since then many different technologies have been developed. Cox and Williamson give a complete overview of hydrogen technologies (Cox & Williamson, 1997). The basic theory behind the electrolyser is simple: water is split into oxygen and hydrogen (H₂O becomes H₂ and O₂). The actual process is more complicated and includes many process steps, as demonstrated in Figure 16. This fluid schematic shows a Solid Polymer Electrolyte (SPE) electrolyser, which is a type of Polymer Electrolyte Membrane (PEM) electrolyser, as designed by Nuttall in 1977

(Nuttall, 1977). Since then several other types of electrolyzers have been developed. Schmidt et al. compare electrolyzers based on expert reviews and predict the future performances. They compare alkaline electrolysis cells (AEC), proton exchange membrane electrolysis cells (PEMEC) and solid oxide electrolysis cells (SOEC), their basic operating systems are shown in Figure 17 (Schmidt, et al., 2017).

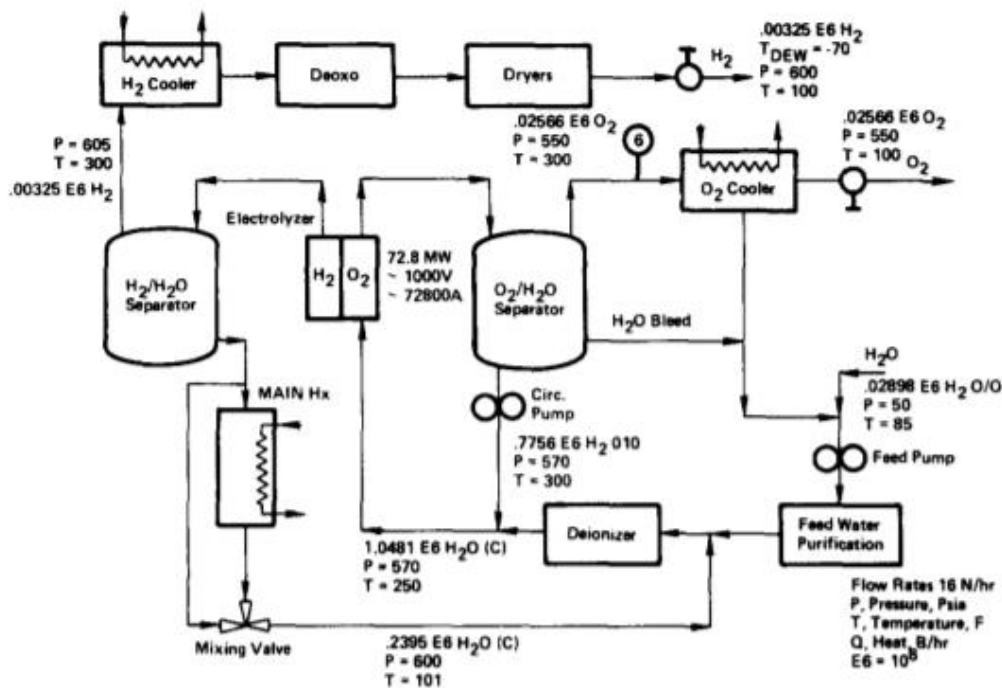


Figure 16: System fluid schematic as designed by Nuttall (Nuttall, 1977)

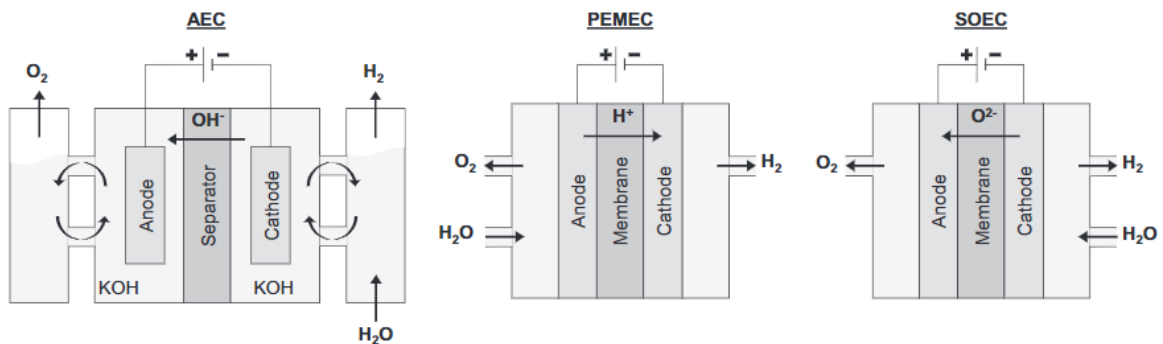


Figure 17: Schematic depiction of alkaline electrolysis (AEC), proton exchange membrane electrolysis (PEMEC) and solid oxide electrolysis cells (SOEC) (Schmidt, et al., 2017)

These three technologies are each on a different level of maturity. AEC is the oldest technology; it is fully developed and is the incumbent technology. PEMEC is currently scaling up and is already used commercially. SOEC is still being developed on lab scale. The majority of experts states PEMEC will be the dominant technology in 2030, and all experts involved in the study agree that AEC will be replaced almost completely.

An even newer technology to mention is the battolyser. The battolyser is a battery and electrolyser in one, as electricity is stored in a nickel-iron battery, which produces hydrogen when fully charged (Mulder, Weninger, Middelkoop, Ooms, & Schreuders, 2017). This combination seems to be ideal for energy storage purposes, as it combines efficient short term and long-term energy storage into one

technology. The first demonstration battolyser is to be built in 2019, predictions for 2030 are difficult to make, but given the high uncertainty and limited availability of information the battolyser will not be selected for this comparison (Mulder, Weninger, Middelkoop, Ooms, & Schreuders, 2017).

In this report the PEMEC is therefore selected as the technology to further investigate for use in simulation. An important feature of the PEMFC is that it can follow a varying load, if the fuel cell is kept on hot standby (Matute, Yusta, & Correias, 2019).

7.2.2. Transport and storage

The transport and storage of hydrogen were already touched upon in chapter 5.3. For large scale storage of hydrogen underground storage is necessary. Underground hydrogen storage already happens in three locations with salt caverns in the USA and the UK (Van Gessel, Breunese, Juez Larré, Huijskes, & Remmelts, 2018). Van Gessel et al. have created a comprehensive study on underground storage potential of the Netherlands, including identification of underground storage locations suitable for hydrogen storage. The nearest suitable salt caverns are in the province of South Holland, as was visible in Figure 11 on page 17. Hydrogen must be transported from the electrolyser to the salt cavern, this is done using pipelines and compressors (Wlodek, Laciak, Kurowska, & Wegrzyn, 2016).

7.2.3. Regeneration of electricity

The production of electricity from hydrogen can be done in several ways. The simplest way is to combust hydrogen in a hydrogen turbine. However, high temperatures are reached, and efficiencies are low (Kraftwerk Forschung, 1999). For that reason, hydrogen fuel cells are ultimately considered the better alternative. Comparisons of different fuel cell types have been done before by IEA and the US department of Energy (IEA, 2015), (Fuel cell technologies office, 2015). The comparison by IEA is given in Table 4. The selected technology was the PEM fuel cell, based on startup time, cost per hour of lifetime, efficiency and available sizes. Included in the comparison by the Fuel cell technologies office are the challenges with regards to these technologies. All fuel cells come with challenges, PEM fuel cells are sensitive to poisoning by fuel impurities and contain expensive catalysts but are still considered the best technology for this system (Fuel cell technologies office, 2015). Simulations in this study will be based on PEM fuel cells.

Table 4: Comparison of fuel cell types as done by IEA (IEA, 2015). FC stands for fuel cell, PEM stands for polymer electric membrane, SO stands for solid oxide, PA stands for phosphoric acid fuel cell, MC stands for molten carbonate fuel cell.

Application	Power or capacity	Efficiency *	Initial investment cost	Life time	Maturity
Alkaline FC	Up to 250 kW	~50% (HHV)	USD 200-700/kW	5 000-8 000 hours	Early market
PEMFC stationary	0.5-400 kW	32%-49% (HHV)	USD 3 000-4 000/kW	~60 000 hours	Early market
PEMFC mobile	80-100 kW	Up to 60% (HHV)	USD ~500/kW	<5 000 hours	Early market
SOFC	Up to 200 kW	50%-70% (HHV)	USD 3 000-4 000/kW	Up to 90 000 hours	Demonstration
PAFC	Up to 11 MW	30%-40% (HHV)	USD 4 000-5 000/kW	30 000-60 000 hours	Mature
MCFC	KW to several MW	More than 60% (HHV)	USD 4 000-6 000/kW	20 000-30 000 hours	Early market

* = Unless otherwise stated efficiencies are based on LHV.

** = All investment costs refer to the energy output.

7.3. Ammonia technology selection

After selection of the hydrogen system components the ammonia system can be designed. The predicted dominant technologies for 2030 will be selected for further modeling. In this case the system components are nitrogen capture, ammonia production, storage, transport and regeneration of electricity.

7.3.1. Nitrogen capture from air

Nitrogen makes up 78% of air, which means it is available everywhere for ammonia production, however, nitrogen does have to be separated from air. In order to do so three types of processes can be used; cryogenic air separation units (ASU), pressure swing absorption (PSA) and membrane generators. Cryogenic air separation units are the typical technology for large scale air separation. The liquefied nitrogen is stored in tanks and transported over the road (Gas Generation Team, 2013).

Alternatively, for onsite nitrogen generation two types of systems can be used; PSA and membrane generators, both are described by Ivanova and Lewis (Ivanova & Lewis, 2012). In PSA systems air is pumped into a nitrogen adsorbing substance (e.g. a carbon molecular sieve) under high pressure, O_2 and CO_2 are captured, while nitrogen passes through. Once the adsorbers are saturated the pressure is reduced, causing the adsorbers to release the oxygen. In reality the system contains more steps and is more complex, as is illustrated by Figure 18. Membrane generators use the difference in molecule size for generation of nitrogen. Air is pressurized and flows by membranes that allow O_2 , CO_2 and other impurities to pass. The impurities are taken out as permeate, the nitrogen passes on. Selection of the nitrogen system is done based on the required nitrogen purity and nitrogen flowrate. Ivanova and Lewis have created an image to easily select the best technology, the image is given in Figure 19. The selection was validated during conversation with Hans Vrijenhoef, ammonia expert and founder/director of Proton Ventures (Vrijenhoef, personal conversation, 2020).

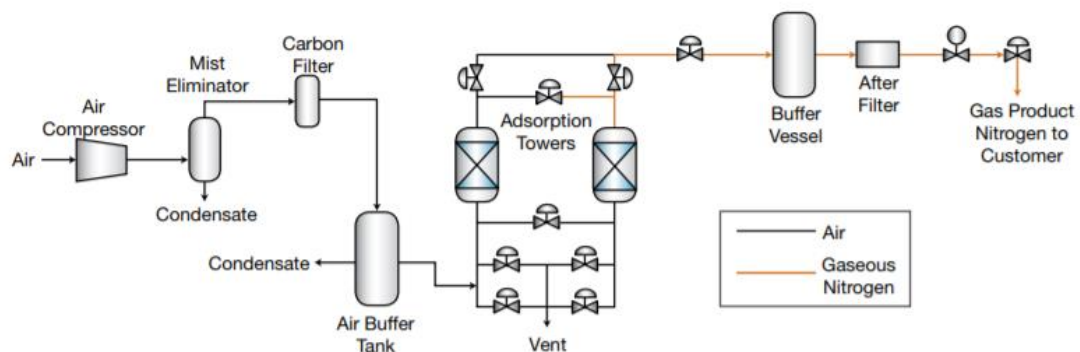


Figure 18: System steps in a PSA nitrogen separation plant (Ivanova & Lewis, 2012)

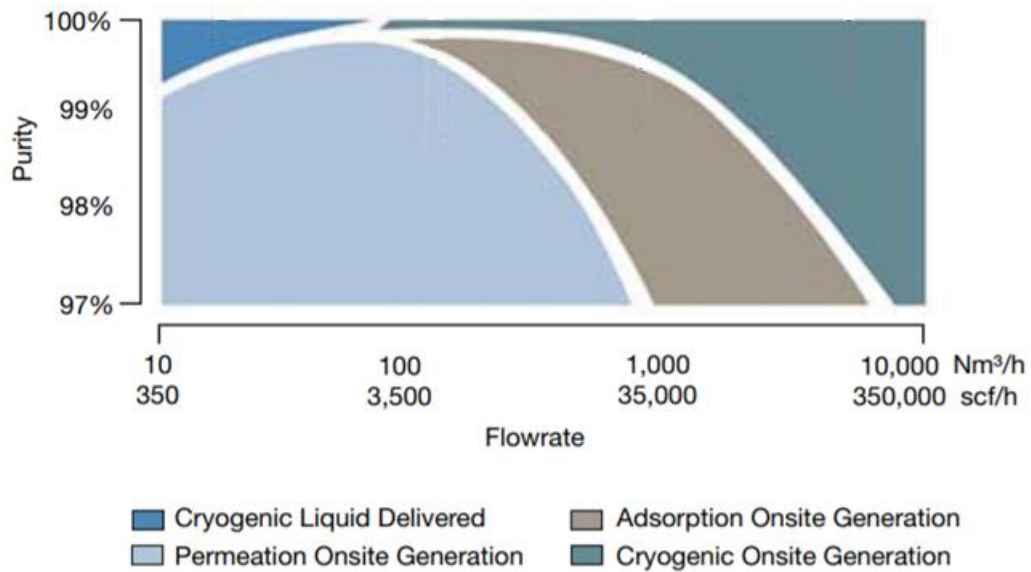


Figure 19: Tool for selection of the right nitrogen separation type based on purity and flowrate (Ivanova & Lewis, 2012)

7.3.2. Ammonia production

Ammonia production from nitrogen and hydrogen is typically done thermochemically in the Haber-Bosch process (Gür, 2018). This process was developed by Haber in 1913, which means the technology is incredibly mature. In the Haber-Bosch process hydrogen (H_2) and nitrogen (N_2) are heated, pressurized and led over several catalyst beds to form ammonia (NH_3). Different operators use different temperatures, pressures and catalysts. In general, the process takes place under 200-350 bar pressure at temperatures of 300-550 °C and uses an iron based catalyst (Klerke, Christensen, Nørskov, & Vegge, 2008). Performances of the system differ, but Klerke et al. have found that the production of one tonne of ammonia will cost 1.5 GJ to produce, while one tonne of ammonia contains 28.4 GJ. A schematic view of a Haber-Bosch plant is shown in

Figure 20. Nielsen et al have created a complete and comprehensive overview of ammonia processes and technologies, read their book for more information (Nielsen, et al., 1995). The Haber-Bosch process has until now mostly been used to produce artificial fertilizers, for VRES energy storage the system will have to follow a load, which might prove to be problematic. According to Hans Vrijenhoef, switching a Haber-Bosch reactor on and off causes material stresses, leading to a reduced lifetime. The alternative is presented by Cheema and Krewer. They have experimented with varying hydrogen inflow streams and found a way to vary the production of ammonia between 33-100% of maximum production rate (Cheema & Krewer, 2018).

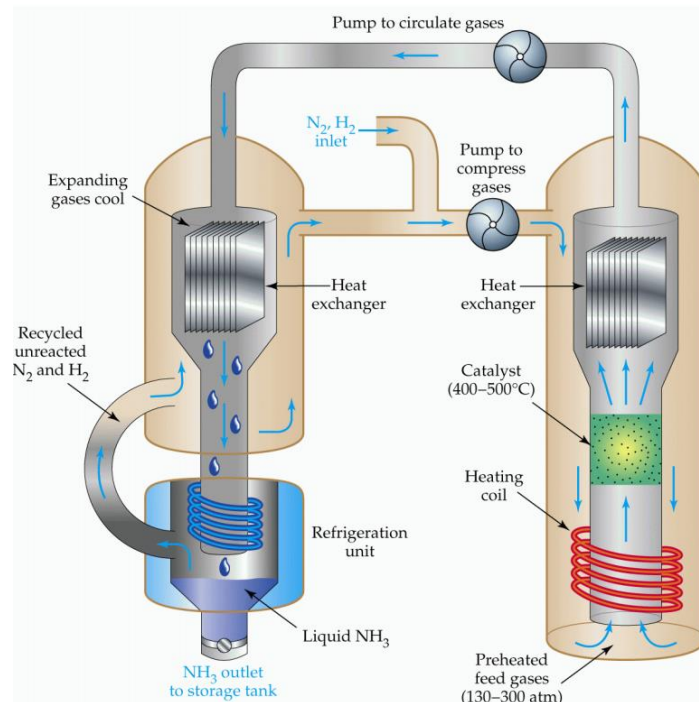


Figure 20: Schematic representation of a simplified Haber-Bosch system (Goetheer, 2018)

A different, more recently developed route for ammonia synthesis is the electrochemical route. Ammonia can be formed from nitrogen and hydrogen electrochemically, or ammonia can be produced directly from water and nitrogen, skipping the hydrogen production step. In this direct process nitrogen (N_2) is reacted with purified water (H_2O) to produce ammonia (NH_3). Both processes are schematically depicted in Figure 21.

Even newer is the electrochemical technology that produces ammonia directly from air and water. This technology was developed by Lan and Tao and is currently still being tested on lab scale (Lan & Tao, 2013). The direct production of ammonia would bypass nitrogen capture and hydrogen production completely. This technology therefore shows a lot of advantages, should it develop and reach commercial scales.

While the newer technologies are developing fast and have some very relevant advantages compared to the Haber-Bosch process, they are not expected to have reached large scales commercially before 2030. For that reason, the Haber-Bosch process is selected for further modelling.

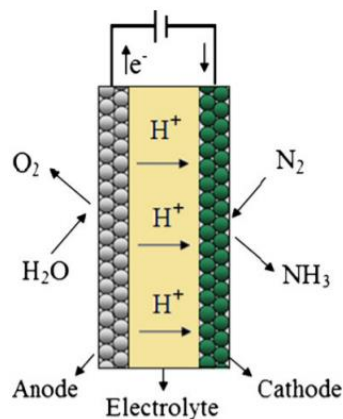


Figure 21: Schematic representation of electrochemical ammonia production (Amar, Lan, Petit, & Tao, 2011)

7.3.3. Ammonia storage and transport

One of the major advantages of ammonia over hydrogen is that it is easily liquefied, which drastically increases the volumetric energy density. Ammonia has a condensation temperature of $-33\text{ }^{\circ}\text{C}$ at atmospheric pressure and a condensation pressure of 3.32 bar at room temperature ($20\text{ }^{\circ}\text{C}$). It is therefore typically stored as a liquid. Liquefaction can be achieved through cooling, pressurizing, or a combination of the two. Nielsen et al. distinguish between these three types of storage by the maximum capacity they can hold. They state pressurized storage tanks (no cooling) have a maximum capacity of 270 tonne ammonia, refrigerated and pressurized spheres have a maximum capacity of 450-2750 tonnes of ammonia and refrigerated storage tanks (1 atm) have a maximum capacity of 45000 tonnes of ammonia (Nielsen, et al., 1995). Given the large amount of energy that must be stored in case of seasonal storage applications, the assumed technology in this report is refrigerated tanks. These tanks are designed specifically for ammonia storage and contain a feedback loop to keep boiled-off ammonia in the system (Morgan, Manwell, & MacGowan, 2014).

Transportation of liquid ammonia is also a very mature technology. Nielsen et al. report ammonia transportation in tanks, over road, rail and water. Transportation through pipelines is a more recent development but is already done commercially over long distances in the US and in Russia (ISPT, 2017). The type of transport is dependent of distance and flow.

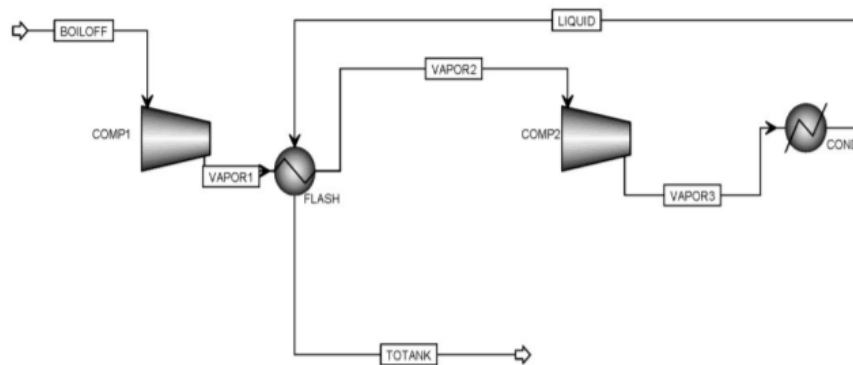


Figure 22: Schematic illustration of a simplified ammonia storage loop (Morgan, Manwell, & MacGowan, 2014)

7.3.4. Regeneration

Regeneration can be done in three ways; by cracking ammonia back to hydrogen and nitrogen, by direct ammonia fuel cells and by ammonia combustion. Cracking hydrogen back to nitrogen and hydrogen is done in an ammonia cracker, using catalysts at high temperatures (ISPT, 2017). After cracking, the hydrogen is fed into a hydrogen fuel cell. This double step increases the cost and complexity of the PtXtP system, where possible it should be replaced with a direct ammonia-to-power technology.

Ammonia turbines are being developed but are currently not sold off-the-shelf (Kobayashi, Hayakawa, Kunkuma, Somarathne, & Okafor, 2019). Developments for ammonia combustion are moving fast, and according to Hans Vrijenhoef ammonia turbines are ready for production (Hans Vrijenhoef, personal conversation, 2019). However, challenges these turbines face are the slow combustion of ammonia and the high combustion temperatures, causing formation of NO_x .

The second direct ammonia-to-power conversion option is a direct ammonia fuel cell (DAFC). These ammonia fuel cells are SOFC's, they operate at temperatures between $650\text{-}1000\text{ }^{\circ}\text{C}$ and use catalysts (Patel & Petri, 2006). These fuel cells show great potential, both in efficiency and cost, but have to be

kept warm for quick response time. For further modeling these direct ammonia SOFC's are selected. This selection was based on the availability of data and reduction of cost and complexity of the system.

7.4. Methane technology selection

The power-to-methane-to-power system, like that of ammonia and hydrogen, contains many process steps, each of which have several technologies showing potential. The steps are CO₂ capture, methane production, storage, transport and regeneration of electricity. The technologies are selected based on their predicted performance in 2030.

7.4.1. CO₂ capture

Methane is produced from CO₂ and hydrogen, which means CO₂ must be won first. CO₂ can come from several sources: air, seawater or flue gasses. The easiest source is flue gasses, due to high concentrations of CO₂. However, flue gasses come from the combustion of fossil fuels, meaning the CO₂ still has a fossil source. Unless the CO₂ that is released during regeneration is captured and reused this means the exhaust of fossil CO₂ is postponed, but not prevented and the system is still fossil dependent. In order to store energy in a fully fossil-free system, CO₂ must be captured from seawater or air.

The direct air capture of CO₂ is developing fast, and several types of CO₂ capture technology are available already. CO₂ can be taken out air using chemical separation, cryogenic separation or membrane separation (ICEF, 2018). Challenging is the low concentration of CO₂ in air (0.4%) which means huge streams of air must be filtered to gather a significant volume of CO₂. This results in energy consumption (both electrical and heat) and high costs (ICEF, 2018).

New technologies are created to extract CO₂ from seawater (Eisaman, et al., 2012). However, in seawater the concentration of CO₂ is even lower (90 mg/kg), and no demonstration plants have been developed yet (Floor Anthoni, 2010). For this reason, CO₂ capture from air is selected as the dominant technology.

7.4.2. Methane production

Methane production from hydrogen and CO₂ can be done thermochemically and electrochemically. The thermochemical way is the oldest and is called the Sabatier reaction. The Sabatier reaction takes place at high temperatures and under influence of catalysts (Van Leeuwen, 2018). The exact temperatures, pressures and catalysts differ per operator. Variability of the process is difficult, but can be achieved by reducing the share of hydrogen in the inflow stream of the reactor (Gorre, Ortloff, & Van Leeuwen, 2019).

Electrochemical production of methane is easier to vary, but current electrochemical processes are still limited in their flowrate and purity of output (Manthiram, Beberwyck, & Alivisatos, 2014). In addition, the process is expensive, and no large-scale demonstration plants exist yet. For these reasons the Sabatier reactor was selected to be the technology to simulate.

7.4.3. Storage and transport

Methane is the main component of natural gas, as is used in the Dutch gas grid. Problems with earthquakes due to gas drilling in Groningen (North of the Netherlands) have led to the decision that the Netherlands should drastically reduce the use of natural gas, new houses are built without a gas grid connection, and existing houses are taken off the gas grid gradually (Rijksoverheid, 2019). By 2022, gas extraction in Groningen should be stopped completely (Rijksoverheid, 2018).

This reduction in gas production and usage creates unused capacity in the gas grid, which can be used for storage and distribution of green methane (Gür, 2018). In order to do so, methane must be transported to a gas injection point, which is done using pipelines. Before introduction to the natural gas grid, methane must be checked on quality and compressed in a pre-injection station (Van Leeuwen, 2018). The nearest feed-in station is in 's Hertogenbosch, in the South of the Netherlands, as can be seen in Figure 23.

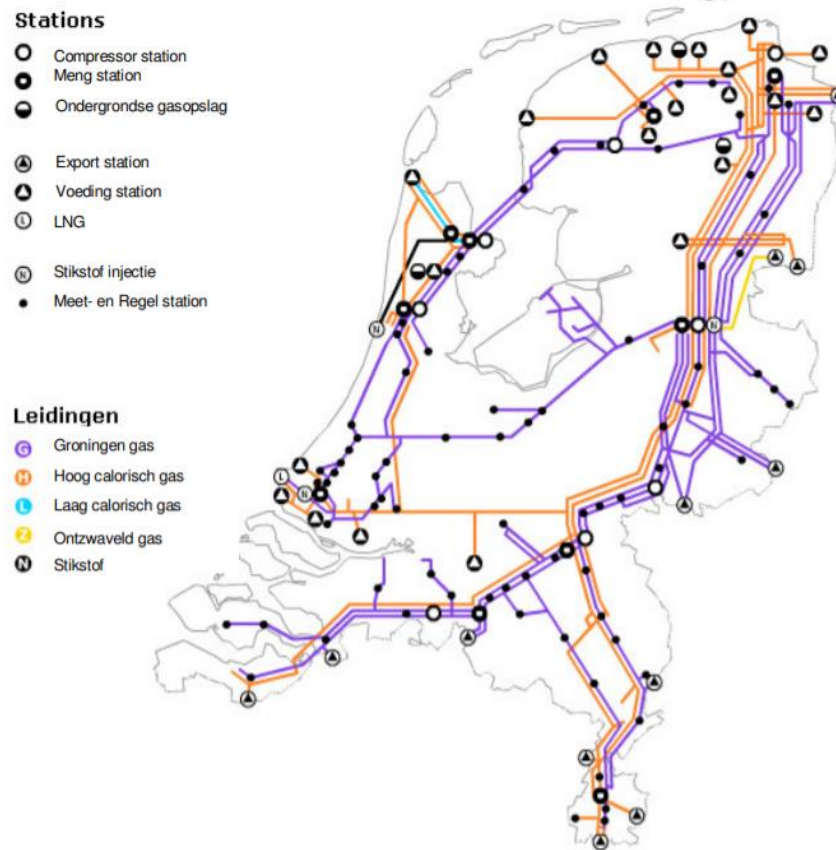


Figure 23: Map of the natural gas grid as owned by Gasunie, the feed-in stations are marked by a black circle with a white triangle inside (Gielisse, Dröge, & Kuik, 2018).

7.4.4. Regeneration

As for methane storage and transport, the current natural gas system can also be used for electricity regeneration of methane. Natural gas is combusted in gas fired turbines to generate steam, which is used to drive a generator. These gas turbines are already connected to the grid and are owned by Gasunie. The generation of electricity from natural gas will be reduced, which means no additional investment has to be done for regeneration of electricity from methane, as the gas turbines can be repurposed (Gasunie, 2018). The costs for regeneration are therefore limited to the operational costs of the natural gas generator. Use of the existing grid is therefore a big advantage of the Power-to-Methane-to-Power system.

7.5. Conclusion

In this chapter technologies were selected for each of the system components. This literature research also uncovered potential bottlenecks for these technologies. The bottlenecks are summarized in the table below. The selected technologies will be simulated in a series of models to compare their theoretical performances in a VRES system. The model is described in the next chapter.

8. The model

As stated before, PtXtP system components are already in a demonstration phase or beyond. The innovation is in the application as an energy storage system. The purpose of the model is to simulate all system components in a VRES use case to identify bottlenecks and to compare system performances and cost.

8.1. Assumptions

The model is created to simulate a VRES grid and different PtXtP systems over the course of one year. The model is created in Simulink, with a timestep of one hour. This step time was selected because it is small enough for simulation of large-scale energy storage, while reducing the runtime of the model. As such, no balancing is done for mismatches over periods shorter than one hour. All system components are modelled as black boxes. The entire PtXtP system is considered a closed system. As stated in the methodology, electricity goes in and comes out, intermediate exchanges of electricity or hydrogen between the system components are done without financial compensation between component owners. This also implies the produced energy carriers are always converted back to energy, never sold.

8.2. Outputs

As stated before, the purpose of the model is to evaluate the PtXtP performance and cost. The performance of the system is measured as the grid exchange that can be prevented by use of the storage system. The system is connected to a wind park and electricity demand that are exactly equal after one year, which means any losses in the energy system, as well as system under sizing result in grid exchange. The second output is the cost of the system on a yearly basis, using the annualized CAPEX, fixed OPEX and variable OPEX. To evaluate the system components individually the cost and energy use per system component are compared, so the output is given per system component as well.

8.3. Inputs

The PtXtP system components are modelled as black boxes. Each system component performs a conversion step and has an impact on the system efficiency, cost, grid interaction and curtailment. The impact is determined by the main characteristics of the system component, which are CAPEX, OPEX, conversion efficiency, electricity use, heat use and ramp time. These system properties are gathered from literature, chapter 9 gives the input values for each component.

In order to accurately evaluate the storage performance a somewhat realistic use case must be simulated. The first inputs are therefore the Dutch demand and power generation from a 1 GW wind park.

8.4. Model structure

The basic structure of the model is relatively simple, as is shown in Figure 24. The demand and generation are unbalanced, creating a mismatch. This mismatch is primarily handled by the production of X in case of an electricity surplus, and by regeneration of power from X in case of an electricity deficit. Exceptions occur when no storage capacity is available, or when the regeneration or X production power capacity are exceeded. In case of an electricity surplus while the storage capacity is full, the wind power must be curtailed. In case of an electricity deficit, when the storage capacity is

empty, the demand will have to be met by other parties in the electricity grid. This is the simplest illustration of the model structure; the more detailed structure will be given after more information about the details of the system are determined.

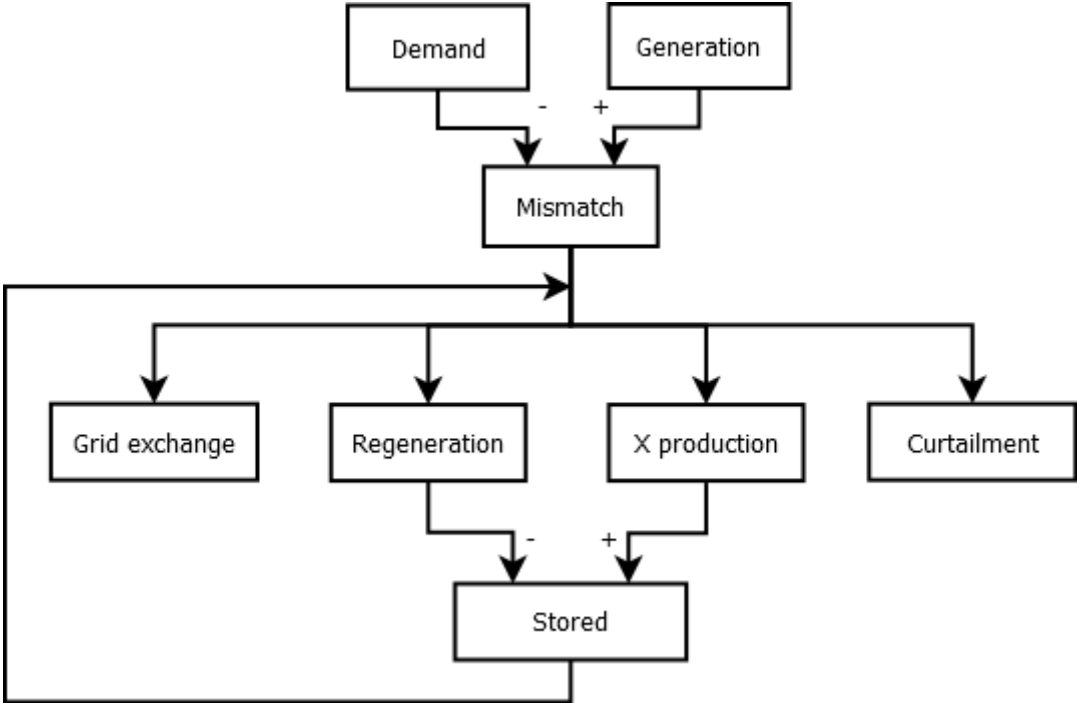


Figure 24: Simplified schematic of the intended model structure. Each arrow represents a process step.

8.5. Limitations

The model is a strongly simplified representation of the storage system. As such the system was optimized specifically to meet the given demand, it was not sized for energy security. In addition, no heat integration was done to maintain a low level of complexity. Other limitations that follow from assumptions are the elimination of mismatches within the hour, the assumption that the entire system is owned by one party, eliminating intermediate transactions, and not including the option of fuel or feedstock production (PtX). A limitation to the use of the model in this thesis is the running time of one year (8760 hours). The model is defined as such that after one year it is back at its initial states, so that no windup occurs and all energy in and out of the system is accounted for.

9. Overview of model input values

In order to simulate the performance of the PtXtP systems data on the performance of different system components was gathered. The cost, efficiency and energy use of each system component was found in as many sources as possible, in order to create the model as accurately as possible. Extensive literature research and interviews have resulted in a current and comprehensive overview of knowledge regarding PtXtP systems. The sources of the information are given in the footnotes. The result is the set of assumptions and references as presented in the tables below.

9.1. General assumptions

Dollar/Euro conversion	€1.00=\$1.11
Energy content of hydrogen	120 MJ/kg (LHV), 0.0333 MWh/kg
Energy content of methane	50.0 MJ/kg (LHV), 0.0139 MWh/kg
Energy content of ammonia	18.6 MJ/kg (LHV), 0.00517 MWh/kg
Fixed OPEX ¹ as function of CAPEX (unless otherwise indicated)	4%
Interest rate	5%

¹Fixed OPEX is defined as the yearly operational cost, like parcel rent and labor cost.

9.2. Electricity input

Generation	Hourly wind data 2018	1 GW ¹
Demand	Hourly demand data 2018	2.3335% of Dutch demand ²
Electricity	DC cable	0.985 cables ³ , 0.90 for rectifier, transformers, converters ⁴
	AC distribution grid	0.959 ⁵

¹ ENTSO-E hourly wind generation data for 2018 was used. The installed capacity of 957 MW was scaled up to 1 GW by simple multiplication. (Open Power System Data, 2019)

² Based on data from the ENTSO-E power statistics Platform. The total demand is scaled down to match the wind energy production of 2018 and achieve a net yearly mismatch of 0. (Open Power System Data, 2019)

³ Based on 800 kV cables for 50km, assuming energy losses of 3% per 100 km (IEA ETSAP, 2014)

⁴ Estimation based on 3 or 4 conversion steps of 97% efficiency (Jung, Lempidis, Marklein, & Steffen, 2016), (Kyriaki-Nefeli & Demoulias, 2013)

⁵ Scaled up from 2018 values. In 2018 5 TWh of losses occurred for an energy demand of 116.5 TWh. This relates to 5.8 TWh for the predicted 135 TWh in 2030, or 95.9% efficiency. In 2018, 5 TWh of energy was lost during transmission and distribution of 116.5 TWh (Tennet, 2019). These losses are assumed to correlate linearly with the increase in energy consumption, which means for distribution of 135 TWh the losses are estimated to be 5.8 TWh, or 4.1%. This translates to a multiplication of the energy consumption in the model by a factor of 1.043 to compensate for grid losses.

9.3. Carriers

This system component aims to map the parameters of the storage system feedstock. For production of hydrogen purified water is required. For production of ammonia nitrogen is required and for production of methane CO₂ is required as input. While the capture of CO₂ and nitrogen is usually done batch-wise, nitrogen capture, CO₂ capture and water purification are included in this model only in the form of cost and electricity use per kg. This implies an assumption of unlimited supply and unlimited flow. In reality the need for a CO₂ or nitrogen buffer may arise. The impact of the buffer is already included in the price and energy use per kg and is not investigated dynamically in this thesis.

	Carbon dioxide	Nitrogen	Demi-water
Technology type	Direct air capture (DAC)	PSA ⁶	Membrane filtration
Cost (€/kg)	0.0427-0.27 0.11 ^{7,8,9}	0.010-0.225 0.015 ^{10,11,12,14}	0.000976-0.00171 0.0014 ¹³
Electricity use (kWh/kg)	0.194-0.45 0.37 ⁷	0.282-0.468 0.375 ¹⁴	0.0005 ¹³
Heat use (kWh/kg)	0-2.25 1.24 ¹⁵	0 ¹⁴	0 ¹³
TRL	7	9+	9+
Nr of sources	3	10+	1

⁶ Based on system size estimations and design rules (Ivanova & Lewis, 2012), as well as flexibility of the system.

⁷ Based on the weighted average of four scenario's in a detailed engineering and cost analysis for a 1 Mt-CO₂/year direct air capture plant (Keith, Holmes, St. Angelo, & Heidel, 2018). Cost of 0.056 €/kg does not include the costs for energy.

⁸ Based on predictions for the Global thermostat plant described in the ICEF roadmap (ICEF, 2018). The value of 0.05 €/kg is a rough estimation, possibly based on near zero energy prices.

⁹ Cost of 180-300 \$/ton CO₂, electricity use of 1.3-1.8 GJ/ton CO₂, and heat use of 5.3-8.1 GJ/ton CO₂. Results in 0.16-0.27 €/kg, 0.3611-0.5 kWh_e/kg and 1.47-2.25 kWh/kg heat (Realmonte, et al., 2019).

¹⁰ Based on analysis of nitrogen purchase by purity gas. Costs include energy, delivery, vessels and profit. The given values are 0.17-1.89 \$/m³, (standard conditions), which is equal to 0.225-2.25 €/kg (Purity gas, 2017). The cost for energy is assumed to be 90% of the total price, leaving 10% of the price for system, maintenance etc. (Flowe nitrogen systems, n.a.).

¹¹ Based on purchase of liquid nitrogen, 0.216 €/kg, this does include energy and transportation cost, but does not include cost of on-site tanks, maintenance or labor (Gaspur gas tech CO. , 2019). The cost for energy is assumed to be 90% of the total price, leaving 10% of the price for system, maintenance etc. (Flowe nitrogen systems, n.a.).

¹² Based on rough estimations done by Hans Vrijenhoef. Estimated Capex of €10,000,000 for 240 ton/day N₂ production, 4% Opex per year, 20 years lifetime leads to 0.01 €/kg.

¹³ Average of two technologies, one ion exchange system and one membrane filtration system. The energy consumption of the ion exchange system (Van den Vijver, 2007).

¹⁴ Based on 99.5-99.99% purity. 56-93 kW required for 100 SCFM N₂ flow, which is equal to 0.282-0.468 kWh/kg (Flowe nitrogen systems, n.a.).

¹⁵ Selected scenario is high in electricity use but does not use heat. Other scenarios use 0.077 kWh electric per kg but consume 1.458 kWh of natural gas. (Keith, Holmes, St. Angelo, & Heidel, 2018)

9.4. Generation

	Hydrogen	Ammonia	Methane
Technology type	PEM electrolyser	Haber Bosch reactor	Sabatier reactor
CAPEX+ fixed OPEX ¹ (€/((kg _{out} /h)/year))	4,400-7,620 6,000 ^{16,17,18,19,20}	282-840 550 ^{21,22,23,24}	216-488 290 ^{25,26,27}
Chemical efficiency/ selectivity (%)	100 ^{16,18,19}	100 ²⁸	95-100 96 ^{29,30}
Electricity use (kWh/kg _{output})	6-13.3 ^{16,18,19} 10 +2% standby ^{31,32}	1.3-3.5 ²² 1.3 ³³ , 2% standby ³⁴	0.75-0.8 ^{32,25} 0.78 +4.7% standby ³²
Heat use (MJ/kg _{output})	0	0.1 ²²	0
Ramp time (h)	<1	33-100% in <1 ³⁵	40-100% in <1 ³⁶
TRL	7	9	8
Nr of cases	10+	7	7

¹Fixed OPEX is defined as the yearly operational cost, like parcel rent and labor cost. CAPEX refers to the annualized CAPEX, which is calculated as follows: $Annualized\ CAPEX = CAPEX \cdot \frac{i}{1 - \frac{1}{(1+i)^T}}$. Where i is the interest rate, and T is lifetime in years.

¹⁶ Annualized CAPEX of €4.76 per GJ yearly output, equal to 150,110 €/MW/year. Efficiency of 70% (446 kWh/GJ) (ISPT, 2019).

¹⁷ Based on CAPEX for a 100 MW system. 160 M€ for 100 MW system, 2% yearly OPEX, assumed 20 years lifetime, leads to 160,000 €/MW/year. (ISPT, 2019)

¹⁸ Interpolation of data: 932 €/kW in 2025, 334 €/kW in 2050. 882 €/kW in 2030. Fixed OPEX of 4%. Lifetime of 30 years. 92,610 €/MW/year. (HyUnder, 2014)

¹⁹ Based on data from IEA, Table 15, 800,000 \$/MW with a lifetime of 75,000 hours, 5% yearly OPEX. Assumed on-time of 40%, leads to a lifetime of 20 years, and 100,000 €/MW/year. Efficiency of 70% (IEA, 2015).

²⁰ 1 MW with an efficiency of 70% is equal to 21 kg/h, all prices in €/MW/year are converted to €/(kg/h)/year by division with 21. Average CAPEX is 126,000 €/MW/year or 6,000 €/(kg_{H2}/h)/year.

²¹ Weighted average. The prices that included the entire system were multiplied with a factor 0.6, to find the cost of only the ammonia production component.

²² Current cost: Annualized CAPEX 0.86 M€ for 20,000 ton per year, lifetime of 20 years. CAPEX is 381 €/(kg_{NH3}/h)/year. OPEX is 87 €/(kg NH₃/h)/year. A total of 470 €/(kg_{NH3}/h)/year Includes N₂ capture and NH₃ cracker. Electricity use of 1.3 kWh/kg for small scale, 3.5 kWh/kg and other energy use of 0.1 MJ/kg (ISPT, 2019).

²³ Based on 5 currently realized projects in the USA. (700-2300, average of 1,510 \$/(ton/year)) 568-1400 €/(kg_{NH3}/hr)/year, the weighted average is at 1050 €/(kg_{NH3}/h)/year. Includes N₂ capture. (Vrijenhoef, 2017)

²⁴ Based on conversations with Hans Vrijenhoef. Estimation of 50 M€ for a HB reactor with 300 ton/day output, lifetime of 20 years. With scale up in the future 500,000 \$/MW is possible according to Hans Vrijenhoef. CAPEX of 186-320 €/(kg/h)/year, OPEX of 116-200 €/(kg/h)/year. Total of 300-520 €/(kg/h)/year

²⁵ 979 kton/year at 315 M€, lifetime of 20 years, equal to 225 €/(kg/h)/year. Fixed OPEX of 4%, adds 112 €/(kg/h)/year. Total of 340 €/(kg/h)/year (ISPT, 2019). Energy use of 15.56 kWh/GJ of output product, is equal to 0.778 kWh/kg CH₄.

²⁶ Based on three selected values for larger scale methanation plants: 110 €/kW_{ch4}, 130 €/kW_{ch4}, 250 €/kW_{ch4}, 20 years lifetime. The average is 180 €/(kg/h)/year. The fixed OPEX is assumed to be 4% of capex, or 90 €/(kg/h)/year. Final value is 270 €/(kg/h)/year, a range of 216-488. (Van Leeuwen, 2018)

²⁷ This value is a weighted average. These values are current prices, the price in 2030 might be lower, if economies of scale arise.

²⁸ Chemical efficiency. No H₂ is lost in the process, dissolved hydrogen and nitrogen in ammonia out flow are recirculated according to Hans Vrijenhoef.

²⁹ Based on the 96% purity that is guaranteed by ETOGAS (Benjaminsson, Benjaminsson, & Boogh Rudberg, 2013).

³⁰ Selectivity of 95-100% for methane. CO₂ conversion is between 72 and 100%, but this can be recycled (Junaedi, et al., 2010).

³¹ Electrolyser's operating pressure and temperature are maintained for quick response, consuming 2% of maximum power (Matute, Yusta, & Correias, 2019).

³² Electrolyser of 1000 kW uses 5-39 kW_e at hot standby, which is equal to 2.45%. The methanation unit for a 1000kW electrolyser uses 47 kW on stand-by (Frank, Ruoss, Gorre, & Friedl, 2018).

³³ 1.3 kWh/kg was selected because this value does not include the capture of N₂ and therefore prevents double counting.

³⁴ The Haber-Bosch reactor functions at high temperatures and pressures (Leighty, 2008), energy required to maintain the pressure and temperature are not available in literature. To create a fair comparison, the standby electricity use was assumed to be 2%, same as the electrolyzers.

³⁵ Maximum variation range of hydrogen inflow for same process efficiency (Cheema & Krewer, 2018).

³⁶ Reducing the inflow stream 40% of the maximum H₂ results in similar efficiencies, but lower methane production (Gorre, Ortloff, & Van Leeuwen, 2019)

9.5. Storage system

	Battery	Hydrogen²		Ammonia	Methane
Technology type	Lithium-ion: LTO	Salt cavern (200 bar)	Tank	Cooled tank	Injection station
Use limitations	DoD: 92.5%	Max Power: 10 bar/day ⁴³			
CAPEX+ fixed OPEX ¹ (€/(MWh _{cap.})/year)	9,000-39,900 21,900 ^{37,38}	0.56-18,5 5.3 ^{39,40,41,42,43,44} + 955-1,390 1170 ^{45,46} €/((kg _{H2} /h)/year)	4-68 9.3 ^{47,48,49} + 1170 ^{45,46} €/((kg _{H2} /h)/year)	0.2331-68 23.7 ^{50,51,52,53,54,55}	4,700-58,500 9,800 €/year ⁵⁶

³⁷ LTO batteries (long lifetime, high efficiency and competing cost). CAPEX of 200-550 \$/kWh, weighted average of 450 \$/kWh, 20.000 cycles. (IRENA, 2017). Given roundtrip efficiency is 97%.

³⁸ This study bundles 19 studies and gives an estimation of 124-338 \$/kWh for 2030, (weighted average of 207\$/kWh). Lifetime of 15 years, 1 cycle per day, this assumption is rough and rather low (Cole & Frazier, 2019). Given roundtrip efficiency is 85%.

³⁹ 470 €/kg_{H2}, 120 MJ/kg= 14,100 €/MWh, lifetime of 30 years, 4% OPEX results in 1480 €/MWh/year (Larscheid, Lück, & Moser, 2018)

⁴⁰ 50 €/m³, 1 m³ contains 8.5 kg (Van Leeuwen, 2018). The result is 176.5 €/MWh, 4% OPEX, 30 year lifetime equals 18.5 €/MWh/year. (Londe, 2018)

⁴¹ Three values: 0.3 \$/kWh, 9€/m³, 0.02 \$/kWh, average at 1.2 €/kg. Equal to 36 €/MWh. 2% OPEX, 30 year lifetime. 3 €/MWh/year. (Van Leeuwen, 2018)

⁴² For caverns, cushion gas, compressors and pipeline: 1.60 \$/kg. 30 years lifetime, 4% OPEX. Results in 4.52 €/MWh/year. (Kobos, Klise, Borns, & Klise, 2011)

⁴³ €1,111,111 for 213,333 MWh. 30 year lifetime, 4% OPEX. Results in 0.57 €/MWh/year. Does not include any installations. (ISPT, 2019)

⁴⁴ Weighted average, the value by Larscheid, Lück and Moser is not included because it is an outlier.

⁴⁵ Compressor for 300 €/kW, dryer for 6€/kW + 4% opex, lifetime of 15 years. Total of 1390 €/((kg/h)/year). (Michalski, et al., 2017)

⁴⁶ 400 kg/h compression (60 to 200 Bar) costs 3.185 M€. Lifetime of 20 years, 4% OPEX. 955 €/((kg_{H2}/h)/year). 1.1 kWh/kg. (Tractebel, Engie and Hincio, 2017)

⁴⁷ Average of 11 studies, ranging between 23 and 102 €/m³. 53 €/m³, 200 bar, 20 years lifetime, OPEX of 1.5%. This results in 9.3 €/MWh/year (Van Leeuwen, 2018).

⁴⁸ CAPEX of 13-29 \$/kg for H₂ storage at 350 bar. Lifetime of 20 years, 4% OPEX. Results in a range of 42.1-93.9, average of 68 €/MWh/year (James, Houchins, Huya-Kouadio, & DeSantis, 2016).

⁴⁹ The cost by Van Leeuwen were selected because of the lower pressure and number of sources.

⁵⁰ 50 M€ for 50,000 m³, 609 kg/m³, 30 year lifetime, 2.5% OPEX. Total of 68.6 €/MWh/year. 10 kWh/ton electricity use. Excluding infrastructure. (ISPT, 2019)

⁵¹ 25M\$ for 60 short kton tank, 30 year lifetime, extremely low OPEX of 30,000 \$/year. Results in 6.9€/MWh/year. (Leighty, Costs of Delivered Energy from Large-scale, Diverse, Stranded, Renewable resources. Transmitted and Firmed as Electricity, Gaseous hydrogen and ammonia, 2006).

⁵² \$100,000 for 30,000-gal storage tank underground. 609 kg/m³, 30 years lifetime, 4% OPEX. Results in 0.2331 €/MWh/year (Wittrig, 2018).

⁵³ Based on estimations by Hans Vrijenhoef. 25 M€ for 30 kton NH₃. 30 years lifetime, 4% OPEX. Results in 17 €/MWh/year.

⁵⁴ 5\$/gallon for large scale. Or, 15M\$ for 30 kton NH₃. 609 kg/m³, 30 years lifetime, 4% OPEX. Results in 39 €/MWh/year or 9.2 €/MWh/year. (Leighty, Energy Storage with Anhydrous Ammonia - Comparison with other energy storage, 2008).

⁵⁵ Average cost for tank is 23.5 €/MWh/year. The cost for the ammonia condenser is \$92,700 for 9 kton, 30 years lifetime, 4% OPEX, results in 0.2 €/MWh/year (Morgan, Techno-Economic Feasibility Study of Ammonia plants powered by offshore wind, 2013).

⁵⁶ 75,000 €, 30 years lifetime, OPEX of 4,900 €/year, results in a total of 9,800 €/year. Includes quality check and injection into distribution grid. (Van Leeuwen, 2018).

Efficiency ³ (%)	85-97 91% ^{37,38}	98 %/year ⁵⁷	100%	100%/year ⁵⁸	100%
Electricity use (kWh/kg)	n.a.	1.06 ^{59, 46}	1.06 ⁵⁹	10 ⁻⁶ -0.1 0.1 ^{50,60,61} + 3 kWh/ktonne capacity ⁶¹	0.09 ⁶²
TRL	7	6	9	9	9
Nr of cases	10+	8	10+	6	4

¹ Fixed OPEX is defined as the yearly operational cost, like parcel rent and labor cost. CAPEX refers to the annualized CAPEX, which is calculated as follows: $Annualized\ CAPEX = CAPEX \cdot \frac{i}{1 - \frac{1}{(1+i)^T}}$. Where i is the interest rate, and T is lifetime in years.

² The storage tank is used as a hydrogen buffer in ammonia and methane storage systems. The hydrogen salt cavern is used for large scale storage of hydrogen.

³ The efficiency of the PtXtP systems is defined as the output mass over the input mass, as there is no significant mass flow in and out of the batteries, their efficiency is defined as the electric output over the electric input.

$$\eta = \frac{output_e}{mass\ flow\ in * LHV}, \text{ or } \eta = \frac{output_e}{input_e}$$

⁵⁷ Chemical efficiency, 1-3% loss per year, through leaks or reactions. (Tsoutsos, 2010)

⁵⁸ Boil-off for storage at -33 °C at 0.04%/day, 27 kW compressor necessary to counter this for a 9 kton tank. (Morgan, Manwell, & MacGowan, Wind-powered ammonia fuel production for remote islands: A case study, 2014)

⁵⁹ 1 kWh/kg for compressor, 0.02 kWh/kg for dryer. 1.02 kWh/kg. (Michalski, et al., 2017)

⁶⁰ Two stage compressors required for the ammonia condenser of 8 and 4.75 kW, for a NH₃ flow of 0.033 kg/s. This equals 0.1 kWh/kg. (Morgan, Techno-Economic Feasibility Study of Ammonia plants powered by offshore wind, 2013)

⁶¹ 27 kW compressor and condenser for a 9,000 ton capacity tank. (Morgan, Manwell, & MacGowan, Wind-powered ammonia fuel production for remote islands: A case study, 2014)

⁶² 230 kJ/Nm³ for completion compression. 0.72 kg/Nm³. (Croezen, Van Swigchem, Kortmann, & Rooijers, 2005).

9.6. Transport system

	Hydrogen	Ammonia	Methane
Distance	50 km, two-way	0 km, onsite storage	30 km, one-way
CAPEX + fixed OPEX ¹ (€/km/year)	24,400-45,700 47,000 ^{63,64,65,66}	170-200 €/MW/km 0 ^{67,68}	5,300-13,600 9,000 ^{69,70}
Electricity use (kWh/kg, one-way)	0.017 ⁷¹	n.a. ⁶⁸	0.012 ⁷²
TRL	8	9	9
Number of sources	10	1	2

¹Fixed OPEX is defined as the yearly operational cost, like parcel rent and labor cost. CAPEX refers to the annualized CAPEX, which is calculated as follows: $Annualized\ CAPEX = CAPEX \cdot \frac{i}{1 - \frac{1}{(1+i)^T}}$. Where i is the interest rate, and T is lifetime in years.

⁶³ Annualized CAPEX of 17,575 €/y/km, OPEX of 28,120 €/y/km, 40 years lifetime, total 21,800 kg/h (ISPT, 2019).

⁶⁴ 300,000 €/km, 200,000 € equipment, 35 years lifetime. 2% OPEX. 24,300 €/km/year and 16,200 €/year equipment cost (Tractebel, Engie and Hincio, 2017).

⁶⁵ For 300 mm diameter, 600 €/m, lifetime of 35 years, 2% OPEX. Results in 46,642 €/km/year (Mulder & Perey, 2019).

⁶⁶ Based on 3 reports, 0.4-1.1 M€/km. 35 years, 2% OPEX results in 32,400-89,200 €/km/year. Weighted average of 55,142 €/km/year (Van Leeuwen, 2018).

⁶⁷ Cost is given for comparison and is estimated at 170-200 €/MW/km for a pipeline with 10-15 GW capacity (Valera-Medina, Xiao, Owen-Jones, David, & Bowen, 2018).

⁶⁸ Distance of 0 km, CAPEX of the compressor is included in the ammonia system CAPEX.

⁶⁹ Based on two reports. 65,000-100,000 €/km for distribution grid. OPEX of 2%, 35 years lifetime. 6,700 €/km/year (Van Leeuwen, 2018).

⁷⁰ 300,000 \$/mile, with 35 years lifetime and 2% OPEX this results in 13,600 €/km/year (SARI Energy, n.a.)

⁷¹ Compressor power (Van Leeuwen, 2018) for a pressure drop from 50 to 48 Bar over a 50 km pipeline (one-way) (Wlodek, Laciak, Kurowska, & Wegrzyn, 2016). Initial compression is included in storage energy.

⁷² Compressor power calculation (Van Leeuwen, 2018) and a calculated pressure drop from 50 to 40 Bar for a 30 km pipeline (one-way) (Wlodek, Laciak, Kurowska, & Wegrzyn, 2016)

9.7. Regeneration

	Hydrogen	Ammonia	Methane
Technology type	PEM Fuel cell	SOFC	CCGT
CAPEX+ fixed OPEX ¹ (€/MW _e /year)	3,200-180,000 67,400 ^{73,74,75,76,77,78,79}	86,000-91,000 88,500 ^{80,81}	32,000 ^{82,83,85}
Ramp time (h)	<1 ^{74,75}	<1 ^{80,81}	<1
Efficiency ² (%)	45-67 58 ^{73,74,75}	35-70% 56% ^{80,81,84}	50-60% ^{85,86} 60%
Heat use	n.a. ⁸⁷	2% ^{80,81,88} of power	n.a.
TRL	6	7	9
Nr. of sources	10+	2 rough estimations	10+

¹Fixed OPEX is defined as the yearly operational cost, like parcel rent and labor cost. CAPEX refers to the annualized CAPEX, which is calculated as follows: $Annualized\ CAPEX = CAPEX \cdot \frac{i}{1 - \frac{1}{(1+i)^T}}$. Where i is the interest rate, and T is lifetime in years.

²The efficiency is defined as the electricity output over the input mass multiplied with the energy content (LHV).

$$\eta = \frac{output_e}{mass\ flow\ in * LHV}$$

⁷³ 500 €/kW_e by 2030. 60,000 hours lifetime (17 years, 40% on-time). Results in 64,350 €/MW/year. AC system efficiency of 50 kWh/kg, or 58% efficiency (Hydrogen Europe, 2018).

⁷⁴ Predicted for 2030: 830 \$/kW in 2030. Lifetime of 80,000 hours or 23 years (40% on time). OPEX of 5%. Total of 70,400 €/MW/year. Efficiency of 54% (HHV) is equal to 63% (LHV), assuming 25°C H₂ input. (IEA, 2015)

⁷⁵ Current values: 1,600-3,000 €/kW, 20 years lifetime, 4% OPEX. Results in 192,388 €/MW/year. Efficiency of 45-55%. (Tractebel, Engie and Hinicio, 2017).

⁷⁶ Current values: 200-1500 €/kW, lifetime of 20 years is assumed, 4% OPEX. Equals 24,000-180,000 €/MW/year. Efficiency of 50-60% (Zhang, et al., 2019).

⁷⁷ Prediction of system cost in high volume production: 30-40 \$/kW, assumed 20 years lifetime, 4% OPEX. Equals 3,200-4,300 €/MW/year (Miller, et al., 2016)

⁷⁸ 2025, based on 100,000-500,000 produced units: 36-40 \$/kW: Results in 3,900-4,300 €/MW/year. Efficiency 52% (Wilson, Kleen, & Papageorgopoulos, 2017).

⁷⁹ Extremely large differences between current prices and future predictions. The highest values are for current cost. The lowest values are from the same group and are considered outliers. The average between the IEA and Hydrogen Europe was selected to be the most accurate value.

⁸⁰ Based on SOFC for NG, similar system cost, but with 8 years set back in development. 670 €/kW, 17 years lifetime, 4% OPEX. Results in 86,200 €/MW/year. Efficiency of 55% (Van Nielen, 2016).

⁸¹ Current price of 1,575 \$/kW_e, potential price reduction over 10 years of approximately 60% (Afif, et al., 2016). This results in 470 \$/kW. Lifetime of 40,000 hours (40% on-time), 4% OPEX. Results in 91,000 €/MW_e/year. Efficiency of 35-40% currently, 35-60% in the future (Patel & Petri, 2006).

⁸² Only OPEX, purchase is not required in the case of using a current turbine. 4% of CAPEX, CAPEX is expected to be 900 \$/kW_e, 20 year lifetime. Results in fixed OPEX of 32,000 €/MW_e/year.

⁸³ Gas turbine price of 550 €/kW and a lifetime of 30 years (Bertuccioli, et al., 2014).

⁸⁴ According to Hans Vrijenhoef ammonia fuel cells can reach efficiencies of 60-70%.

⁸⁵ Cost of 900\$/kW, Efficiency of 20-35% for turbine, combined cycle results in 50-60% efficiency (NREL, 2017).

⁸⁶ Efficiency of 54-60% in 2020 (Etsap, 2010).

⁸⁷ Low temperature PEM cells (80 °C) were selected to allow easy switching, heat use can therefore be neglected

⁸⁸ This value was not given numerically in any reports. The high operation temperature is similar to that of the electrolyser, similar energy use was assumed.

10.Scenarios

The aim of the model is to compare the selected storage technologies for large scale energy storage on their performance in a variable renewable energy storage system. All scenarios are based on the same electricity input: the wind generation and electricity demand of 2018. They are designed to identify certain bottlenecks for each technology and for different use cases. The base case is that of no storage system at all. The purpose of the scenarios is to identify system bottlenecks. The scenarios start with the simplest ones; first no storage, then hydrogen, followed by the methane scenarios and finally the ammonia scenarios. All the scenarios include the same wind generation and transport losses from the wind park to shore and distribution losses.

10.1. System performance scenarios

10.1.1. No storage

This scenario is added as a base case and is the simplest model. No storage system is connected, which means all surplus of electricity will have to be prevented (curtailed) and all deficits of electricity will have to be compensated by the grid. A diagram of the model is given in Figure 25. For this simple model a screenshot of the Simulink is also provided, to give an insight in the type of modelling that's done. For more complex scenarios this is no longer an option due to readability.

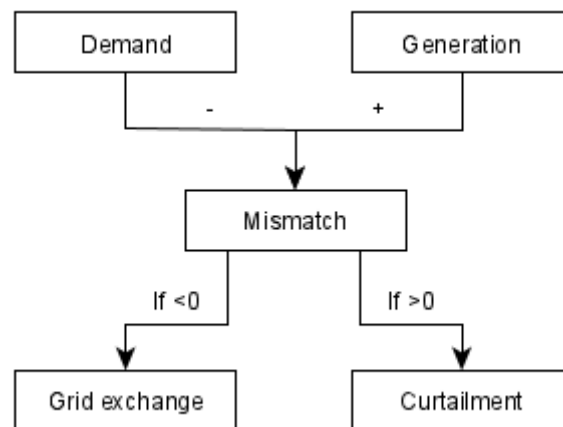


Figure 25: Simplified diagram of the model for a no-storage scenario

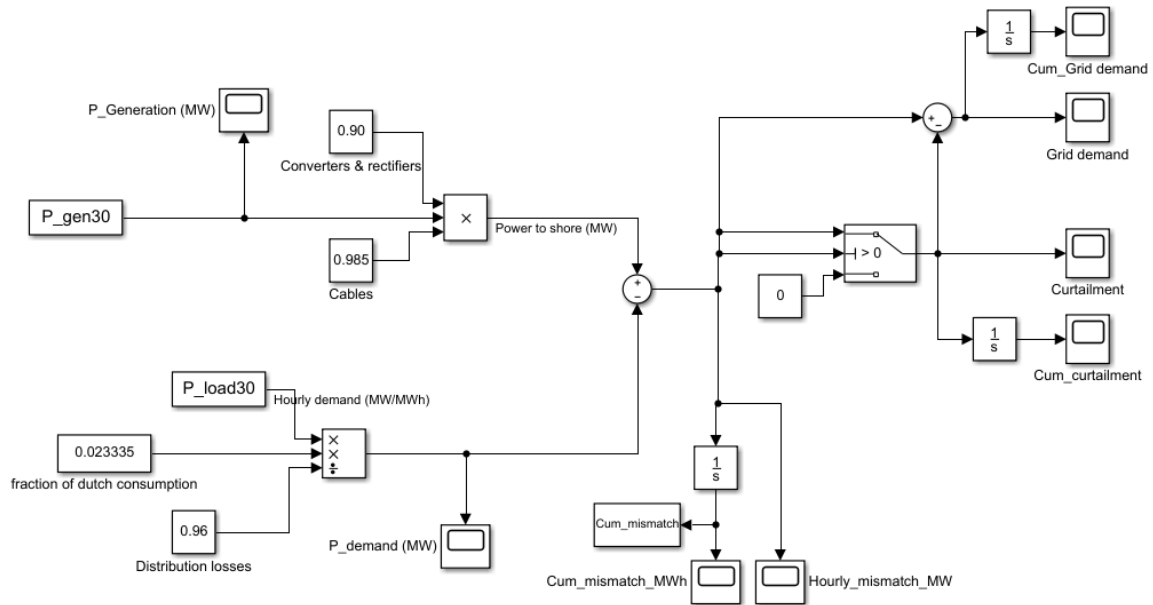


Figure 26: Image of the model in Simulink for illustration of the type of model that was used. This figure shows the no storage scenario. P_{gen30} is the hourly electricity generation from the wind park, P_{load30} is the hourly demand. After correction for losses, the mismatch is monitored as curtailment when it is >0 , and as grid demand when it is <0 . The cumulative mismatch at the end of the year is zero.

10.1.2. H₂

In the first hydrogen scenario the energy storage system is comprised of an electrolyser, fuel cell, salt cavern and pipes. A simplified illustration of the model is given in Figure 27, a map of the scenario is given in Figure 28. The electrolyser and fuel cell must be sized, this is done by running several scenarios with different sizes. In all these scenarios the ratio of fuel cell to electrolyser is 1:1, based on the ratio between the maximum deficit and surplus power (-490:509 or 1:1). System sizes are varied in steps of 100 MW initially, but the step size is reduced to 25 MW around the selected value. The solution that reduces the impact on the grid the most is selected; this system size will be used in all following scenarios.

The second design decision is the initial fill state of the hydrogen cavern. Starting with an empty storage cavern would not create realistic results. It would result in high grid demand at the start of the year, when no storage buffer exists yet. Instead, the simulation was run, and the fill state at the end of the year was taken as the initial state for the actual simulation. This is the equivalent of running the simulation for the second year. The difference between the initial state and final state of the simulation is counted as grid exchange to result in a net storage difference of zero per year. The hydrogen cavern content is not limited, the maximum content is taken as the eventual hydrogen capacity of the cavern. The pipelines are modelled in the same way; their capacity is not limited, the size of the pipeline meets the maximum hydrogen output of the electrolyser, and as such is a result. The results of these scenarios are given in the next chapter.

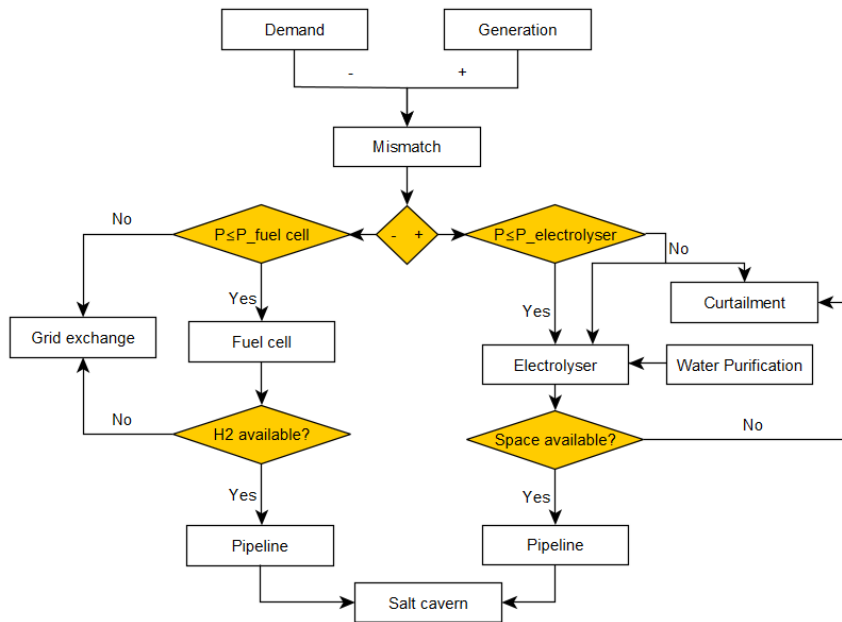


Figure 27: Simplified schematic representation of the model for the hydrogen scenario

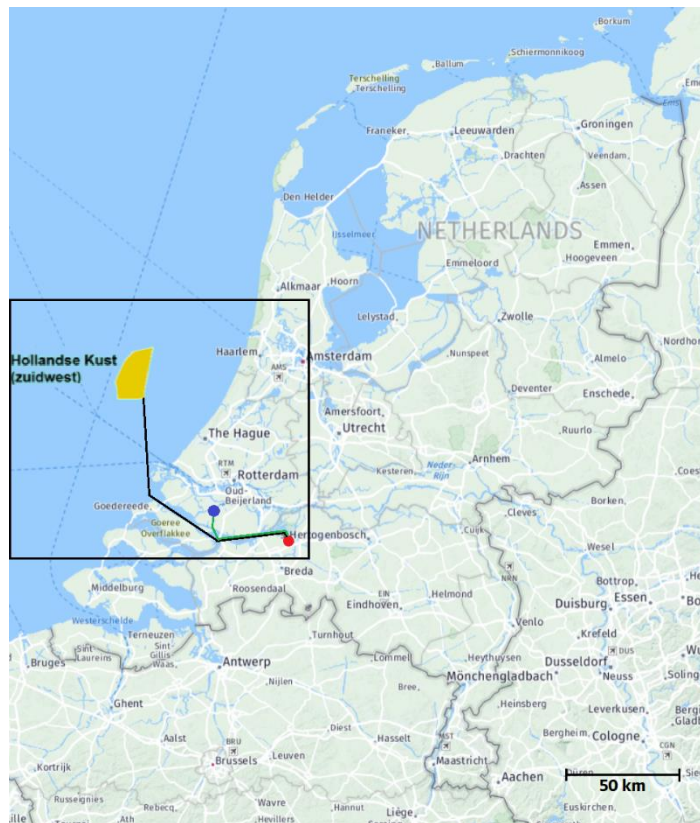


Figure 28: Map illustrating the hydrogen scenario. Yellow is one of the designated areas for future wind parks. Black is the DC cable connecting the wind park to the shore. Red is the grid connection point, where the fuel cell and electrolyser are located. Blue is the salt cavern location and green is the hydrogen pipeline connecting them.



Figure 29: Zoomed in image of Figure 28.

10.1.3. H2 - full load

One of the purposes of this thesis is to evaluate the effect of the VRES use on the performance of the system. A comparison must therefore be made to a system under constant use. To make a fair comparison the model in this scenario is kept exactly the same as the previous scenario. The only difference is that the electrolyser and fuel cell will be kept running at maximum capacity.

10.1.4. Ammonia - Constant production

Literature research proved that hydrogen is difficult to store and transport. For easy storage and transport ammonia is produced from hydrogen and nitrogen. Ammonia is then liquified and stored in an on-site ammonia tank. The distance of transportation is so small it is negligible, instead the compressors and condensers are included in the storage system. A schematic overview of the system is given in Figure 30. Due to the nature of the ammonia storage tank all system components can be in the same location, the map that corresponds with this scenario is therefore simple. It is given in Figure 32.

Up to now, the Haber-Bosch process has mostly been used in continuous operation. Hans Vrijenhoef indicated that switching the Haber-Bosch reactor on and off would result in unwanted material stresses (Vrijenhoef, personal conversation, 2020). Haber-Bosch reactors are therefore better used continuously. Hydrogen production on the other hand is fluctuating with the wind energy production, which means a hydrogen buffer must be installed. The ammonia SOFC is equal in size to the H₂ fuel cell. The HB reactor is sized in such a way that all stored hydrogen is converted to ammonia, and no additional hydrogen is required. The buffer size is not limited, the simulation will show the required size of the hydrogen buffer. Figure 31 shows the buffer content and buffer sizing. The ammonia tank is limited only to being empty, the maximum ammonia content is taken as the ammonia tank size. The initial fill of the ammonia tank is determined in the same way as the initial fill of the hydrogen cavern. The simulation is run once, the end value is taken as the initial value for the second run. The difference between the two is considered grid demand.

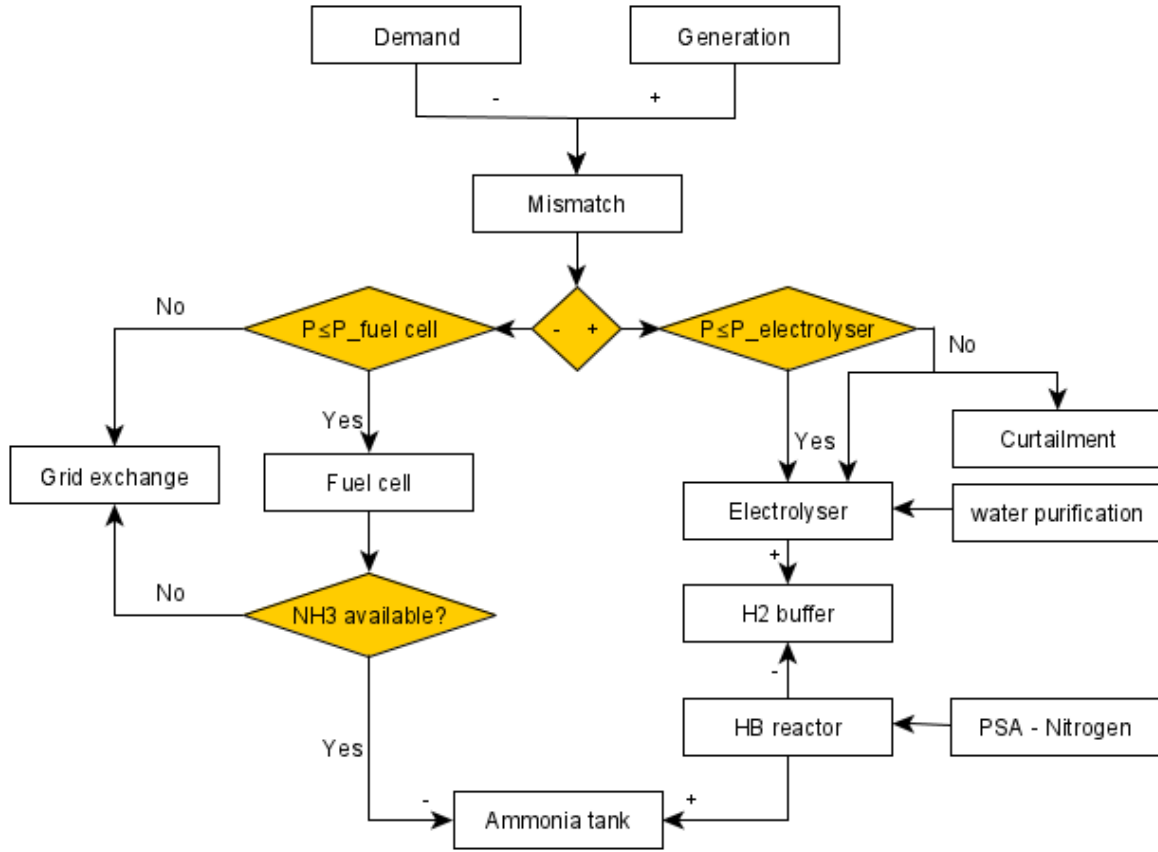


Figure 30: Simplified schematic view of the constant Haber-Bosch scenario

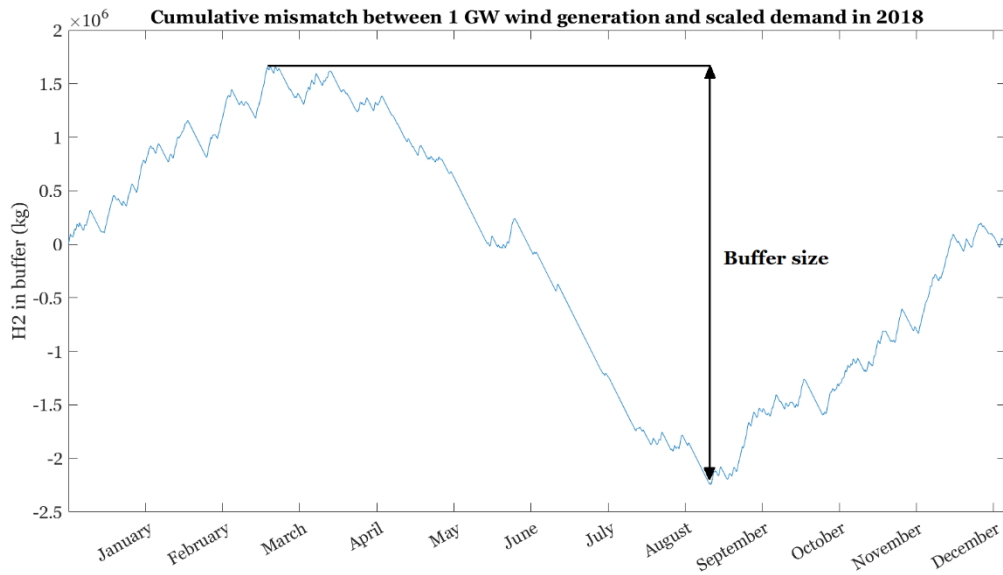


Figure 31: Hydrogen buffer content and size

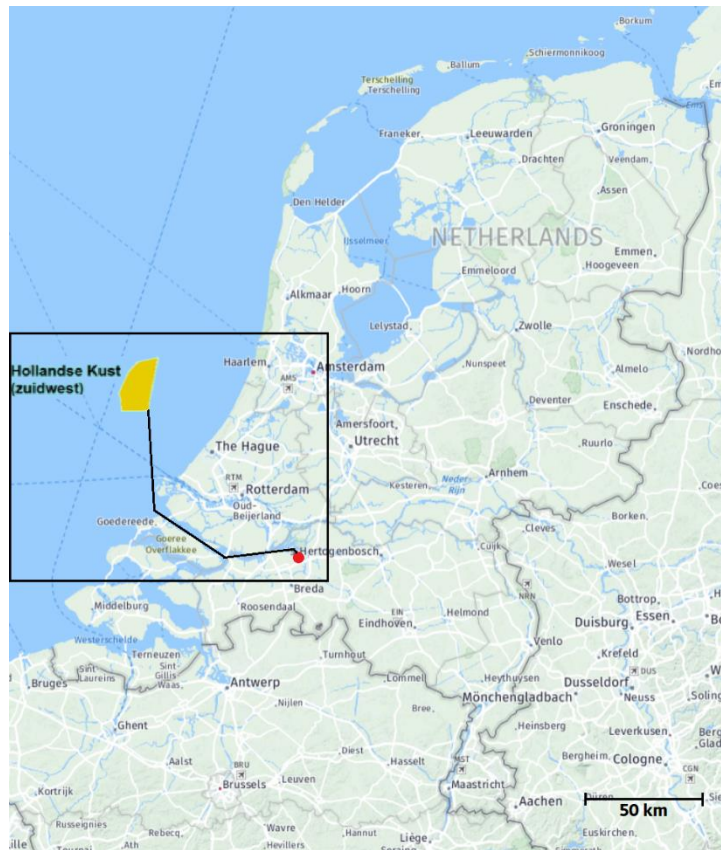


Figure 32: Map of the ammonia system. Yellow is one of the designated areas for future wind parks. Black is the DC cable connecting the wind park to the shore. Red is the storage site containing the grid connection point, ammonia tank, Haber-Bosch reactor and Fuel cell.



Figure 33: Zoomed in image of Figure 32.

10.1.5. Ammonia – Flexible production

The previous scenario simulates continuous ammonia production, because those are the most optimal conditions for the HB reactor. However, to match the variable production of hydrogen a flexible HB process is more optimal from a system perspective. The literature study showed the process has a minimum load of 33%, without switching the reactor completely off (Cheema & Krewer, 2018). This second ammonia scenario aims to assess the impact of flexible HB on the required hydrogen buffer

size. Like in the previous scenario, the reduced cost and energy use of transport and storage are weighed against the increased cost and energy use of the HB reactor and ammonia fuel cell.

The HB sizing in this scenario is again done in such a way that the buffer is exactly empty at the end of the year. The initial value of the ammonia tank is taken at the end of the first simulation run, the reduced content of the tank at the end of the year is considered grid exchange. The HB reactor in this scenario fluctuates with the wind generation, in times of low wind generation the HB reactor functions at 33% of its maximum capacity. This is the only systemic difference with the previous scenario.

10.1.6. Ammonia – Full load

Like for hydrogen, for ammonia too the effect of the VRES use on the performance of the system is evaluated. The comparison is again made to a system under constant use at full capacity. To make a fair comparison the model in this scenario is kept the same as the previous scenario. The HB reactor is again scaled to meet the hydrogen production exactly.

10.1.7. Methane

Methane performs similarly to the Haber-Bosch system in flexibility. Where the HB reactor can be varied between 33% and 100%, the methane reactor can only be varied between 40% and 100% (Gorre, Ortloff, & Van Leeuwen, 2019). The consequences of this limited flexibility will become clear from the simulation with ammonia. In this methane scenario a different bottleneck is investigated. The Sabatier reaction uses CO₂ from DAC, which is an energy intensive process. The question is whether the energy consumed for CO₂ capture is offset by the transport, storage and regeneration advantages. A schematic of the methane system is presented in Figure 34. It consists of an electrolyser, hydrogen buffer, Sabatier reactor, pipeline, gas injection station and gas turbines. The gas turbine is already part of the grid and does not have to be built specifically for this purpose. Figure 35 gives a map of the scenario.

The Sabatier system sizing was done in the same way as the HB sizing. The reactor is scaled so that at the end of the year, all hydrogen has been converted to methane. The pipeline is scaled to the maximum throughput, the DAC is completely flexible. Methane is stored in the natural gas grid, which means the produced methane must be transported to the nearest gas injection station, which is located in 's Hertogenbosch, 30 km from the grid connection. The grid is assumed to have unlimited storage space. At the end of the year the net demand from the grid is considered to be grid exchange.

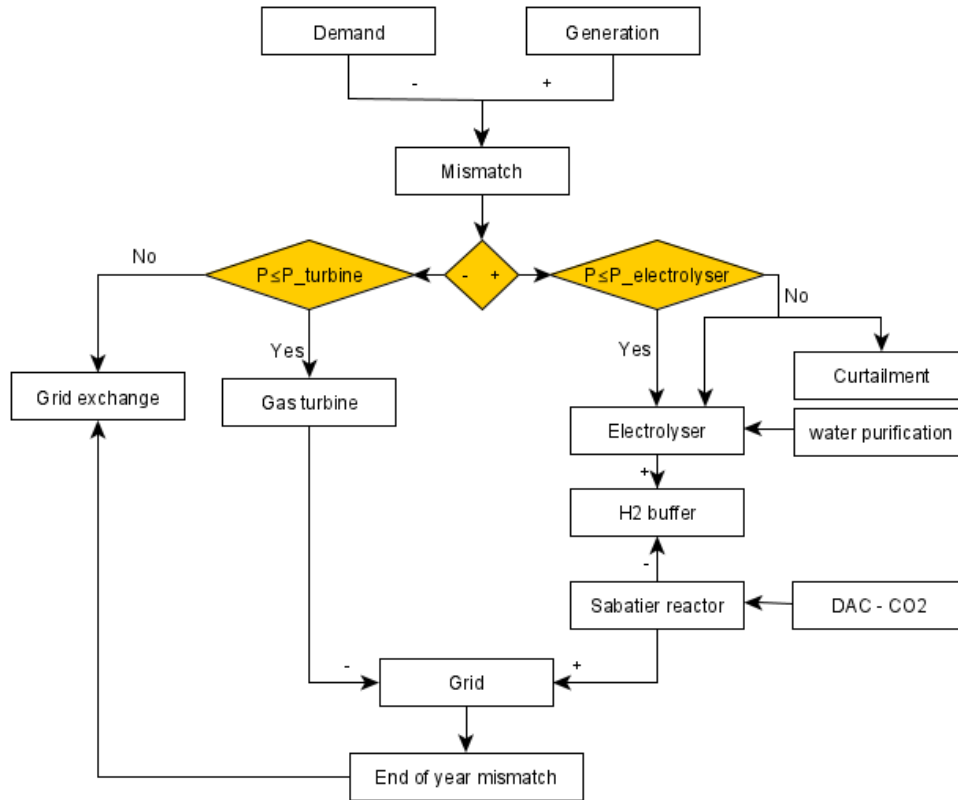


Figure 34: schematic representation of the methane storage system

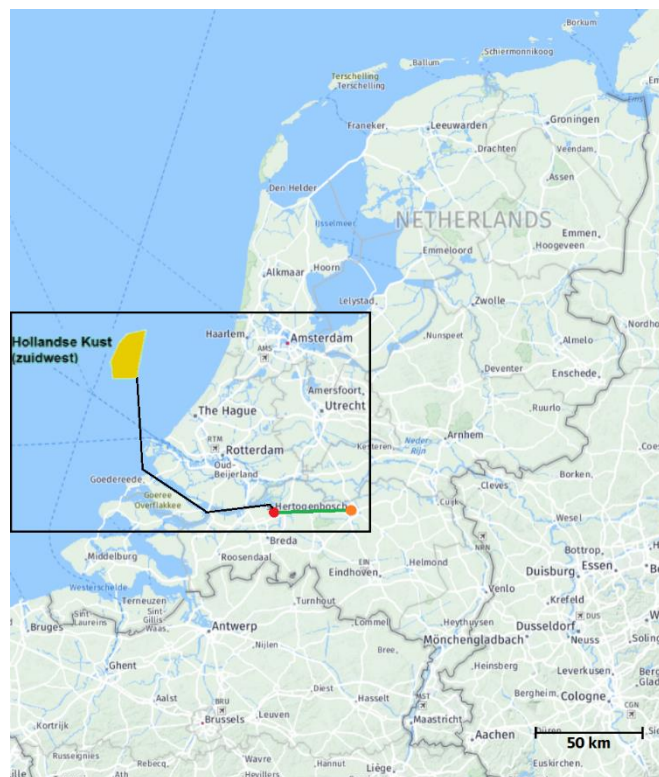


Figure 35: Map of the methane scenario, yellow represents the designated area for future wind parks. Black is the DC cable connecting the wind park to the shore. Red is the grid connection point, where the fuel cell and Sabatier reactor are located. Orange is the gas injection station, the hydrogen pipeline connecting them is marked green. The gas turbine can be any gas turbine already connected to the gas and electricity grid.



Figure 36: Zoomed-in image of Figure 35.

10.1.8. Methane – Full load

The methane system, as well as the hydrogen and ammonia system, was also simulated under full working hours. Both the electrolyser and fuel cell are used at maximum capacity (425 MW), to investigate the potential of the system when it is run full time. The entire system is kept the same, the Sabatier reactor is scaled to meet the hydrogen production exactly.

10.2. Added value of storage

The alternative to energy storage is to oversize the wind park and curtail energy in times of low demand or strong wind. The downside is the added cost and area of wind parks required to meet this demand. For larger wind parks the grid exchange is reduced, so an important question is how much grid demand is acceptable. In 2030, 70% of all electricity generation is to come from renewable sources. This means a backup generator using fossil fuels could be used to meet demand in times of low wind generation power. This backup generator could be used to meet up to 30% of the demand.

This scenario is created to investigate the required oversizing of the wind park to reduce the grid demand in a system with storage and a system without storage. Based on previous scenarios the best storage system is selected and compared with a no-storage scenario. Wind generation is linearly scaled, and the grid exchange for systems with and without storage is compared.

11. Results

11.1. Scenario results

11.1.1. No storage

The no-storage scenario was created to set a baseline. All the mismatch is curtailed or compensated by the grid. The system sizing was done so that the generated electricity and the electricity consumed in one year are equal. The cumulative mismatch over the year was therefore 0.

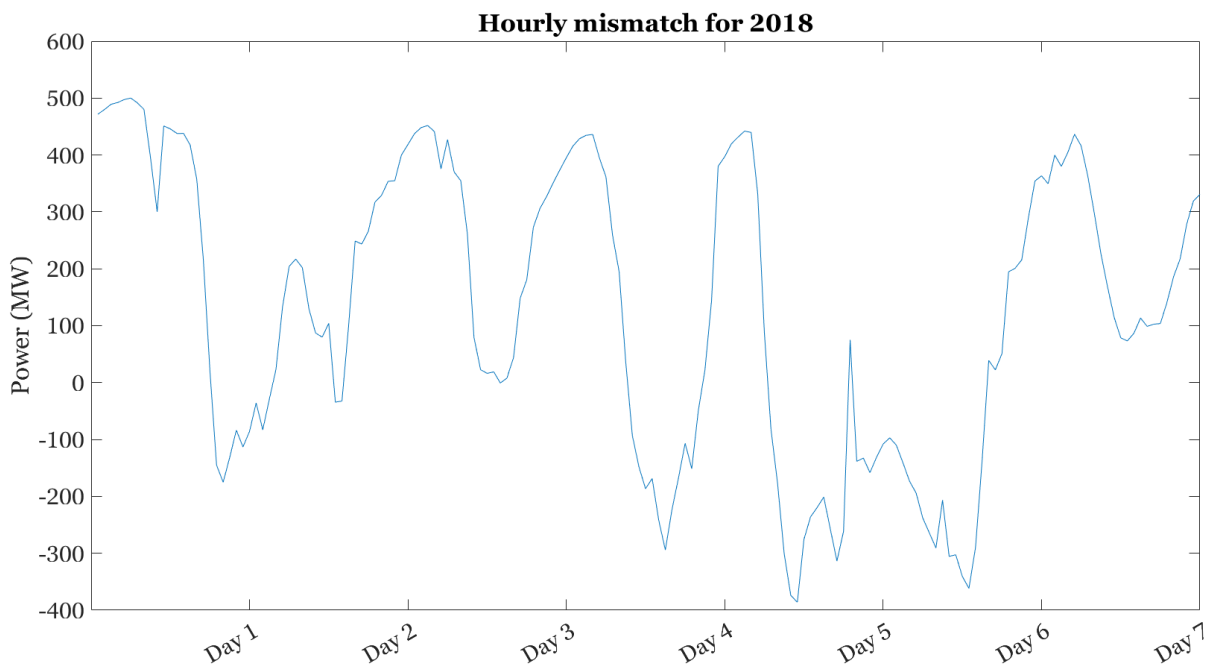


Figure 37: Hourly mismatch of week 1 for 2018

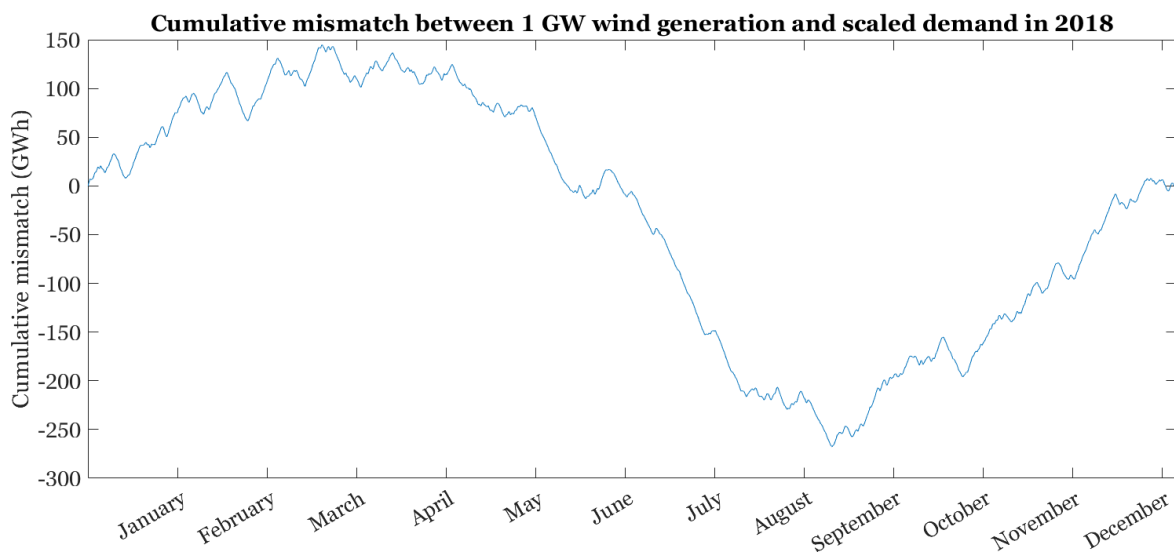


Figure 38: Cumulative mismatch between wind generation and electricity demand in MWh in the year 2018, generated from data from the Open Power Systems Data (Open Power System Data, 2019).

Table 5: Output of simulations for the scenario of a 1 GW wind plant generating electricity for the Dutch energy grid, without storage.

Storage system cost	0
Curtailement	1.06 TWh
Grid demand	1.06 TWh
Net electricity mismatch	0
Total demand	3.28 TWh

11.1.2. Hydrogen

The impact of system size on cost and grid interaction is shown in Figure 39. Grid interaction initially reduces with electrolyser and fuel cell size, while the cost almost linearly increases. Based on these simulations the optimal size was selected to be 425 MW, based on the minimized grid interaction. For larger systems the grid interaction increases rather than decreases due to the additional energy use of the system. Given the system sizing of 425 MW the same outputs were gathered from the system as for the no-storage base case. The result is shown in Table 6. The annual electricity delivered to the grid to meet demand is 367.6 GWh, the system cost is 106 M€, which results in a levelized cost of storage of 288 €/MWh stored. The relative system component costs are given in Figure 40. The roundtrip efficiency calculated from the theoretical values would be 41%, based on the efficiency of the fuel cell and the electrolyser. According to this model, the electricity delivered by the system and electricity stored by the system result in a round trip efficiency of 35%, which is significantly lower, and is closer to the roundtrip efficiency for a hydrogen storage system as found in literature (Table 3), which was 38%. The difference lies in the energy use of the system. The complete hydrogen storage system consumes 96 GWh of electricity per year. The contributions of the individual system components are given in Figure 41.

Table 6: Output of simulations for the scenario of a 1 GW wind plant generating electricity for the Dutch energy grid, connected to a hydrogen storage system

Annualized storage system cost ¹	97.7 M€
Levelized cost of storage ¹	264 €/MWh _{output}
Additional levelized cost of energy ²	37 €/MWh
Roundtrip efficiency ³	35%
Curtailement	6.45 GWh
Grid demand	689 GWh
Fuel cell size	425 MW
Electrolyser size	425 MW
Pipeline size	9000 kg/h
Salt cavern size	1.67 ktonne H ₂

¹ The annualized CAPEX is calculated as indicated below, where i is the interest rate, and T is the lifetime in years. This definition is used in many other reports, including the HyChain report (ISPT, 2019).

$$\text{Annualized CAPEX} = \text{CAPEX} \cdot \frac{i}{1 - \frac{1}{(1+i)^T}}$$

² Storage system cost divided by the number of MWh delivered by the storage system

² Cost added to consumers electricity price due to the cost of storage. Calculated as storage system cost divided by the number of MWh's of demand met (direct demand-generation match + energy delivered by the storage system)

³ Defined as the electricity input divided by the energy delivered by the storage system

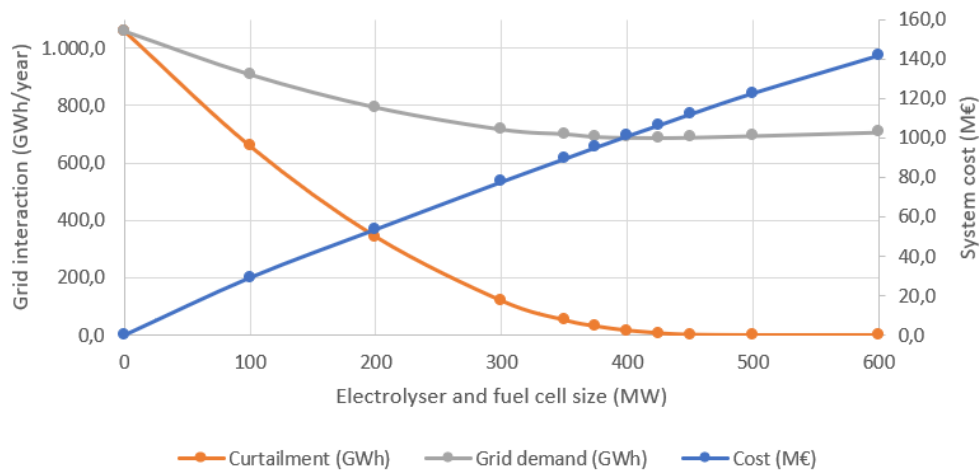


Figure 39: Relation between system size, system cost and grid interaction

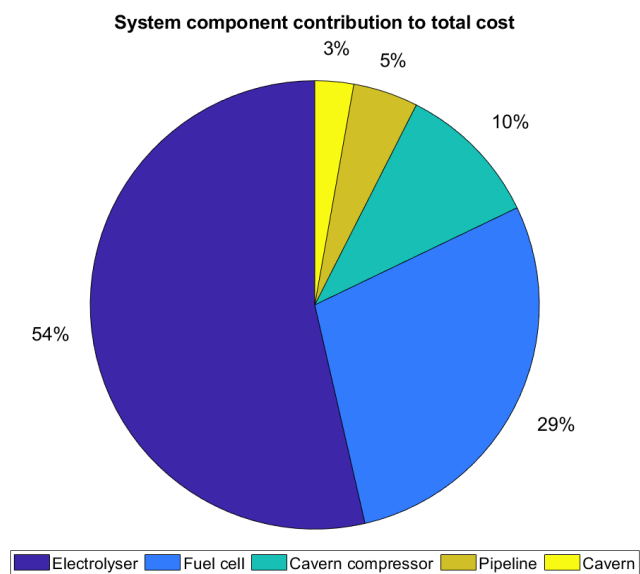


Figure 40: Contribution of system components to storage system costs (CAPEX and OPEX). Storage system cost is 97.7 M€.

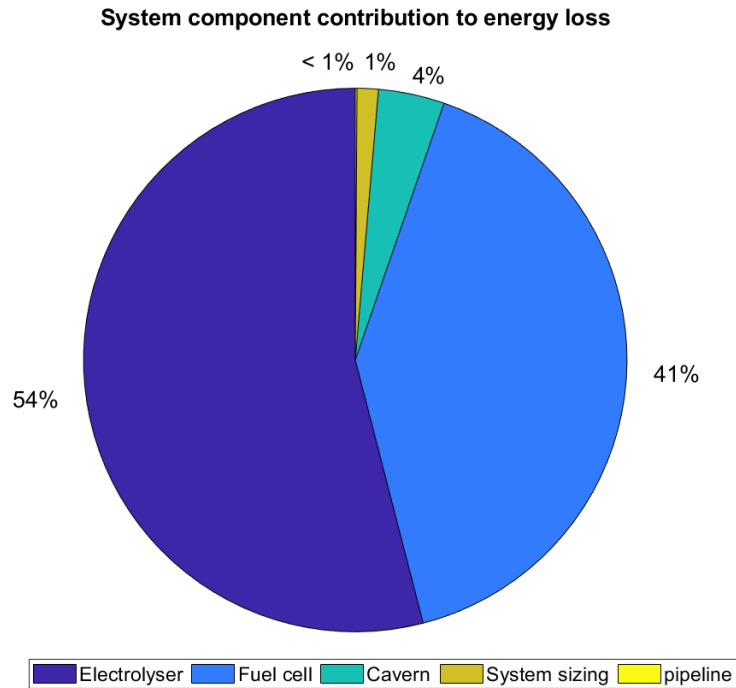


Figure 41: Contribution of system components to storage system energy use. The total energy loss in the storage system is 686 GWh per year (65% of 1.06 TWh).

11.1.3. H2 under full load

The previous scenario showed the performance of the hydrogen system when used as an energy storage system in a VRES grid. The efficiency and cost for a system that runs full time are expected to be lower, because the standby power losses will be relatively smaller, and the system costs will be divided over a larger energy output. The table below gives the result of the system when it is used at max capacity constantly, so 425 MW into the electrolyser and 425 MW out of the fuel cell.

The table shows the storage system costs are not significantly changed. The minor change is caused by the elimination of the hydrogen cavern. When both systems run at full capacity hydrogen is consumed faster than it is produced. A net electricity shortage is created, which must be taken from the external grid and no hydrogen is stored in the cavern. The pipelines are still included in the system.

The cost per MWh delivered is significantly lower. Mostly due to the strongly increased electricity output. The electricity output of the storage system is 1.352 TWh, while the electricity input is 3.723 TWh. This increased electricity output results in a levelized cost of storage of 72 €/MWh. The efficiency is increased slightly, to 36.3%. This can be explained by the relatively lower stand-by electricity losses, as the output increases and the standby power consumption remains the same. In reality the efficiency of a PtXtP system connected to VRES might be reduced more by variable efficiencies, these variable efficiencies will have to be examined further before they can be incorporated in the model.

Table 7: Output of simulations for the scenario of a hydrogen storage system containing a 425 MW electrolyser and 425 MW fuel cell running at full capacity for one year. Compared to the same hydrogen storage system connected to a 1 GW wind plant and a Dutch demand cycle.

	H ₂ in VRES	H ₂ full load
Storage system cost	97.7 M€	98.0 M€
Levelized cost of storage ¹	264 €/MWh _{output}	72 €/MWh _{output}
Roundtrip efficiency ²	35.0%	36.3%

Curtailment	0.00645 TWh	0
Grid demand	0.689 TWh	2.371 TWh
Salt cavern size	1.67 kt H ₂	n.a.

¹ Storage system cost divided by the number of MWh delivered by the storage system

² Defined as the electricity input divided by the energy delivered by the storage system

11.1.4. Ammonia – constant

The first result is the size of the hydrogen buffer. In the hydrogen scenario a hydrogen cavern with a hydrogen capacity of 1.67 kt of hydrogen was required to store all produced hydrogen. The scenario with constant ammonia production aims to reduce the transport and storage cost of hydrogen. In order to do so the ammonia reactor was scaled so that all hydrogen produced in one year was converted to ammonia. A larger HB reactor would result in an additional demand for hydrogen, a smaller reactor would result in accumulation of hydrogen, effectively wasting it as it cannot be used in the ammonia fuel cell. The required hydrogen buffer size to keep a HB reactor this size running, however, is 4.2 kt. The required hydrogen buffer in that case is larger than the original hydrogen storage capacity required. To store this buffer a salt cavern should be used, which brings us back to the system as described in the hydrogen scenario.

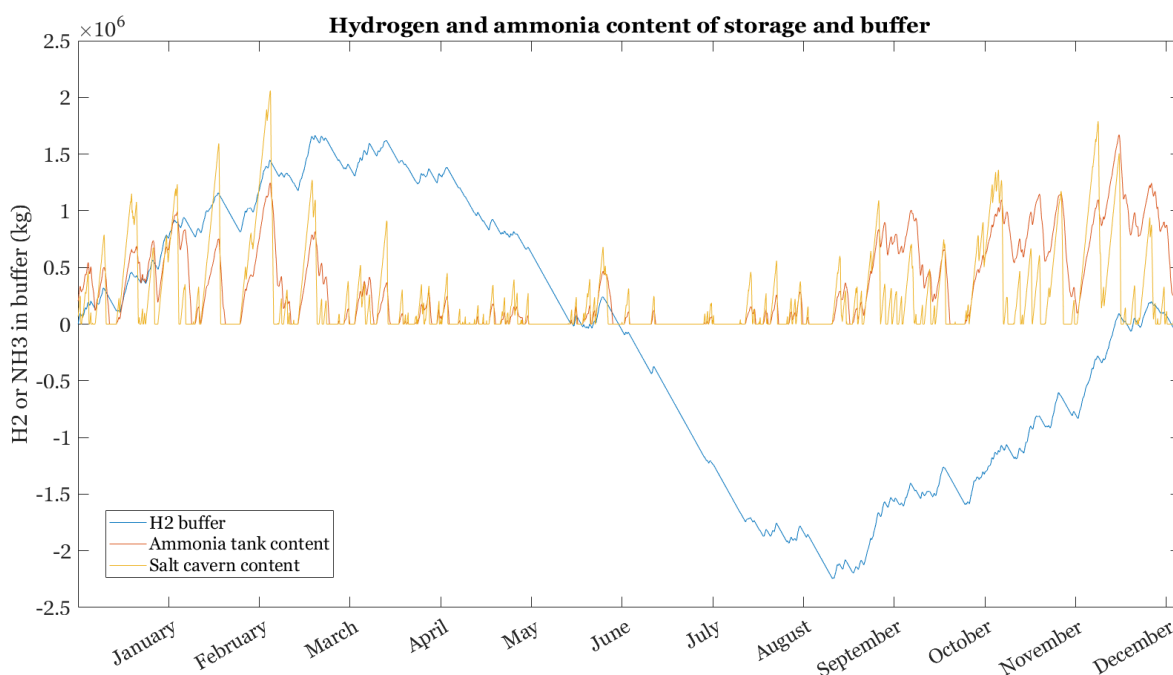


Figure 42: Ammonia and hydrogen content of the salt cavern, hydrogen buffer and ammonia tank

The alternative is to limit the hydrogen storage capacity and import hydrogen from external sources. Increasing the production of hydrogen from the electrolyser would defeat the purpose of the storage system, as it would result in additional grid exchange at times when the wind production is low, and a mismatch already exists.

The conclusion is that a continuously running HB reactor is not a solution for large-scale energy storage. More detailed results are discussed in the flexible ammonia scenario. This doesn't mean constant HB processes can't serve a purpose in the energy transition. Ammonia transport is still cheaper than hydrogen storage, so a possibly useful application could be long distance transport. This is one of the business cases Proton Ventures pursues (Vrijenhoef, personal conversation, 2020).

Table 8: Output of simulations for the scenario of a 1 GW wind plant generating electricity for the Dutch energy grid, connected to an ammonia storage system with a HB reactor running constantly.

Storage system cost	110 M€ (buffer cost not included)
Levelized cost of storage ¹	590 €/MWh _{output}
Additional levelized cost of energy ²	45 €/MWh
Roundtrip efficiency ³	17.5%
Curtailement	2.655 GWh
Grid demand	871.5 GWh
HB reactor size	12,486 kg/h
Hydrogen buffer size	4.2 kt H ₂
Ammonia storage tank	2.54 kt NH ₃

¹ Storage system cost divided by the number of MWh delivered by the storage system

² Cost added to consumers electricity price due to the cost of storage. Calculated as storage system cost divided by the number of MWh's of demand met (direct demand-generation match + energy delivered by the storage system)

³ Defined as the electricity input divided by the energy delivered by the storage system

11.1.5. Ammonia – flexible production

The previous scenario has proven that constant production of ammonia serves no purpose in large-scale energy storage for the grid. This scenario assumed a variable HB process. The first interesting result is the HB system sizing. The HB reactor with constant NH₃ production needed a max. capacity of 11,316 kg NH₃ per hour to process all hydrogen produced by the electrolyser. For flexible production the max. capacity must be increased to 18,803 kg NH₃ per hour, a 66% increase, which influences the investment cost.

The second effect is on the required size of the hydrogen buffer. The hydrogen buffer size can be reduced to 2.44 kt of hydrogen. While this is significantly lower than the buffer required for constant ammonia production (4.2 kt), it is still bigger than the hydrogen buffer for energy storage in hydrogen. To provide this buffer a salt cavern should be used, meaning no transport or storage complications can be prevented. In addition, the roundtrip efficiency is slightly lower than in the constant HB scenario due to the increased energy use of the HB reactor.

Table 9: Output of simulations for the scenario of a 1 GW wind plant generating electricity for the Dutch energy grid, connected to an ammonia storage system with a HB reactor with flexible operation between 33% and 100% of full capacity.

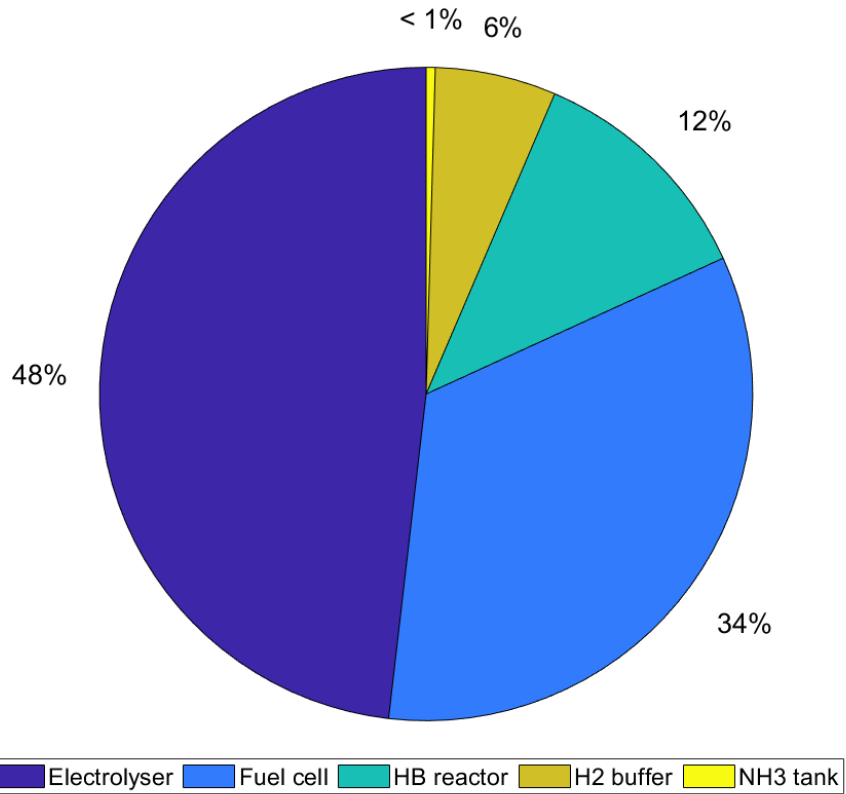
Storage system cost	111.6 M€
Levelized cost of storage ¹	630 €/MWh _{output}
Additional levelized cost of energy ²	46.5 €/MWh
Roundtrip efficiency ³	16.7%
Curtailement	1.128 GWh
Grid demand	880.3 GWh
Fuel cell size	425 MW _e
Electrolyser size	425 MW _e
HB reactor size	21,500 kg/h
Hydrogen buffer size	2.44 kt H ₂
Ammonia storage tank	3.86 kt NH ₃

¹ Storage system cost divided by the number of MWh delivered by the storage system

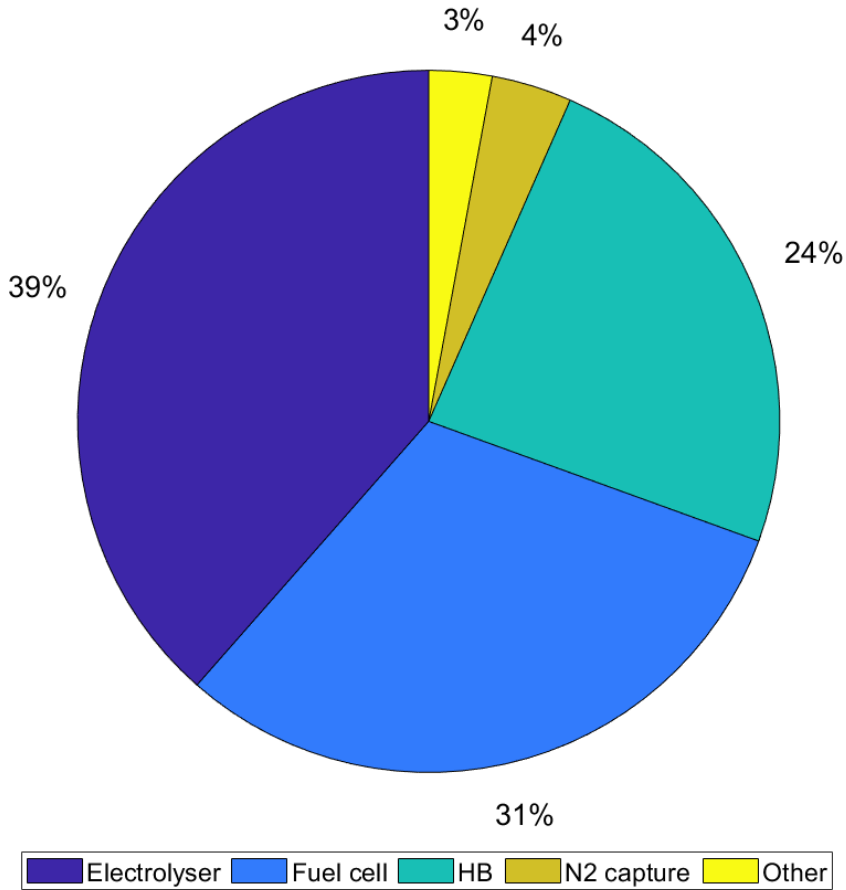
² Cost added to consumers electricity price due to the cost of storage. Calculated as storage system cost divided by the number of MWh's of demand met (direct demand-generation match + energy delivered by the storage system)

³ Defined as the electricity input divided by the energy delivered by the storage system

System component contribution to total cost



System component contribution to energy use



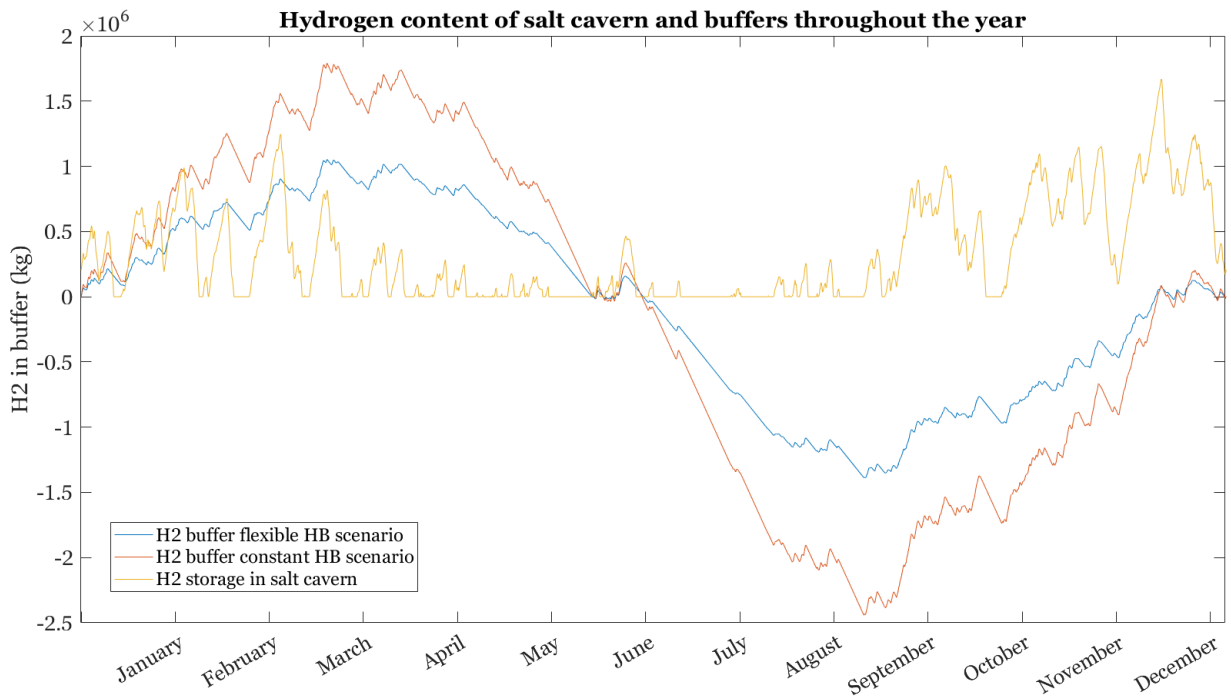


Figure 43: H₂ storage in hydrogen buffers with hydrogen storage in salt cavern as a reference

The trade-off between system size and system flexibility will always exist. The required HB size and hydrogen buffer size for this system are plotted against the system flexibility in Figure 44. Where the installed required HB capacity increases with increasing flexibility, while the H₂ buffer size decreases.

For energy storage in ammonia an on-site hydrogen storage buffer is necessary, these currently store up to 1000 kg per tank (Van Leeuwen, 2018). Even with a flexibility of 1-100% output an ammonia energy storage system requires a buffer with a hydrogen capacity of 150,000 kg H₂, or 150 tanks.

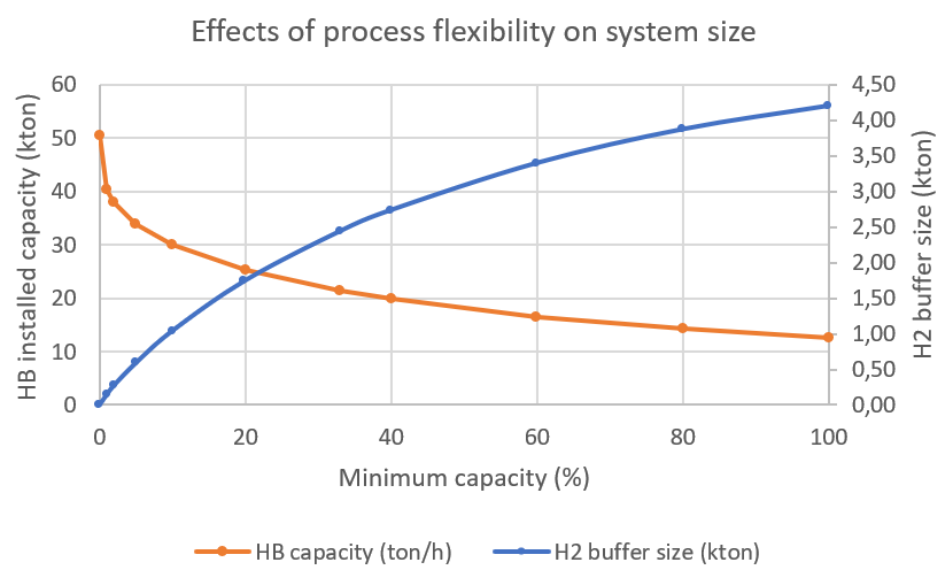


Figure 44: The impact of flexible system use on system size

11.1.6. Ammonia – full load

The purpose of this scenario is to compare the performance of the ammonia system in a grid with VRES to the normal condition of full load running. The Storage system cost is increased to 125 M€, which is

explained by the increase of the required ammonia reactor size. The levelized cost are reduced significantly, which is explained by the increased output of the system.

Interestingly, the roundtrip efficiency of this full load system is smaller than that of the NH₃ system when connected to a VRES source. This can be explained by the large electricity use of the Haber-Bosch reactor. Given that the fuel cell is already run at maximum capacity, the electricity use of the system must be provided by the grid. ives the contribution of different system components to the electricity use.

Table 10: Output of simulations for the scenario of an ammonia storage system containing a 425 MW electrolyser and 425 MW ammonia fuel cell running at full capacity for one year, connected to a HB reactor. Compared to the same ammonia storage system connected to a 1 GW wind plant and a Dutch demand cycle, where the HB reactor has a minimum load of 33%.

	NH ₃ in VRES (constant production)	NH ₃ full load
Storage system cost	111.6 M€	125 M€
Levelized cost of storage	630 €/MWh _{output}	278 €/MWh _{output}
Roundtrip efficiency	16.7%	12%
Curtailment	1.128 GWh	0
Grid demand	880.3 GWh	3.273 TWh
Fuel cell size	425 MW _e	425 MW _e
Electrolyser size	425 MW _e	425 MW _e
HB reactor size	21,500 kg/h	50,500 kg/h
Hydrogen buffer size	2.44 kt H ₂	0

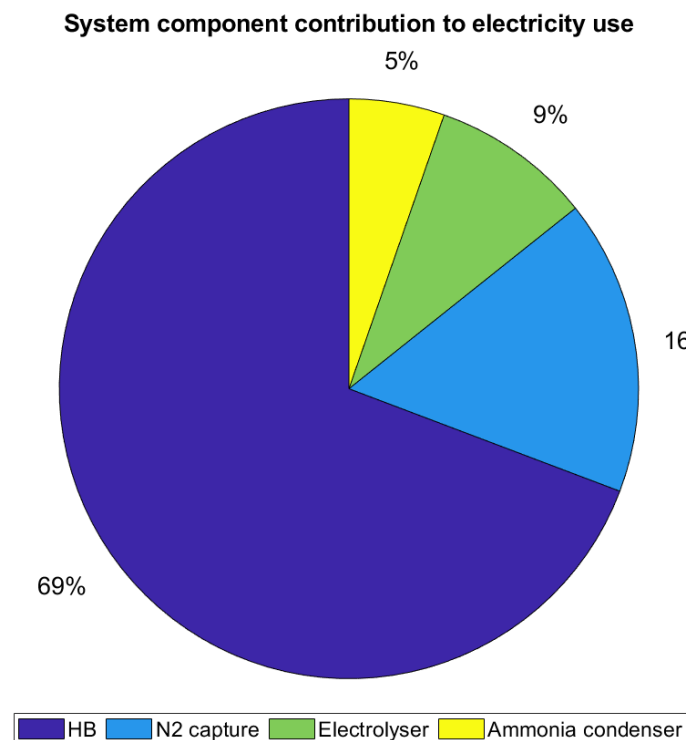


Figure 45: Breakdown of system electricity use

11.1.7. Methane

The purpose of this scenario is to identify bottlenecks in the methane storage system, the results are given in Table 11. The first thing that's interesting to mention is the system cost. The methane system cost is lower than the cost of the hydrogen or the ammonia system. This cost reduction is achieved using the existing gas grid and turbine. For comparison: the purchase of a new gas turbine would have increased the system cost by 15.2 M€, assuming a gas turbine price of 550 €/kW and a lifetime of 30 years (Bertuccioli, et al., 2014). The storage system cost would be 110 M€, which is more expensive than the hydrogen system, but slightly less expensive than the ammonia system.

Table 11: Output of simulations for the scenario of a 1 GW wind plant generating electricity for the Dutch energy grid, connected to a methane storage system with a Sabatier reactor with flexible operation between 40% and 100% of full capacity.

Storage system cost	95.9 M€
Levelized cost of storage ¹	276 €/MWh _{output}
Additional levelized cost of energy ²	37.4 €/MWh
Roundtrip efficiency ³	32.5%
Curtailement	2 GWh
Grid demand	712,7 GWh
Sabatier reactor size	9800 kg/h
Hydrogen buffer size	2.8 kt

¹ Storage system cost divided by the number of MWh delivered by the storage system

² Cost added to consumers electricity price due to the cost of storage. Calculated as storage system cost divided by the number of MWh's of demand met (direct demand-generation match + energy delivered by the storage system)

³ Defined as the electricity input divided by the energy delivered by the storage system

The previous ammonia scenarios proved that the poor flexibility of the system results in hydrogen buffers roughly the size of the salt cavern used in the hydrogen scenario. The buffer required for a flexible methane system (40-100%) has a capacity of 2.8 kt of H₂. The scenario with a constant Sabatier reactor is therefore not included in this thesis. The same conclusion can be drawn as for ammonia, the conversion of hydrogen into methane does not prevent or replace any of the hydrogen storage or transport system components.

The second bottleneck to be investigated is the CO₂ capture. Literature study showed that the use of CO₂ from air is one of the most problematic components of the methane PtXtP system, as it is costly and energy consuming. Breakdowns of the cost and energy consumption of the system are given in Figure 46 and Figure 47.

Interesting for this scenario is that the DAC system does indeed contribute strongly to the energy use of the system (25%), but the roundtrip efficiency is still high. Important to know about the energy use of the system is that the Sabatier reaction contributes a negative energy consumption, which means it adds energy to the system. This can be explained by the fact that CO₂ and H₂ react exothermally, which means heat and, in this case, chemical energy is added to the system. With every kg H₂ that goes into the reactor 3.84 kg of CH₄ is created. The energy content of 1 kg of hydrogen is 120 MJ, the energy content of methane is 50 MJ per kg. This leads to a net gain of energy when hydrogen is added to the reactor. These outcomes answer the question of feasibility of the DAC system. While the DAC system is indeed responsible for a significant share of the energy losses, the Sabatier systems compensates this energy loss.

System component contribution to energy use

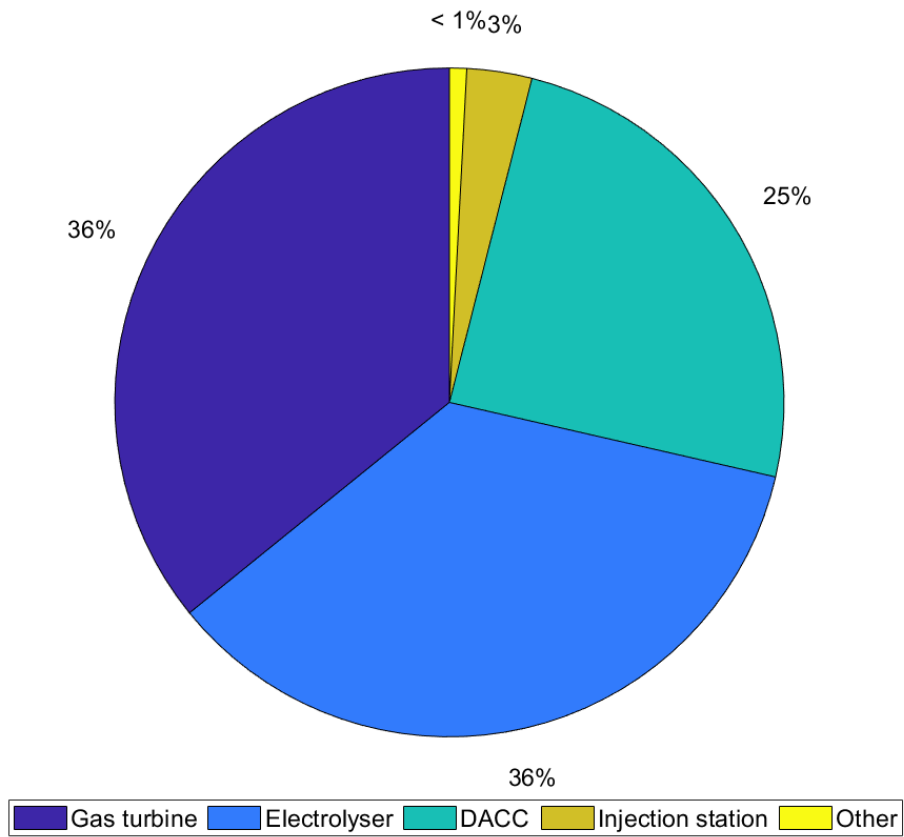


Figure 46: Contribution of system components to total system energy use. Total system energy use is 979 GWh, not included is the Sabatier reactor that adds 244 GWh of energy per year.

System component contribution to total cost

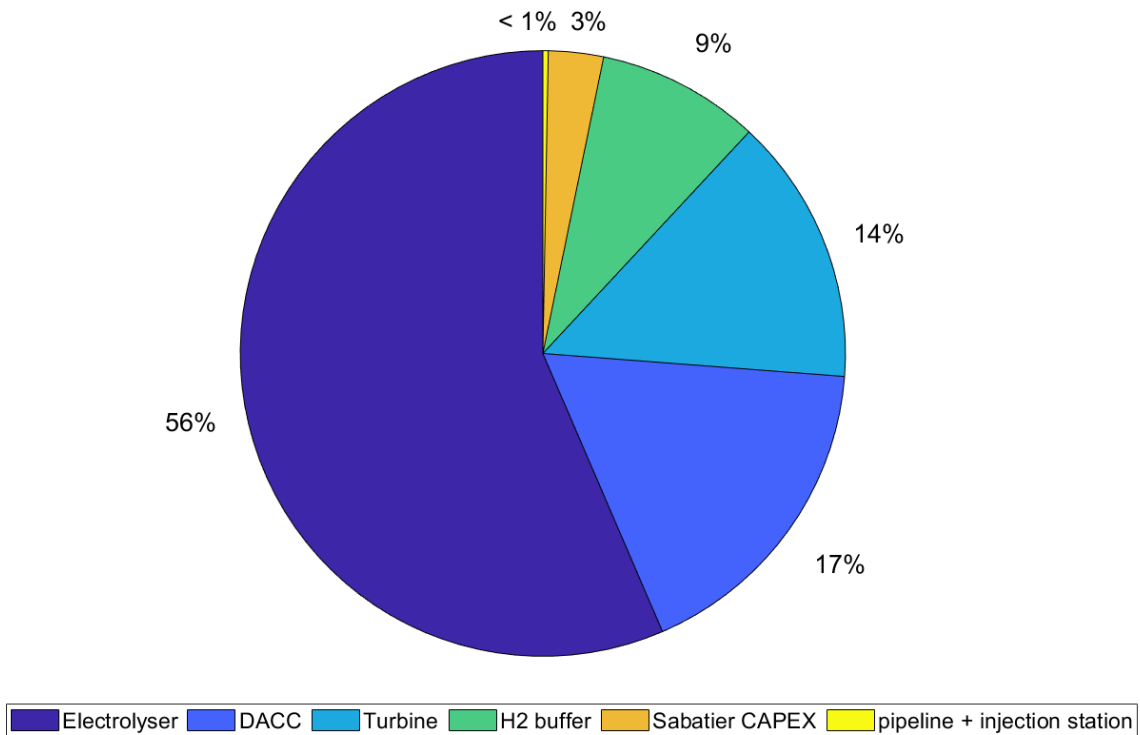


Figure 47: Contribution of system components to storage system cost. Total system energy cost is 95 M€.

11.1.8. Methane – full load

As for the hydrogen and ammonia systems, the methane system was also simulated under full-load conditions. The results are given in Table 12. The result that immediately jumps out is the storage system cost. The system cost has increased to 161 M€, most of which is the cost for CO₂ capture. A breakdown of the costs is given in Figure 48. Figure 48 shows that 54% of the cost are attributed to CO₂ capture. In cases of intense system use price reduction of CO₂ storage technologies becomes the top priority for system price reduction. While the cost of the system is high, the levelized cost of storage at 98 €/MWh is not far from that of the hydrogen system under full load and far below the levelized cost of storage for ammonia.

The second interesting figure in the table of results is the efficiency. The efficiency of the system has increased, which can be explained by the size of the Sabatier reactor. The Sabatier reactor size was increased to nearly 30,000 kg of methane per hour. For every kg of methane produced energy is added to the system, resulting in a higher efficiency than the hydrogen system. The question is whether this is realistic. The implications of this will be discussed in the sensitivity analysis in chapter 0.

Table 12: Output of simulations for the scenario of an ammonia storage system containing a 425 MW electrolyser and 425 MW gas turbine running at full capacity for one year, connected to a Sabatier reactor. Compared to the same methane storage system connected to a 1 GW wind plant and a Dutch demand cycle, where the Sabatier reactor has a minimum load of 40%.

	Methane in VRES	Methane under full load
Storage system cost	95.9 M€	161 M€
Levelized cost of storage	276.4 €/MWh _{output}	98 €/MWh _{output}
Roundtrip efficiency	32.5%	43.9%
Curtailement	2 GWh	0 GWh
Grid demand	712,7 GWh	2.1 TWh
Sabatier reactor size	9800 kg/h	29988 kg/h
Hydrogen buffer size	2.8 kt	0 kt

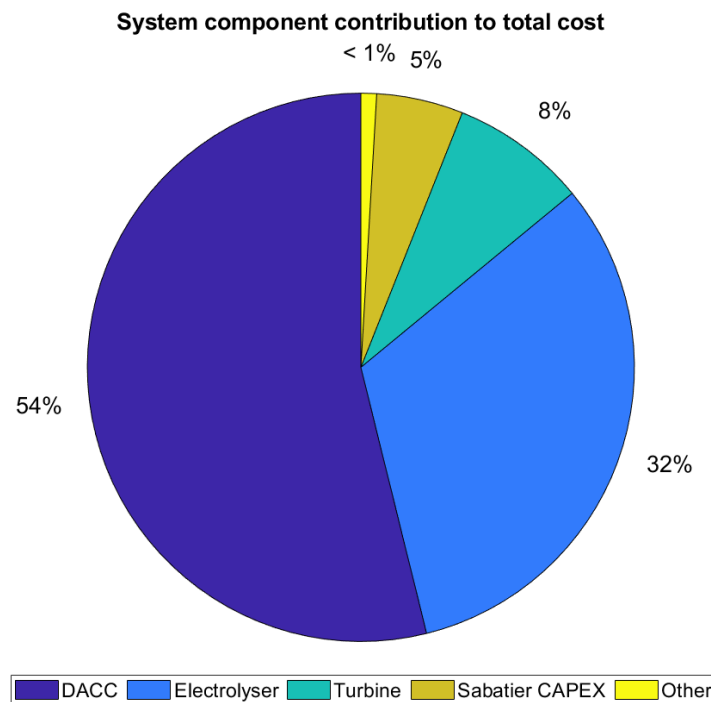


Figure 48: Breakdown of costs for a methane PtXtP system under constant maximum load.

11.2. Added value of storage

This scenario was created to assess the impact of a storage system on grid interaction. It also compares the storage system to the alternative of oversizing the wind park and curtailing. The results are given in Figure 49 and Figure 50. The total demand in this system is 3.3 TWh, the annually generated wind energy is also 3.3 TWh. Assuming a 70% renewable electricity generation, where the other 30% comes from fossil backup generators, means 1.1 TWh of grid exchange is acceptable. The 1 GW wind park without storage creates a grid exchange of less than 1.1 TWh, which means the system without storage can also reach sustainability goals. However, the same result can be achieved with a wind park of 0.65 GW, if a hydrogen storage system is implemented. This reduction in wind park size reduces the wind park cost and reduces the area required for wind generation.

As shown in Figure 49 and Figure 50, the storage system becomes more important when the share of grid interaction is reduced. A scenario with zero grid interaction is possible by scaling up the wind park to 1.45 GW when implementing a storage system. This becomes relevant when planning for the electricity grid in 2050, with 100% renewable electricity generation. Figure 50 shows that even a 25 GW wind park would not reduce the grid exchange below 150 GWh (4.5%). The conclusion is that the storage system is not vital for achieving the sustainability goals of 2030 but could reduce the size of the wind park with 35%. For further reduction of grid exchange energy storage becomes more relevant and even indispensable.

The investment cost of a 1 GW offshore wind park is 1,600-1,900 €/kW, with 41 €/kW/year OPEX (PBL, 2019). Assuming a lifetime of 25 years this is equal to an annualized cost of 154-176 M€ for a 1 GW wind park. The wind park can be reduced with 35%, which is equal to 54-62 M€. Given the cost of a hydrogen storage system required for a 650 GW wind park is 63.5 M€, this means for 70% renewable energy penetration the cost of oversizing is slightly lower or equal to the invest in a storage system. The cost of a storage system scales roughly linearly, while the wind park oversizing increases exponentially. Investment in a large-scale storage system is therefore economically feasible for VRES shares of 70% and higher.

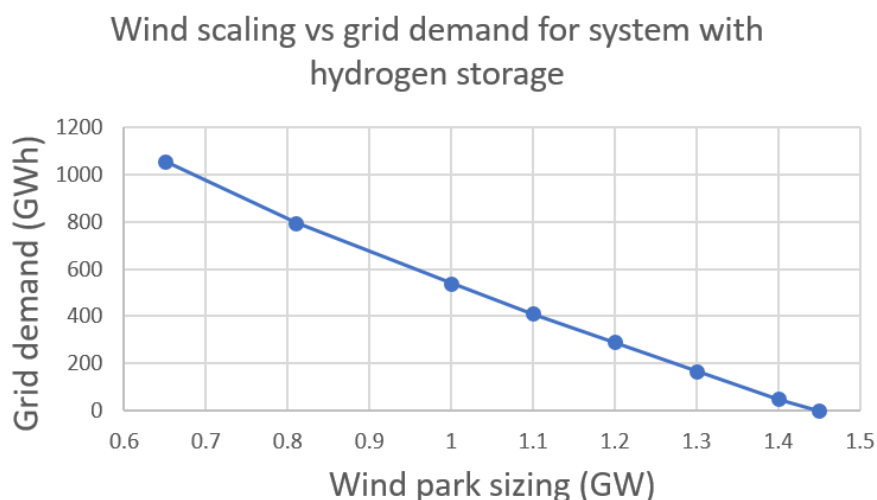


Figure 49: Tradeoff between system oversizing and grid demand for a system with hydrogen storage, in case of a yearly demand of 3.28 TWh.

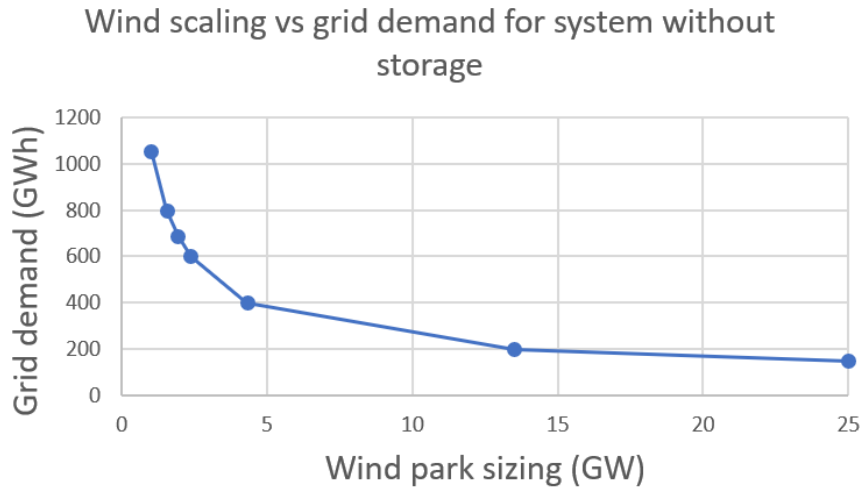


Figure 50: Tradeoff between system oversizing and grid demand for a system without storage, in case of a yearly demand of 3.28 TWh.

11.3. Comparison

All scenarios have been run and results have been discussed in the previous sub-chapter. This sub-chapter will compare the performances of the different systems, compares the different system components and evaluates the impact of the VRES input on the performance of the system. The systems are compared based on the KPI's as identified in the methodology, the KPI's are system cost, levelized cost of storage, roundtrip efficiency and potential capacity in the Netherlands. The potential capacity in the Netherlands is taken from literature (Van Gessel, Breunese, Juez Larré, Huijskes, & Remmelts, 2018). For each energy carrier the results of the flexible, VRES scenario is gathered in Table 13. As a reference, the PHES and CAES information is also presented in the table. Important to keep in mind is that the PHES and CAES values are not specified for use in a VRES system, a direct comparison is therefore not possible. The values are meant to be used as a frame of reference.

Table 13: Gathered results of all PtXtP technologies in VRES systems. The no storage scenario consists of a 1 GW wind park and matching average Dutch electricity use. The H₂ scenario contains a 425 MW electrolyser and fuel cell. The NH₃ scenario contains an electrolyser, ammonia fuel cell and HB reactor with a minimum load of 33%. The CH₄ scenario contains an electrolyser, gas turbine and Sabatier reactor with a minimum load of 40%. PHES and CAES information given for frame of reference.

	No storage	H ₂	Flexible NH ₃	Flexible CH ₄	PHES	CAES
Storage system cost (M€)	0	97.7	111.6	95.9	n.a.	n.a.
Levelized cost of storage (€/MWh _{output})	n.a.	264	630	276.4	6.3-24	27-49
Roundtrip efficiency	100%	35%	16.7%	32.5%	75-85%	60%
Potential capacity	n.a.	456 TWh	n.a.	1939 TWh	0	0-0.55 TWh
Hydrogen buffer size	n.a.	1.67 kt	2.44 kt	2.8 kt	n.a.	n.a.
Grid demand	1.056	689 GWh	880.3	712.7		

11.3.1. Bottlenecks

The scenarios were designed to test bottlenecks as found in literature research. The bottlenecks as identified in chapter 0 are presented again in Table 14, which is adapted from Table 3 in chapter 6.6.

Table 14: Representation of technological bottlenecks as identified in literature. The system components are feedstocks used for energy storage ('carrier', e.g. purified water to produce H₂, CO₂ for creation of methane), the absorption of hydrogen or electricity ('production'), transport, storage and electricity or hydrogen regeneration.

	Hydrogen (g)	Methane	Ammonia
Carrier	++	--	++
Production/ 'charging'	+	+	+
Transport	+	++	+
Storage	-	++	+
Regeneration/ 'discharging'	+	++	+

The most problematic system components in the hydrogen system are transport and storage. Hydrogen pipelines are more expensive than gas pipelines because of leak risks and metal embrittlement (NIST, 2015). Hydrogen storage in tanks is both expensive and dangerous. The production of methane and ammonia would prevent the need for hydrogen storage and transport. The first important conclusion drawn from the simulations is that methane and ammonia production in the Haber-Bosch and Sabatier reactor do not prevent the need for hydrogen storage and transport. The hydrogen buffers required are in fact bigger than the hydrogen storage capacity in a hydrogen storage system.

For methane the bottleneck identified was the capture of CO₂. The simulations have shown that DAC is indeed an energy intensive and costly procedure. However, the costs and energy use of the DAC system seem to be compensated by the energy efficiency of the system and the use of the existing gas grid.

For ammonia systems the problematic area is regeneration. The storage system requires a 425 MW fuel cell to balance the demand and mismatch. Ammonia can be regenerated in SOFC's, but this is a new technology and fuel cell research is focused mostly on hydrogen fuel cells. The question that remains is if ammonia fuel cells scale up fast enough to meet this 425 MW target.

A potential bottleneck for all system components was the system size. No PtXtP plant of this size exists yet. The HB and Sabatier reactor sizes required in these scenarios are not exceptionally large (ISPT, 2019). The electrolyser size of 425 MW is larger than any functioning electrolysers at this moment, but ISPT has already started the development of a 1 GW electrolyser, which should be built between 2025 and 2030 (ISPT, 2019). Fuel cells are not scaled up as fast. Fuel cells with a scale of 1-10 MW are predicted to be available by 2030 (Gigler & Weeda, 2018). The scale up of fuel cells is slow because fuel cell stacks are easier to scale out than up. This means the future PtXtP would require 43 10 MW fuel cells.

The storage components of the system should also be checked for size. The size of the hydrogen caverns required is 1.67-2.8 kt of H₂, this is equal to 0.019-0.032 bcm of hydrogen, assuming an 85% working volume and 100 bar pressure (Van Gessel, Breunese, Juez Larré, Huijskes, & Remmelts, 2018). Caverns this small are not available in South-Holland, as was assumed in this thesis. Instead, smaller

caverns (<0.5) should be located, for example in Noord-Brabant or off-shore, as is shown in Figure 51. The ammonia tank necessary to store all energy should be able to contain nearly 4 kt of ammonia. The typical ammonia tank can contain 50,000 m³ of ammonia, which is equal to 34.1 kt, assuming a density of 682 kg/m³ (Westfalen, 2015). This means the ammonia tank sizing is not problematic.

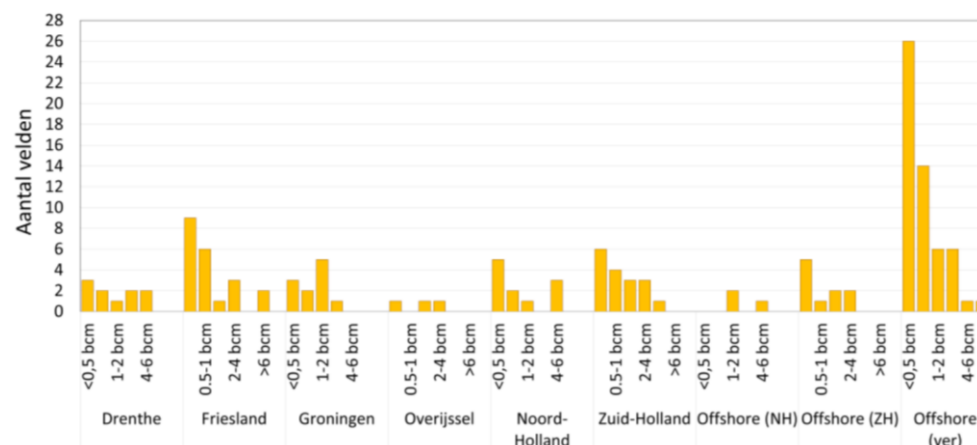


Figure 51: Numbers of caverns suitable for hydrogen storage per size and location. The y-axis shows the number of fields. (Van Gessel, Breunese, Juez Larré, Huijskes, & Remmelts, 2018).

11.3.2. VRES application

One of the questions raised in this report is the impact of a VRES grid on the performance of the system. The results of the VRES and full load simulations are given in have not resulted in a straightforward answer for the impact on system efficiency. The efficiency of the H₂ system is influenced negatively by the VRES application, this is due to the relative increase of standby power use. The efficiency of the ammonia system is influenced positively by the VRES use, which can be explained by the smaller size of the ammonia reactor. The methane system is influenced positively by the increase of the Sabatier reactor. This is because the found input values lead to a net generation of energy in the Sabatier reactor.

Table 15: Gathered results of system performance when connected to the 1 GW wind park and Dutch electricity demand, compared to system performance under full load (425 MW in and 425 MW out for one year)

	H ₂ in VRES	H ₂ full load	NH ₃ in VRES	NH ₃ full load	CH ₄ in VRES	CH ₄ full load
Storage system cost (M€)	106	98	111.6	125	95	161
Levelized cost of storage (€/MWh)	288	72	630	278	276.4	98
Roundtrip efficiency	35%	36.3%	16.7%	11%	32.5%	43.9%

Comparison between the VRES and full load scenarios does show the levelized cost of energy storage increases in all cases in a VRES system. In these scenarios the levelized cost of storage is increased by a factor 2.2-4. The scenario with the strongest cost increase is H₂ because it is the most CAPEX heavy. The system with the smallest increase in cost for VRES is methane, which is explained by the reduced need for CO₂ capture. The conclusion is that the levelized cost of storage increases strongly for VRES storage systems, potentially by a factor 4 for CAPEX dominated systems.

11.3.3. System component comparison

The breakdowns of cost and energy losses are gathered and presented together in Figure 52 (see next page). Figure 52: Overview of system component contributions to cost and energy use for the hydrogen, ammonia and methane storage system in a VRES scenario.

The first observation with regards to the system cost is that the electrolyser makes up about half of the cost for each system. Fuel cells are expensive too, and even the gas turbine for which only the OPEX is paid contributes significantly to the cost. This means the cost of conversion of energy is way more expensive than the cost of storage and transport. Energy losses can also be attributed mostly to the electrolyser. This can be explained by its low efficiency, but also by the fact that the fuel cells are at the beginning of the conversion chain. The energy input into the electrolyser is therefore larger than the energy input into the fuel cells, as a portion of the energy is already lost before reaching the fuel cell. The conclusion is that any efficiency improvements or cost reductions done on the electrolyser will have the biggest effect on the overall system efficiency and cost. Significant improvements can also be achieved by improvement of the fuel cells and carbon capture system. Unlike the predictions based on literature, transport and storage of hydrogen are not the main contributors to cost or energy loss in a large-scale energy storage system. This may of course differ for other applications, e.g. energy transport over large distances.

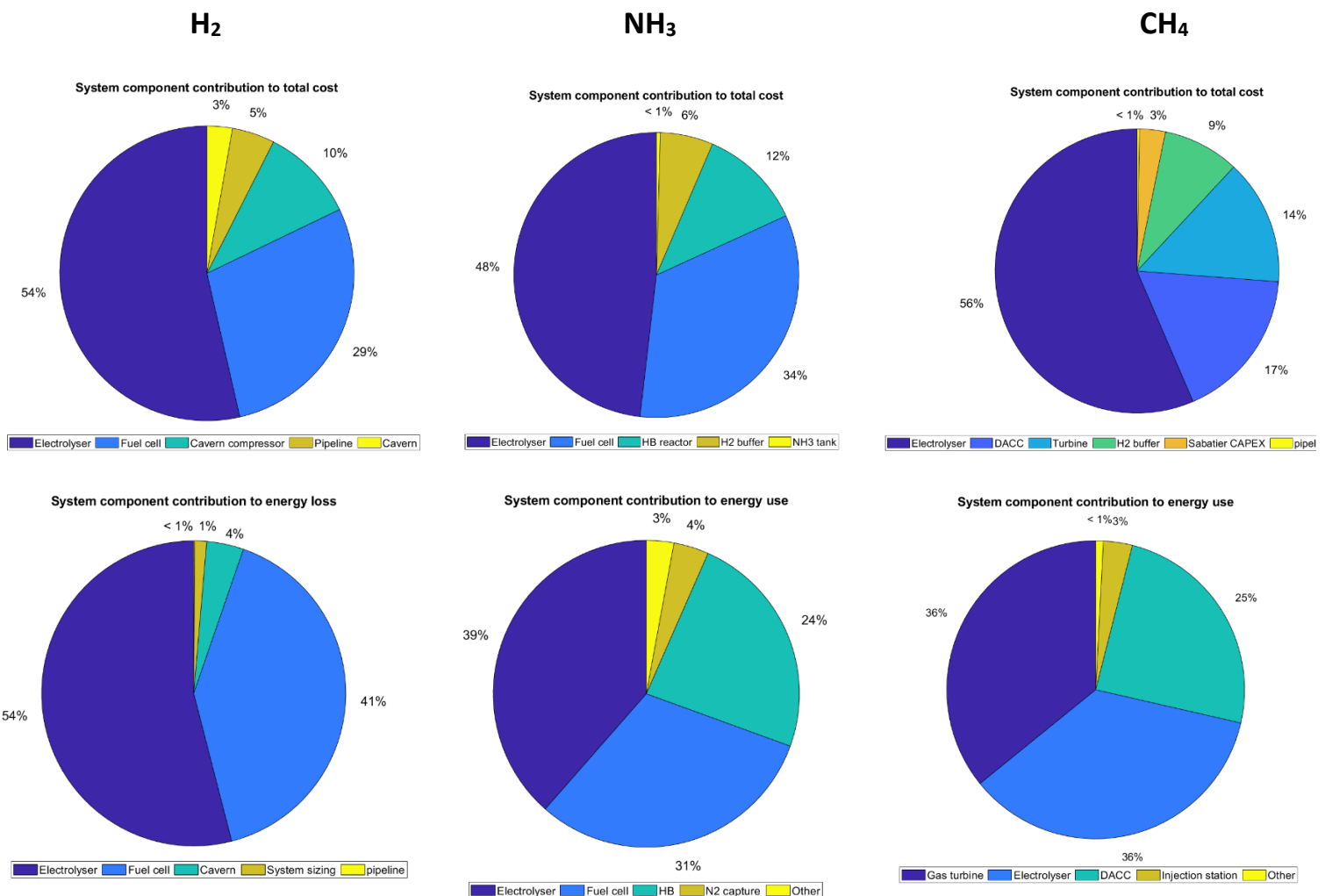


Figure 52: Overview of system component contributions to cost and energy use for the hydrogen, ammonia and methane storage system in a VRES scenario.

12. Sensitivity analysis

The results of the designed scenarios were discussed in the previous chapter. However, before drawing any conclusions the accuracy of the models must be tested. In order to do so several testing scenarios were designed. The first step is to evaluate the accuracy of the input values. The most impactful system parameters are identified, and the effect of their variations is mapped. This will give insight in the uncertainty of the results. As a second step, scenarios are designed to evaluate the circumstances to which the PtXtP systems were subjected. They represent different use cases, with the aim to evaluate if the generated results are true for other PtXtP system applications too.

12.1. Uncertainty of variables

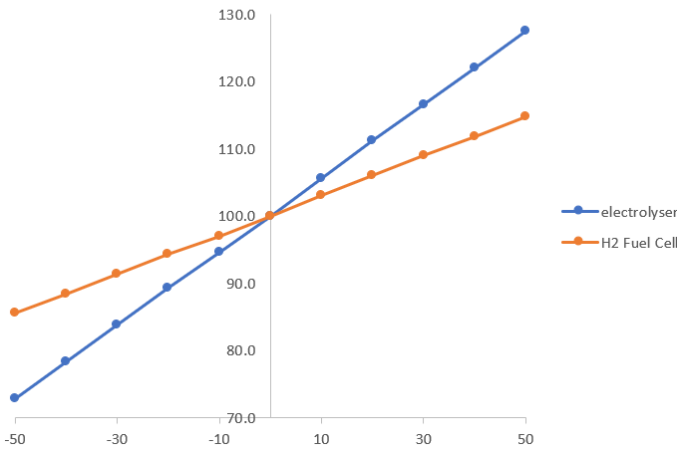
To determine the uncertainty of the models the effect of changing input variables on the output of the model is determined. The outputs are system cost, efficiency and levelized cost of storage. Since the levelized cost of storage is a product of the first two, the effect on system cost and efficiency are evaluated. To reduce the number of variables to be checked, only the variables of the system components with a large impact are evaluated.

For each component the parameter with the most impact is selected and varied between 50% and 150% of its initial value with steps of 10%. The impact on the storage system cost and roundtrip efficiency is then evaluated. The varied characteristics for cost are the electrolyser CAPEX, hydrogen fuel cell CAPEX, ammonia fuel cell CAPEX, HB reactor CAPEX, cost of CO₂ per kg and the gas turbine CAPEX. The impact of different system variables is plotted in the spider diagrams below. Figure 53 contains the spider plots that show the impact of cost related parameters on storage system cost, along with spider diagrams of uncertainty for roundtrip efficiency.

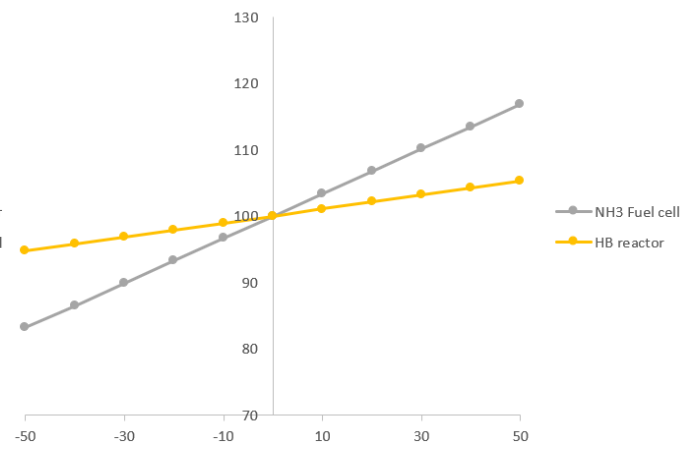
The diagrams show all cost sensitivities are linear, which can be explained by the nature of the variation. As an example, increase of the electrolyser CAPEX with 10% increases the electrolyser cost from 53 to 58.3 M€, adding 5.3 M€ to the storage system cost, this is repeated for each step up to 50% increase or decrease. The same is true for the other characteristics. In the cost calculations the electrolyser CAPEX is the most impactful. However, the range found in literature research is relatively small. More important is the hydrogen fuel cell and the cost of CO₂. These have a large impact on the system cost, and the predicted costs vary strongly in literature. The same is true for the ammonia fuel cell. To identify the most pressing uncertainties, the minimum and maximum of the uncertainty range as identified in chapter 9 are put into the model. The purpose is to identify the uncertainty range of the model output caused by the lack of accurate data. The results are given in Table 16.

The same was done for the roundtrip efficiencies. The components with the biggest impact on roundtrip efficiency are the electrolyser efficiency, hydrogen fuel cell efficiency, HB electricity use, ammonia fuel cell efficiency, Sabatier selectivity and the DAC heat use. The spider graphs illustrating the impact on roundtrip efficiency are given in Figure 53. The impact of these parameters seems linear, but the impact of DAC, Sabatier selectivity and electrolyser efficiency is in fact non-linear. The DAC heat use, Sabatier selectivity and electrolyser efficiency reduce the amount of hydrogen/methane that enters the storage system, reducing the amount of energy needed by other system components. A lower Sabatier selectivity and higher DAC heat use reduce the required size of the HB reactor. However, the non-linear effects are small and near insignificant compared to the direct effects. The diagrams also show that Sabatier selectivity and DAC heat use have a small impact on the roundtrip efficiency. The most critical values are the HB electricity use and ammonia fuel cell efficiency, as can also be concluded from Table 17. These variables have both a large impact and large uncertainty.

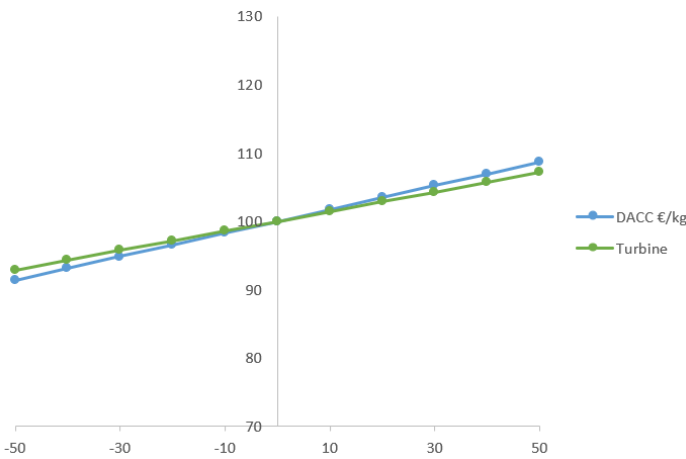
Relative effect of variation of input variables on system cost in the hydrogen storage system



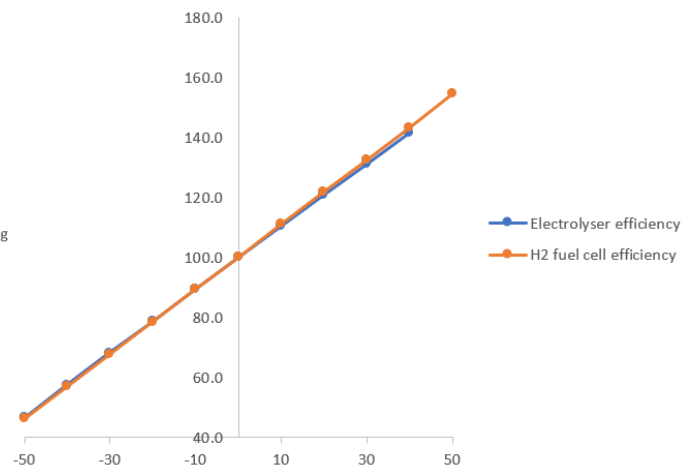
Relative effect of variation of input variables on system cost in an ammonia storage system



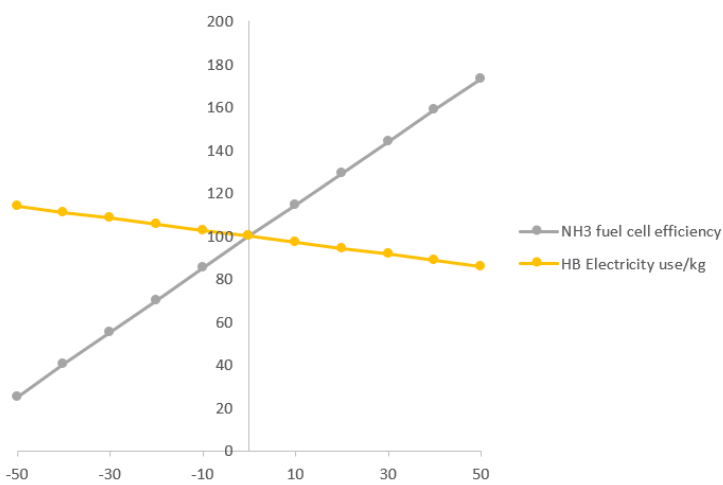
Relative effect of variation of input variables on system cost in a methane storage system



Relative effect of variation of parameters on system efficiency in a hydrogen storage system



Relative effect of variation of input variables on system efficiency



Relative effect of variation of input variables on system efficiency in methane storage system

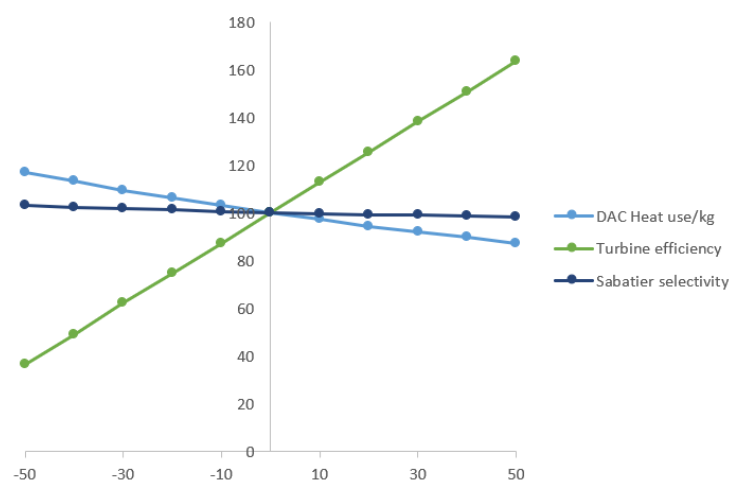


Figure 53: Relative impact of different parameters on the storage system cost and roundtrip efficiency. All axes are expressed in percentages. Cost dependencies are linear, efficiency dependencies contain a slight curvature.

Table 16: Uncertainty ranges of model output for storage system cost for the range of data found in chapter 9.

	Electrolyser	H ₂ fuel cell	HB reactor	NH ₃ fuel cell	DAC cost
Tested scenario	H ₂ in VRES	H ₂ in VRES	flexible NH ₃ in VRES	flexible NH ₃ in VRES	CH ₄ in VRES
Variable	Electrolyser CAPEX (€/((kg/h)/y))	CAPEX (€/MW/y)	CAPEX (€/((kg/h)/y))	CAPEX (€/MW _e /y)	CO ₂ cost (€/kg)
Initial value	6,000	67,400	550	88,500	0.11
Uncertainty range	4,400-7,620	3,200-180,000	282-840	86,000-91,000	0.0427-0.27
Initial system cost	97.7 M€	97.7 M€	111.6 M€	111.6 M€	95.9 M€
Storage system cost range	83.6-112.3	70.6-145.7	106.2-117.9	110.7-112.8	85.5-120.5

Table 17: Uncertainty ranges of model output for roundtrip efficiency based on uncertainty in parameters from chapter 9.

	Electrolyser	H ₂ fuel cell	HB reactor	NH ₃ fuel cell	DAC	Gas turbine
Tested scenario	H ₂ in VRES	H ₂ in VRES	flexible NH ₃ in VRES	flexible NH ₃ in VRES	CH ₄ in VRES	CH ₄ in VRES
Variable	Efficiency	Efficiency	Electricity use per kg	Fuel cell efficiency	Heat use/kg	Turbine efficiency
Initial value	70%	58%	1.3 kWh	56%	1.24 kWh	60%
Uncertainty range	61-82%	45-67%	0.7-3.5 kWh	35-70%	0-2.25 kWh	50-60%
Initial roundtrip efficiency	35%	35%	16.7%	16.7%	32.5%	32.5%
Roundtrip efficiency range	29.9-40.8%	26.2-40.3%	9.1-18.8%	7.2-22.7%	32.4-34.8%	26.4-32.5%

12.2. Use case scenarios

12.2.1. Wind park owner

In all scenarios the storage system was used to match generation and demand, which is a logical application for a VRES grid when considered from the viewpoint of the grid operator, in this case TenneT. In reality, TenneT is not allowed to do any energy storage or delivery into the grid. The system is more likely to be used by the owner of a wind park. In that case the generation shouldn't meet demand, but a constant output instead which is agreed upon in contracts (Zanchi, Porter, & Miller, 2017). This scenario is created to check if the used scenarios are a good test for large-scale energy storage systems in general, not just for demand-generation balancing.

In this scenario the constant output of the system is selected to be the average of the generation, so the net mismatch at the end of the year is zero. The scenario run with the hydrogen storage system. If no changes are noticeable here, there is no point in further simulation of other storage systems.

Table 18: Results of simulation of a hydrogen storage system serving Dutch electricity demand, compared to the simulation output of a hydrogen storage system serving a constant output.

	H ₂ – demand following	H ₂ – constant output
Storage system cost	106 M€	110 M€
Levelized cost of storage	288 €/MWh _{output}	299 €/MWh _{output}
Roundtrip efficiency	35%	35%
Curtailement	6.45 GWh	6.45 GWh
Grid demand	689 GWh	689 GWh
Salt cavern size	1.67 kt H ₂	2.36 kt H ₂
Maximum surplus of electricity	530 (MW)	459 (MW)
Maximum deficit of electricity	480 (MW)	375 (MW)

The scenario shows the mismatch in the new user case has lower peaks, but the requirement for hydrogen storage is increased significantly due to the timing of the peaks. The storage system cost is higher in case of the constant output, which is due to the larger cavern size required. While the changes do have an impact, the impact is not so radical that the other conclusions should be drawn.

12.2.2. H₂ with battery

In all scenarios the electricity mismatch is compensated by the electrolyser and fuel cell. In the previous chapters however, PtXtP was described as an energy storage medium for large scale energy storage (IEA, 2015). PtXtP is less suitable for short term energy storage because of the low conversion efficiency and high cost of power capacity. Once the energy containing chemical is produced the transport and storage are relatively cheap, as can be deduced from the tables in chapter 9. The prediction is that PtXtP systems will always contain short term energy storage media (Energy Storage NL, 2019).

In order to create realistic scenarios batteries were added to the previous system. The batteries could serve two purposes. The first option is to use them as a primary storage system, where the electricity mismatch is initially compensated by energy in the batteries, this might prevent unnecessary efficiencies of PtXtP. The PtXtP is used once the batteries are full or empty; any overflow is redirected to the fuel cell and electrolyser. Figure 54 illustrates a hypothetical scenario where small mismatches can be compensated by a relatively small battery pack, sparing the electrolyser and reducing energy losses.

The second use-case is to use batteries as a buffer for large power surges, which allows for a smaller electrolyser. The mismatch is initially compensated by the electrolyser or fuel cell, any power overflow is stored in the batteries. When the mismatch drops, and the electrolyser or fuel cell have spare capacity, the energy in the batteries is used. Figure 55 illustrates how a secondary battery pack could reduce the pressure on a PtXtP system by spreading peaks. The advantage of this system is the reduction in electrolyser size, which is a large cost component in the PtXtP system (HyUnder, 2014).

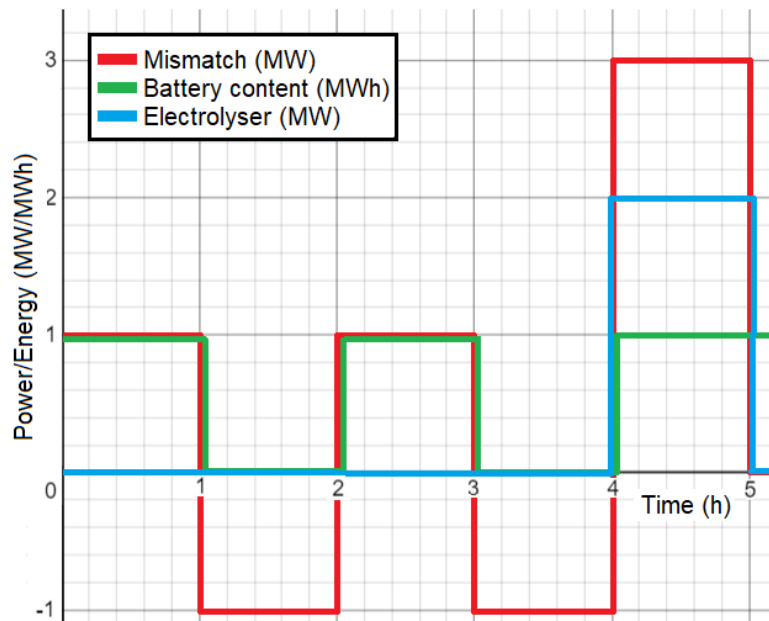


Figure 54: Illustration of the potential advantage of the use of a primary battery system (discrete steps), in this case the battery capacity is limited to 1 MWh.

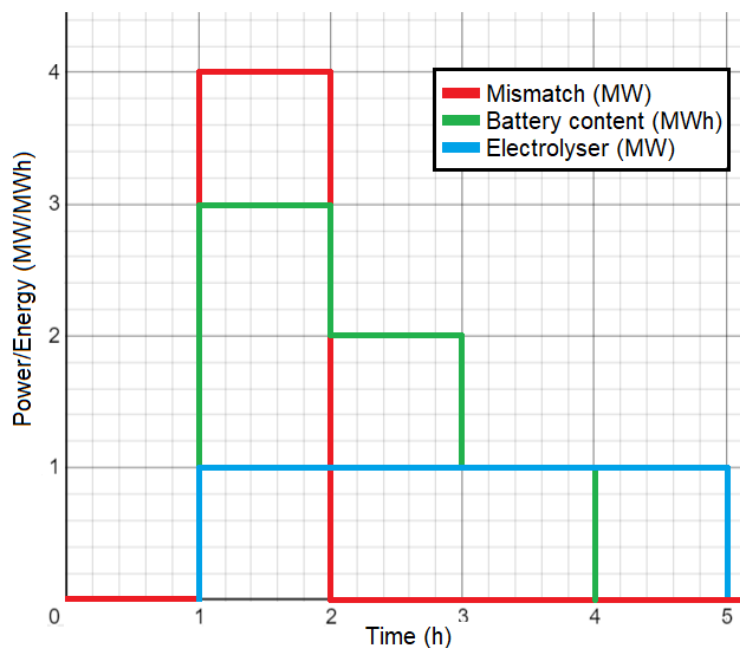


Figure 55: Illustration of potential advantages of a secondary battery storage system (discrete steps), in this case the electrolyser power is limited to 1 MW.

The results of the two scenarios are given in Figure 56 and Figure 57. Both figures show the use of batteries allow for a reduced system size. The fuel cell and electrolyser size in the primary battery system can be reduced from 425 to 300 MW, and results in a slightly lower grid demand (688 to 658 GWh). In the secondary battery system, the fuel cell and electrolyser can also be reduced to 300 MW, but the grid demand is not reduced. For both scenarios the system cost is almost twice as high as for the hydrogen-only scenario (205 M€ instead of 105 M€).

A closer look at the battery systems shows the batteries are used sub-optimally. They only go through the equivalent of 63 cycles each year. This means the potential advantages of added batteries to a storage system could be much higher. The flaw in this simulation is in the control system, the use of a buffer without predictions is near useless (Stikkelman, personal conversation, 2020). A better predictive control system is required to do real predictions, but this is outside the scope of this research. The conclusions to draw from this scenario are that batteries are relatively expensive and efficient (which was known before the start of this thesis), and that the addition of batteries to the system influences the system sizing of fuel cell and electrolyser positively, but at a cost. The other scenarios are designed without batteries, this scenario shows that the outcome of those might turn out to be too pessimistic.

Table 19: Output of simulations for the scenario of a 1 GW wind plant generating electricity for the Dutch energy grid, connected to a hydrogen storage system, without batteries, compared to a system with primary or secondary batteries.

	H ₂ , no batteries	With primary battery system	Secondary battery system
Storage system cost	106 M€	207,3 M€	205 M€
Levelized cost of storage	288 €/MWh	519 €/MWh	549 €/MWh
Roundtrip efficiency	35%	38%	35%
Curtailement	64.5 GWh	3.49 GWh	6.45 GWh
Grid demand	0.689 TWh	0.658 TWh	0.683
Fuel cell size	425 MW	300 MW	300
Electrolyser size	425 MW	300 MW	300
Pipeline size	9000 kg/h	6300 kg/h	6300
Salt cavern size	1.67 kt H ₂	2.151 kt H ₂	1.7 kt H ₂

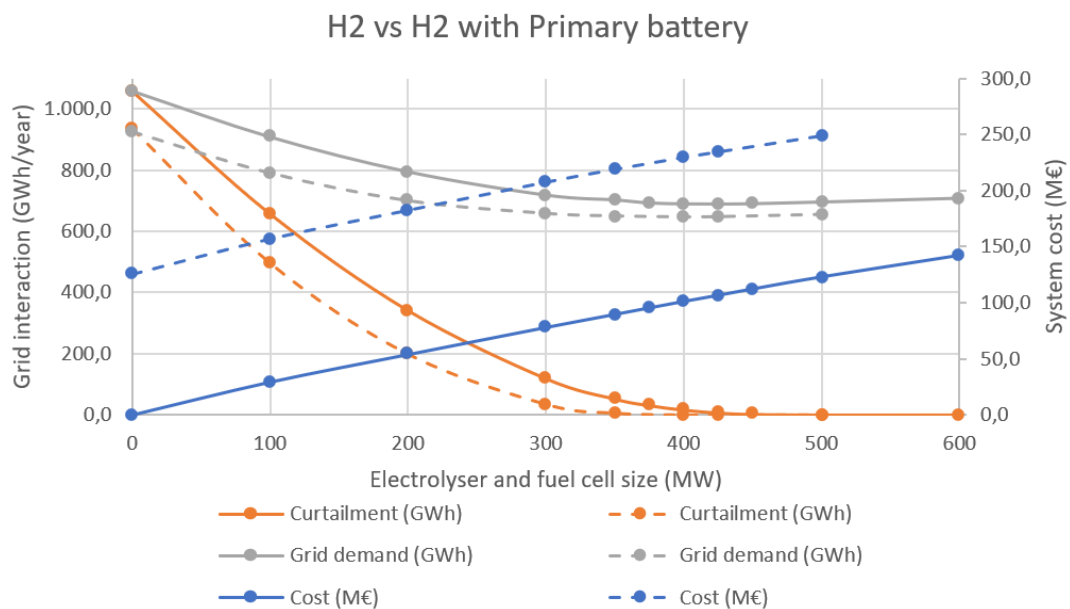


Figure 56: Performance of a storage system containing a hydrogen storage system and primary batteries. Continuous lines indicate the hydrogen system without batteries, dotted lines indicate the mixed system.

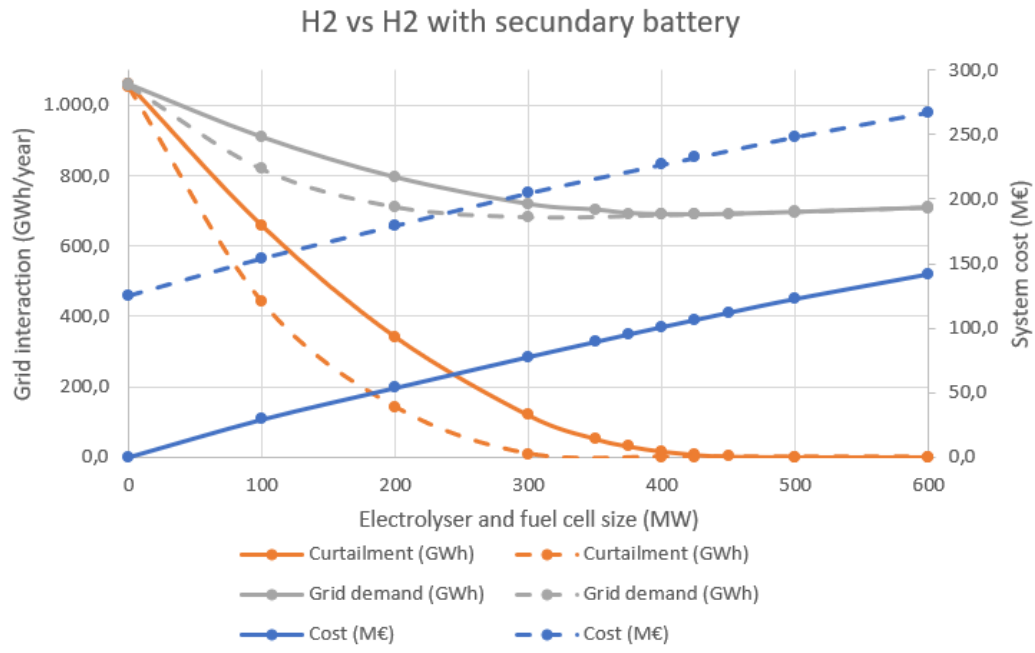


Figure 57: Performance of a storage system containing a hydrogen storage system and secondary batteries. Continuous lines indicate the hydrogen system without batteries, dotted lines indicate the mixed system.

12.2.3. Different year as input

The model was based on hourly data of demand and wind generation in 2018. This scenario is designed to check the performance of the system and the validity of the model in another year, in this case 2017. Data was taken from the same platform and modified in the same way to create the 2030 equivalents. The resulting net mismatch is still zero, as that is how the data is defined, but the fluctuations differ. The maximum mismatch in 2017 is 590 MW, rather than 530. The minimum mismatch in 2017 is -500 MW, rather than -480. The mean mismatch is still zero. The results of the system for 2017 and 2018 are given in Table 20. While there are some differences, the differences are small enough to say the performance of the system is not significantly influenced by the input year.

Table 20: Comparison of simulation outcomes of a hydrogen storage system when connected to a 1 GW wind generation profile based on the year 2017 and 2018 for comparison and validation of the model's assumptions. Table shows there is no significant difference in system performance due to the wind profile.

	2017	2018
Storage system cost	97.9 M€	97.7 M€
Levelized cost of storage	265 €/MWh	264 €/MWh
Roundtrip efficiency	35%	35%
Curtailment	10 GWh	6.45 GWh
Grid demand	691 GWh	689 GWh
Fuel cell size	425 MW	425 MW
Electrolyser size	425 MW	425 MW
Pipeline size	9000 kg/h	9000 kg/h
Salt cavern size	1.68 kt H ₂	1.67 kt H ₂

13. Conclusion

The purpose of this thesis was to compare different PtXtP systems and map their potential for use as a large-scale energy storage system. The main question of the report was the following:

What is the techno-economic potential of power to x to power technologies for energy storage of variable renewable energy in the Netherlands in 2030?

The following sub-questions were posed:

1. How do PtXtP technologies compare to existing energy storage technologies and to each other?
2. Which PtXtP technologies show the most potential for use as an energy storage technology in 2030?
3. What are the technical limitations to the use of PtXtP technologies as energy storage medium?

Sub-question one was answered in chapter 2. Other large-scale energy storage technologies are CAES and PHES. Both technologies are cheaper, more efficient and have a higher TRL. PtXtP systems will nevertheless be a good supplement to these because the available capacity for CAES and PHES in the Netherlands is not sufficient.

Sub-question 2 was answered in chapter 3. After an extensive comparison of all hydrogen carriers, ammonia, methane and gaseous hydrogen were selected, based on the data presented in the table below.

Table 21: Repetition of Table 3.

	Hydrogen (g)	Hydrogen (l)	Methane	Methanol	Ammonia	Formic Acid	LOHC	Metal
Carrier	++	++	--	--	++	--	--	--
Production/ 'charging'	+	+	+	-	+	-	-	-
Transport	+	-	++	-	+	-	+	--
Storage	-	--	++	++	+	+	++	++
Regeneration/ 'discharging'	+	+	++	+	+	-	-	+
Roundtrip efficiency	38% ¹	34% ¹	28% ¹	27% ¹	30% ¹	25% ²	24% ¹	28% ¹
Points	10	8	11	7	11	9	7	5

In order to answer question 3, the different system components were investigated. The dominant technologies were identified, and potential bottlenecks were found. The dominant technologies were subjected to further investigation to collect input data for the model. The result is a current and elaborate overview of information available on PtXtP system components. The overview was presented in tables in chapter 6.

After that the PtXtP systems were modelled and different scenarios were generated to test the performance of the storage systems. Several conclusions were drawn from the models:

- The required size of the HB and Sabatier system increases strongly with flexibility. An ammonia system with 33%-100% flexibility can be 60% smaller than a 0%-100% system.
- The use of a HB and Sabatier reactor does not prevent the necessity of hydrogen storage and transport. The hydrogen buffers they require are larger than the required hydrogen storage space in a PtH₂tP system. Even with a flexible production range of 1%-100% the hydrogen buffer must have a capacity of at least 150,000 kg.
- The size of fuel cells required to meet demand with the energy of a 1 GW plant is 425 MW. This is larger than any current or expected fuel cells, which means upscaling is an important task.
- CO₂ capture is indeed costly and energy consuming, but the cost and energy used do not negate the advantages of the PtXtP storage system.
- The cost and energy consumption of hydrogen transport and storage are relatively small compared to energy conversion steps. This means the drawbacks for a hydrogen system are less significant than the drawbacks of the ammonia or methane system.
- Using the storage systems intermittently to meet VRES demand increases the levelized cost of storage significantly, in these models the LCOS increased by factor 2.2-4.
- The system component with the highest cost and energy loss is the electrolyser. Cost reduction and efficiency improvement will be most fruitful if they are achieved there.
- The added value of a storage system is significant wind park size reduction. In addition, zero grid exchange can only be achieved when implementing a storage system. With lower shares of grid exchange, storage becomes increasingly more valuable.

The final sub-question asked for a comparison of the different PtXtP systems. The table with results of the systems is given below. The results seem to recommend hydrogen as the best energy carrier. This makes sense, because energy is only transported over short distances (100 km) in case of a large-scale energy storage application. Extra conversion steps create extra losses, cost and complexity. However, the results are not entirely conclusive, as the uncertainty for some system components is high. Especially the ammonia system deals with large uncertainties. In order to create a better comparison more information is needed about the cost of the ammonia and hydrogen fuel cells and the energy consumption of the ammonia reactor.

Table 22: Table containing the output of the most important scenarios, hydrogen in a VRES system, flexible ammonia production in a VRES system and flexible methane production in a VRES system.

	No storage	H ₂ -VRES	NH ₃ -flexible	CH ₄ - flexible
Storage system cost (M€)	0	97	111.6	95
Levelized cost of storage (€/MWh)	n.a.	264	630	276.4
Roundtrip efficiency (%)	100	35	16.7	32.5
Potential capacity in NL (TWh)	n.a.	456	n.a.	1939
Hydrogen buffer size (kt)	n.a.	1.67	2.44	2.8
Grid demand (GWh)	1,056	689	880.3	712.7

The main question of the report was as follows: *What is the techno-economic potential of power to x to power technologies for energy storage of variable renewable electricity in the Netherlands in 2030?*

The short answer is that energy storage is necessary, and no alternatives are available in the Netherlands. PtXtP will therefore have to play a large role in the future Dutch electricity grid. However, use of PtXtP storage will increase the price of electricity and several technological developments, mostly scale-ups, are necessary before a PtXtP system is feasible.

14. Recommendations

Based on the conclusions drawn in the previous chapter several recommendations are done. The first recommendation is to start the development of a (semi-)large-scale hydrogen PtXtP demonstration plant, containing a hydrogen storage cavern. The purpose would be to gather more information on real-time performance of the system. Interesting information to distract from such a demonstration plant are the impact of VRES use on system component lifetime and roundtrip efficiency. For some system components the startup and shutdown energies are already known, as well as the output dependent efficiency, but for most system components these are yet unknown. Implementation of a large-scale PtXtP storage plant will also allow for data collection on the effect of scale-up. A lot of data found in literature and used here was linearly interpolated from small scale systems, which reduces the reliability of the data strongly. When developing a demonstration system, the primary should be on development of the electrolyser and hydrogen cavern. The electrolyser contributes the lion share of the costs and energy losses, which means any improvements there will have a large impact on the entire system performance. The hydrogen storage cavern should receive focus because it is a relatively new and uncertain technology, while there is no alternative to this type of large-scale hydrogen storage. In addition, the model showed the hydrogen storage cavern cannot be avoided with the current technology by using methane or ammonia as hydrogen carriers.

While the system is useful for research purposes, it should already be operational to allow further growth of the share of VRES's in the Dutch electricity grid. The Netherlands currently does not have alternative options for large-scale energy storage, while the necessity for storage will grow strongly. In order to reach a 70% renewable system in 2030 and 100% renewable system in 2050 large shares of VRES will have to be introduced to the grid. The problems occurring in the German electricity grid due to the Energiewende can be reduced and similar problems in the Dutch grid can be prevented if the development of energy storage technologies is prioritized now.

The second recommendation is to allocate means for objective comparative studies. It is important to keep investigating and comparing different energy carriers. Research and industry are strongly linked in this sector and research on this topic is subjected to large numbers of assumptions and broad uncertainties. Research can therefore (unintentionally) give colored results. Many (if not most) of the studies found during the creation of this report were done by parties with an interest in the investigated technology.

Alternatives that were not discussed in this thesis but seem extra valuable after this research are direct methane and ammonia production. These technologies prevent the use of both electrolysers and hydrogen buffers, however, these technologies are new and are difficult to scale up, which most likely means they will not be available on a large scale by 2030.

15. Bibliography

- Afif, A., Radenahmad, N., Cheok, Q., Shams, S., Kim, J., & Azad, A. (2016). Ammonia-fed fuel cells: a comprehensive review. *Renewable and sustainable energy reviews*, 822-835.
- Afman, M., & Rooijers, F. (2017). *Net voor de Toekomst*. Delft: CE Delft.
- Álvarez, A., Bansode, A., Urakawa, A., Bavykina, A. V., Wezendonk, T. A., Makkee, M., . . . Kapteijn, F. (2018). Challenges in the greener production of Formates/Formic Acid, Methanol and DME by Heterogeneously Catalyzed CO₂ Hydrogenation Processes. *Chemical reviews*, 9804-9838.
- Amar, I., Lan, R., Petit, C., & Tao, S. (2011). Solid-state electrochemical synthesis of ammonia: A review. *Solid-state electrochemistry*, Ibrahim A. Amar & Rong Lan & Christophe T. G. Petit &.
- Andersson, J., & Grönkvist, S. (2019). Large-scale storage of hydrogen. *International journal of Hydrogen Energy*, 11901-11919.
- Baier, J., Schneider, G., & Heel, A. (2018). A Cost Estimation for CO₂ reduction and reuse by methanation from cement industry sources in Switzerland. *Frontiers in energy research*, 1-9.
- Benjaminsson, G., Benjaminsson, J., & Boogh Rudberg, R. (2013). *Power-to-gas- A technical review*. Malmö: SGC.
- Bertuccioli, L., Chan, A., Hart, D., Lehner, F., Madden, B., & Standen, E. (2014). *Study on development of water electrolysis in the EU*. Cambridge/Lausanne: Fuel Cells and Hydrogen Joint Undertaking.
- Blanc, P., Ducastel, B., Cazin, J., Al Blooshi, M., Al Dhaheri, S., Ali Al Marzooqi, M., . . . Massabuau, J.-C. (2017). First-Time Implementation of Innovative In situ Biotechnology on an Offshore Platform in Arabian Gulf for Continuous Water Quality Monitoring and Early Leak Detection. *Abu Dhabi International Petroleum Exhibition & Conference* (pp. 1-17). Abu Dhabi: Society of Petroleum Engineers.
- Boemer, J. C., Burges, K., Kumm, T., Zolotarev, P., Lehrer, J., Wajant, P., . . . Brohm, R. (2011). Overview of German Grid Issues and Retrofit of Photovoltaic Power Plants in Germany for the Prevention of Frequency Stability Problems in Abnormal System Conditions of the ENTSO-E Region Continental Europe. *1st International Workshop on Integration of Solar Power into Power Systems*, (pp. 1-6). Aarhus.
- CBS. (2018). *Cijfers - Energie*. Retrieved from Trends in Nederland 2018: <https://longreads.cbs.nl/trends18/economie/cijfers/energie/>
- CBS. (2019, 03 01). *Vooraf meer groene stroom uit zon*. Retrieved from CBS - Nieuws: <https://www.cbs.nl/nl-nl/nieuws/2019/09/vooral-meer-groene-stroom-uit-zon>
- CBS. (2019, 08 13). *Windenergie; elektriciteitsproductie, capaciteit en windaanbod per maand*. Retrieved from CBS Statline: <https://opendata.cbs.nl/statline/#/CBS/nl/dataset/70802NED/table?fromstatweb>
- Cheema, I., & Krewer, U. (2018). Operating envelope of Haber-Bosch process design for power-to-ammonia. *RSC Advances*, 34926-34936.
- Chiyodacorp. (2017, n.a. n.a.). *What is "SPERA HYDROGEN" system?* Retrieved from Chiyoda Corporation: <https://www.chiyodacorp.com/en/service/spera-hydrogen/innovations/>

- Cole, W., & Frazier, W. (2019). *Cost Projections for Utility-Scale battery storage*. Golden: NREL.
- Cox, K. E., & Williamson, K. D. (1997). *Hydrogen: It's technology and implications; Volume I*. Boca Raton: CRC press.
- Croezen, H., Van Swigchem, J., Kortmann, R., & Rooijers, F. (2005). *Energiebesparing in de Nederlandse aardgasketen*. Delft: CE.
- De Boer, H. S., Grond, L., Moll, H., & Benders, R. (2014). The application of power-to-gas, pumped hydro storage and compressed air energy storage in an electricity system at different wind power penetration levels. *Energy*, 360-370.
- Del Peroa, C., Astea, N., Paksoy, H., Haghighat, F., Grillod, S., & Leonforte, F. (2018). Energy storage key performance indicators for building application. *Sustainable cities and society*, 54-65.
- Duong Dang, V., & Steinberg, M. (1977). Production of synthetic methanol from air and water using controlled thermonuclear reactor power—II. Capital investment and production costs. *Energy conversion*, 133-140.
- EASAC. (2017). *Valuing dedicated storage in electricity grids*. Halle: German National Academy of Sciences Leopoldina.
- Eisaman, M., Parajuly, K., Tuganov, A., Eldershaw, C., Chang, N., & Littau, K. (2012). CO₂ extraction from seawater using bipolar membrane electro dialysis. *Energy and environmental science* 5, 1-7.
- Energy Storage NL. (2019). *Nationaal Actieplan Energieopslag en conversie 2019*. Zoetermeer: Energy Storage NL.
- Entso-e. (2018). *Project 1002 - iLand*. Retrieved from TYNDP: https://tyndp.entsoe.eu/tyndp2018/projects/storage_projects/1002
- Entso-e. (2019, 05 06). *monthly hourly load values*. Retrieved from entso-e: https://www.entsoe.eu/data/power-stats/hourly_load/
- eStorage. (2015, 11 30). *Overview of potential locations for new pumped storage plants in EU 15, Switzerland and Norway*. Retrieved from estorage project: http://www.estorage-project.eu/wp-content/uploads/2013/06/eStorage_D4.2-Overview-of-potential-locations-for-new-variable-PSP-in-Europe.pdf
- Etsap. (2010, april). *Gas-Fired Power*. Retrieved from Etsap: https://iea-etsap.org/E-TechDS/PDF/E02-gas_fired_power-GS-AD-gct.pdf
- European Commission. (2017, 02 01). *Energy storage; The role of electricity*. Retrieved from European Commission: <https://ec.europa.eu/energy/en/topics/technology-and-innovation/energy-storage>
- Fischer Scientific. (2007, 12 14). Material Safety Data Sheet: Formic Acid.
- Floor Anthoni, J. (2010, 06 08). *The chemical composition of seawater*. Retrieved from seafriends: <http://www.seafriends.org.nz/oceano/seawater.htm>
- Flowe nitrogen systems. (n.a.). *The Energy Costs Associated with Nitrogen Specifications*. Retrieved from Compressed air best practices: <https://www.airbestpractices.com/system-assessments/air-treatmentn2/energy-costs-associated-nitrogen-specifications>

- Frank, E., Ruoss, F., Gorre, J., & Friedl, M. (2018). Calculation and analysis of efficiencies and annual performances of Power-to-Gas systems. *Applied energy*, 217-231.
- Fuel cell technologies office. (2015, 11). *Climate change*. Retrieved from United Nations: <https://unfccc.int/sites/default/files/resource/DOE%20Fuel%20Cell%20Tech%20Office%20FC%20%20Fact%20Sheet.pdf>
- Fuel cells and hydrogen joint undertaking. (2015). *Commercialization of energy storage in Europe*. n.a.: Fuel cells and hydrogen joint undertaking.
- Gas Generation Team. (2013, July 12). *Pressure Swing Adsorption Technology as an Alternative to Conventional Air Separation Part 3 of 3*. Retrieved from Parker: <http://blog.parker.com/pressure-swing-adsorption-technology-as-an-alternative-to-conventional-air-separation-part-3-of-3>
- Gaspu gas tech CO. . (2019, 06 12). *The investment cost of bottle gas nitrogen and liquid nitrogen*. Retrieved from Gaspu: <http://www.gaspusystem.com/news/shownews.php?id=63>
- Gasunie. (2018). *Verkenning 2050*. Groningen: N.V. Nederlandse Gasunie.
- Gielisse, M., Dröge, M., & Kuik, G. (2018). *Risicoanalyse aardgas transportleidingen*. Groningen: Nederlandse Gasunie.
- Gigler, J., & Weeda, M. (2018). *Outlines of a hydrogen roadmap*. Jörg Gigler, Marcel Weeda: TKI Nieuw gas.
- Goetheer, E. (2018, 09 17). Haber-Bosch: Ammonia. *Fossil-free fuel and feedstock: Lecture 3*. Delft: TU Delft icw TNO.
- Gorre, J., Ortloff, F., & Van Leeuwen, C. (2019). Production costs for synthetic methane in 2030 and 2050 of an optimized Power-to-Gas plant with intermediate hydrogen storage. *Applied Energy*, 1-11.
- Gür, T. M. (2018). Review of electrical energy storage technologies, materials and systems: challenges and prospects for large-scale grid storage. *Energy & environmental science*, 2696-2767.
- Hadjipaschalis, I., Poullikkas, A., & Efthimiou, V. (2009). Overview of current and future energy storage technologies for electric. *Renewable and sustainable energy reviews*, 1513-1522.
- Halpern, J. (1953). Kinetics of the Dissolution of Copper in Aqueous Ammonia. *Journal of the electrochemical society*, 421-428.
- Hydrogen Europe. (2018). Hydrogen, Enabling a zero emission Europe. *Technology roadmaps - Full pack*. n.a.: Hydrogen Europe.
- HyUnder. (2014). *D2.2: Assessment of the Potential, the Actors and Relevant Business Cases for Large Scale and Long Term Storage of Renewable Electricity by Hydrogen Underground Storage in Europe*". Brussels: European commission.
- Ibrahim, H., Ilinca, A., & Perron, J. (2008). Energy storage systems - Characteristics and comparisons. *Renewable and sustainable energy reviews* 12, 1221–1250.
- ICEF. (2018). *Direct air capture of carbon dioxide*. n.a.: ICEF.
- IEA. (2015). *Technology roadmap Hydrogen and fuel cells*. Paris: IEA.

- IEA ETSAP. (2014, April). *Energy Supply Technologies Data*. Retrieved from Technology collaborations program: https://iea-etsap.org/E-TechDS/PDF/E12_el-t&d_KV_Apr2014_GSOK.pdf
- IRENA. (2017). *Electricity storage and renewables: Costs and markets to 2030*. Abu Dhabi: International Renewable Energy Agency.
- ISPT. (2017). *Power to Ammonia: Feasibility study for the value chains and business cases to produce CO₂-free ammonia suitable for various market applications*. n.a.: ISPT.
- ISPT. (2019). *HyChain 3*. n.a.: ISPT.
- ISPT. (2019, March 19). Kick-off for designing a Gigawatt electrolysis plant. *ISPT.eu*, pp. <https://ispt.eu/news/kick-off-for-designing-a-gigawatt-electrolysis-plant/>.
- Ivanova, S., & Lewis, R. (2012). Producing nitrogen via pressure swing adsorption. *CEP - American institute of chemical engineers*, n.a.
- James, B., Houchins, C., Huya-Kouadio, J., & DeSantis, D. (2016). *Final Report: Hydrogen Storage System Cost analysis*. Arlington: Strategic Analysis Inc.
- Junaedi, C., Hawley, K., Walsh, D., Roychoudhury, S., Abney, M., & Perry, J. (2010). *Compact and Lightweight Sabatier Reactor for Carbon Dioxide reduction*. North Haven: American Institute of Aeronautics and Astronautics .
- Jung, M., Lempidis, G., Marklein, R., & Steffen, J. (2016). Multifunctional bidirectional Charging of Electric Vehicles Combined wired and wireless. *Symposium Hybrid- und Elektrofahrzeuge* (p. Marco JungGeorgios LempidisGeorgios LempidisRené MarkleinRené MarkleinShow all 7 authorsJonas SteffenJonas Steffen). Braunschweig: Researchgate.
- Keith, D. W., Holmes, G., St. Angelo, D., & Heidel, K. (2018). A process for capturing CO₂ from the atmosphere. *Joule*, 1573-1594.
- Kibrit, B. (2013). *Pumped hydropower storage in the Netherlands*. Delft: TU Delft.
- Klerke, A., Christensen, C. H., Nørskov, J. K., & Vegge, T. (2008). Ammonia for hydrogen storage: challenges and opportunities. *Royal society of chemistry*, 2304-2310.
- Kobayashi, H., Hayakawa, A., Kunkuma, K., Somarathne, A., & Okafor, E. (2019). Science and technology of ammonia combustion. *Proceedings of the combustion institute*, 109-133.
- Kobos, P. H., Klise, J. T., Borns, D. J., & Klise, G. T. (2011). *A life cycle cost analysis framework for geologic storage of hydrogen : A user's tool*. Albuquerque: Sandia National Laboratories.
- Kraftwerk Forschung. (1999). *Hydrogen gas turbines*. Retrieved from Kraftwerk Forschung: <http://kraftwerkforschung.info/en/hydrogen-gas-turbines/>
- Kyriaki-Nefeli, M., & Demoulias, C. (2013). Minimization of Electrical Losses in Two-Axis Tracking PV Systems. *IEEE Transactions on Power Delivery*, 2445-2455.
- Lan, R., & Tao, S. (2013). Electrochemical synthesis of ammonia from air and water using a Li⁺/H⁺/NH₄⁺ mixed conducting electrolyte. *RSC Advances*, 18016-18021.
- Larscheid, P., Lück, L., & Moser, A. (2018). Potential of new business models for grid integrated water electrolysis. *Renewable energy*, 599-608.

- Leighty, B. (2006, 10 02). Costs of Delivered Energy from Large-scale, Diverse, Stranded, Renewable resources. Transmitted and Firmed as Electricity, Gaseous hydrogen and ammonia. *Ammonia: Key to US Energy Independence* (pp. 1-132). Juneau: The Leighty Foundation.
- Leighty, B. (2008). Energy Storage with Anhydrous Ammonia - Comparison with other energy storage . *Ammonia: The Key to US Energy Independence* (pp. 1-74). Juneau: Leighty Foundation.
- Londe, L. (2018, 02 08). *Hydrogen caverns are a proven, inexpensive and reliable technology*. Retrieved from Medium: <https://medium.com/@CH2ange/louis-londe-technical-director-at-geostock-hydrogen-caverns-are-a-proven-inexpensive-and-346dde79c460>
- Luzzi, A., Lovegrove, K., Filippi, E., Fricker, H., Schmitz-Goeb, M., Chandapillai, M., & Kaneff, S. (1999). Techno-economic analysis of a 10 MWe solar thermal power plant using ammonia based thermochemical energy storage. *Solar energy*, 91-101.
- Manthiram, K., Beberwyck, B., & Alivisatos, P. (2014). Enhanced Electrochemical Methanation of Carbon Dioxide with a Dispersible Nanoscale Copper Catalyst. *Journal of the American chemical association*, 13319-13325.
- Matute, G., Yusta, J., & Correas, C. (2019). Techno-economic modelling of water electrolyzers in the range of several MW to provide grid services while generating hydrogen for different applications: A case study in Spain applied to mobility with FCEVs. *International Journal of Hydrogen Energy*, 17431-17442.
- Methanol institute. (2016). *Methanol safe handling technical bulletin: Atmospheric Above Ground Tank Storage of Methanol*. Washington D.C.: Methanol institute.
- Methanol institute. (2016, 06). *Power generation*. Retrieved from Methanol institute: methanol.org/power-generation/
- Michalski, J., Bünger, U., Crotagino, F., Donadei, S., Schneider, G.-S., Pregger, T., . . . Heide, D. (2017). Hydrogen generation by electrolysis and storage in salt caverns: Potential, economics and systems aspects with regard to the German energy transition. *International journal of hydrogen energy* 42, 13427-13443.
- Miller, E., Papageorgopoulos, D., Stetson, N., Randolph, K., Peterson, D., Cierpik-Gold, K., . . . Satyapa, S. (2016). U.S. Department of Energy Hydrogen and Fuel Cells program: Progress, Challenges and Future Directions. *MRS Advances*, 2839-2855.
- Ministerie van Economische Zaken. (2016). *Energieagenda*. The Hague: Rijksoverheid. Retrieved from Rijksoverheid.
- Moret, S., Dyson, P., & Laurency, G. (2014). Direct synthesis of formic acid from carbon dioxide by hydrogenation in acidic media. *Nature communications*, 1-7.
- Morgan, E. (2013). *Techno-Economic Feasibility Study of Ammonia plants powered by offshore wind*. Amherst: University of Massachusetts Amherst.
- Morgan, E., Manwell, J., & MacGowan, J. (2014). Wind-powered ammonia fuel production for remote islands: A case study. *Renewable Energy* , 51-61.
- Mulder, F., Postma, H., Klop, E., & Visser, H. (2015). *Naar een hoog aandeel van duurzame energie; Opslag is noodzaak voor afstemmen van vraag en aanbod* . Amsterdam: NL ingenieurs.

- Mulder, F., Weninger, B., Middelkoop, J., Ooms, F., & Schreuders, H. (2017). Efficient electricity storage with a battolyser, an integrated Ni–Fe battery and electrolyser. *Energy & Environmental science*, 756-764.
- Mulder, M., & Perey, P. (2019). *Outlook for a Dutch hydrogen market*. Groningen: RUG.
- Müller, T., & Möst, D. (2018). Demand Response Potential: Available when Needed? *Energy policy*, 181-198.
- Nagashima, M. (2018). *Japan's hydrogen strategy and its economical and geopolitical implications*. Paris: Ifri.
- Netbeheer Nederland. (n.a., n.a. n.a.). *Inhoud - Bijlagen*. Retrieved from Energie Cijfers: <https://energiecijfers.info/bijlagen/>
- Nielsen, A., Aika, K., Christiansen, L. J., Dybkjaer, I., Hansen, J. B., Hoylund Nielsen, P. E., . . . Tamaru, K. (1995). *Ammonia: Catalysis and Manufacture*. Lyngby: Haldor Topsoe A/S.
- NIST. (2015). NIST calculates high cost of hydrogen pipelines and shows how to reduce cost. *Fuel cells bulletin*, 14-15.
- NREL. (2017). *Natural Gas Plants*. Retrieved from Annual technology baseline: <https://atb.nrel.gov/electricity/2017/index.html?t=cg>
- Nuttall, L. (1977). Conceptual design of large scale water electrolysis plant using solid polymer electrolyte technology. *International journal of hydrogen energy*, 395-403.
- Office of energy efficiency and renewable energy. (n.a., n.a. n.a.). *Liquid hydrogen delivery*. Retrieved from energy.gov: <https://www.energy.gov/eere/fuelcells/liquid-hydrogen-delivery>
- Onishi, N., Laurency, G., Beller, M., & Himeda, Y. (2018). Recent progress for reversible homogeneous catalytic hydrogen storage in formic acid and in methanol. *Coordination chemistry reviews*, NaoyaOnishiaGáborLaurencybMatthiasBellerYuichiroHimedaa.
- Open Power System Data. (2019, 06 05). *Data platform*. Retrieved from Open Power System Data: https://data.open-power-system-data.org/time_series/2019-06-05
- Patel, P., & Petri, R. (2006). Co-production of Energy and Hydrogen Using NH₃-Fueled SOFC Systems. *Ammonia Fuel Conference 2006* (pp. 1-42). Golden: Fuel cell Energy.
- PBL. (2019). *Costs of offshore wind energy 2018*. The Hague: PBL.
- Purity gas. (2017, 8 21). *Costs of nitrogen gas – how much should you be paying?* Retrieved from Purity: <https://puritygas.ca/nitrogen-gas-costs/>
- Realmonde, G., Drouet, L., Gambhir, A., Glynn, J., Hawkes, A., Köberle, A., & Tavoni, M. (2019). An inter-model assessment of the role of direct air capture in deep mitigation pathways. *Nature communications*, 1-12.
- Rijksoverheid. (2018, 03 29). *Kabinet: einde aan gaswinning in Groningen*. Retrieved from Rijksoverheid: nieuws: <https://www.rijksoverheid.nl/actueel/nieuws/2018/03/29/kabinet-einde-aan-gaswinning-in-groningen>
- Rijksoverheid. (2019, 02 13). *Bestaande woningen aardgasvrij maken*. Retrieved from Rijksoverheid: <https://www.rijksoverheid.nl/onderwerpen/aardgasvrije-wijken/bestaande-gebouwen-aardgasvrij-maken>

- Rijksoverheid. (2019, 05 13). *Maatregelen klimaatakkoord per sector*. Retrieved from Rijksoverheid: <https://www.rijksoverheid.nl/onderwerpen/klimaatakkoord/maatregelen-klimaatakkoord-per-sector>
- Rozzak, R., Firley, L., Rozzak, S., Pfeifer, P., & Kuchta, B. (2016). Hydrogen storage by adsorption in porous materials: Is it possible? *Colloids and Surfaces A: Physicochemical and Engineering Aspects*, 69-76.
- RVO. (2006). *Opslag van elektriciteit: Status en toekomstperspectief voor Nederland, bijlagen: Opslag van energie*. The Hague: RVO.
- SARI Energy. (n.a.). Natural gas value chain: Pipeline transportation. *Global energy markets trade program* (pp. 48-121). n.a.: US Aid. Retrieved from SARI Energy: [https://sari-energy.org/oldsite/PageFiles/What_We_Do/activities/GEMTP/CEE_NATURAL_GAS_VALUE_C HAIN.pdf](https://sari-energy.org/oldsite/PageFiles/What_We_Do/activities/GEMTP/CEE_NATURAL_GAS_VALUE_CHAIN.pdf)
- Schefer, R. W., Houf, W. G., San Marchi, C., Chernicoff, W. P., & Englom, L. (2006). Characterization of leaks from compressed hydrogen dispensing systems and related components. *International journal of hydrogen technology*, 1247-1260.
- Schmidt, O., Gambhir, A., Staffell, L., Hawkes, A., Nelson, J., & Few, S. (2017). Future cost and performance of water electrolysis: An expert elicitation study. *International journal of Hydrogen Energy*, 30470-30492.
- Shin-ichi, O., Nakamori, Y., Eliseo, J. R., Züttel, A., & Craig, J. (2007). Complex Hydrides for Hydrogen Storage. *Chemical reviews*, 4111-4132.
- Teichmann, D., Arlt, W., Wasserscheid, P., & Freymann, R. (2011). A future energy supply based on Liquid Organic Hydrogen Carriers. *Energy and Environmental science*, 2767-2773.
- Teichmann, D., Stark, K., Müller, K., Zöttle, G., Wasserscheid, P., & Arlt, W. (2012). Energy storage in residential and commercial buildings via Liquid Organic Hydrogen Carriers (LOHC). *Energy and environmental science*, 9044-9054.
- Tennet. (2019). *Integrated Annual Report 2018*. Arnhem: TenneT Holding B.V.
- TenneT TSO B.V. (2019). *Concept notitie reikwijdte en detailniveau M.E.R.-procedure Net op Zee IJmuiden Ver Alpha*. Arnhem: TenneT.
- Tixador, P. (2008). Superconducting Magnetic Energy Storage: Status and prospective. *IEEE/CSC & ESAS European superconductivity news forum, No. 3*, 1-14.
- Tractebel, Engie and Hincio. (2017). *Study on early business cases for H2 in energy storage and more broadly power to H2*. Brussels: FCH.
- Tsoutsos, T. (2010). Hybrid wind-energy systems. In J. Kaldellis, *Stand-Alone and Hybrid Wind Energy Systems* (pp. 254-281). n.a.: Woodhead Publishings.
- TU Delft. (2018, 06 12). *Eerste battolyser voor elektriciteitsopslag en waterstofproductie in Groningen dankzij Waddenfonds*. Retrieved from Technische Universiteit Delft: <https://www.tudelft.nl/2018/tu-delft/eerste-battolyser-voor-elektriciteitsopslag-en-waterstofproductie-in-groningen-dankzij-waddenfonds/>

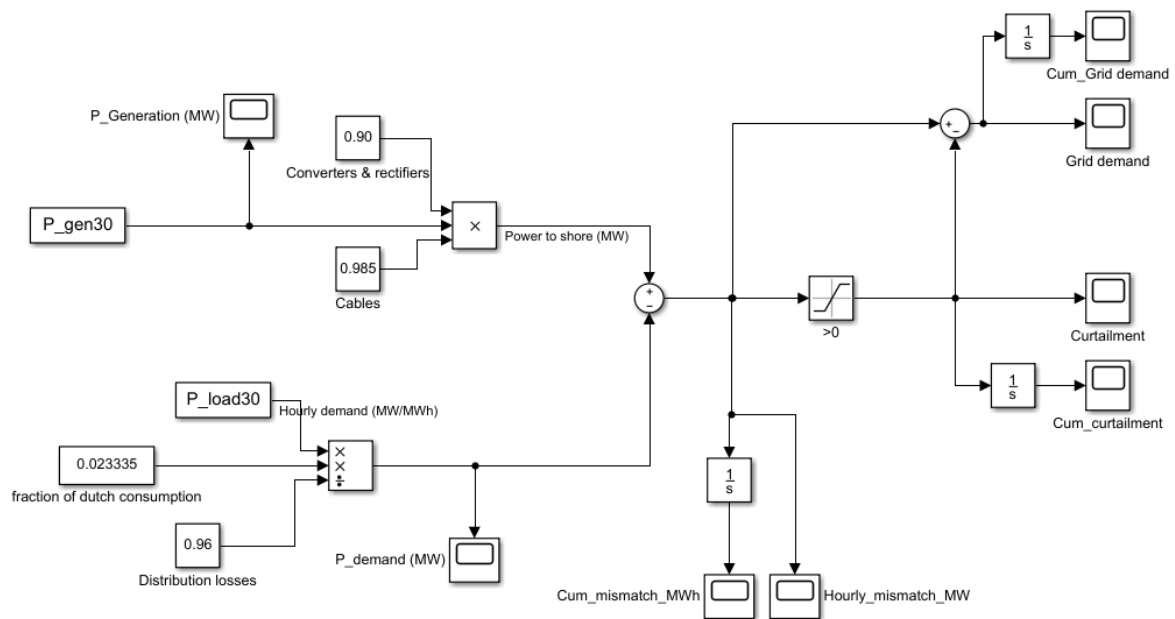
- Valera-Medina, A., Xiao, H., Owen-Jones, M., David, W., & Bowen, P. (2018). Ammonia for power. *Progress in Energy and Combustion Science*, AValera-Medinaa1HXiaoab1MOwen-JonescW.I.F.DavidcdP.J.Bowena1.
- Van den Vijver, A. (2007). Demiwater produceren met membraanfiltratie. *Oppervlaktetechnieken*, 21-23.
- Van Eldik, R., & Hubbard, C. D. (2017). *Inorganic reaction mechanisms*. Seiten: Academic Press Inc.
- Van Gessel, S. F., Breunese, J., Juez Larré, J., Huijskes, T. D., & Remmelts, G. (2018). *Ondergrondse opslag in Nederland - Technische verkenning*. Utrecht: TNO.
- Van Haperen, R. (2016). *Formic Acid as Energy Carrier*. n.a.: Topsector Energie.
- Van Leeuwen, C. (2018). *D8.3: Report on the cost involved with PtG technologies and their potentials accross the EU*. n.a.: Store and Go.
- Van Nielen, S. (2016). *Techno-economic assessment of Solid Oxide Fuel Cells and fuel assisted electrolysis cells in future energy systems*. Delft: TU Delft, Leiden University.
- Vrijenhoef, J. (2017). Opportunities for small scale ammonia production. *Proceedings 7xx* (pp. 1-16). London: International Fertiliser Society.
- Westfalen. (2015). *Ammoniak - onder druk vloeibaar gemaakt*. Retrieved from Westfalen: <https://www.westfalengassen.nl/industriële-gassen/alle-gassen-op-een-rij/applicationdetailviewnl/productdetailviewnl/gas/ammoniak-38-w-1.html>
- Wiebes, E. (2018, 03 n.a.). *Offshore Wind Energy Roadmap 2030*. Retrieved from RVO.nl: <https://english.rvo.nl/sites/default/files/2018/03/Letter-Parliament-Offshore-Wind-Energy-2030.pdf>
- Wilson, A., Kleen, G., & Papageorgopoulos, D. (2017). *Fuel cell system cost - 2017*. n.a.: US Department of Energy .
- Wittrig, S. (2018, 05 30). *Ammonia Fuel - Opportunities, markets and Issues*. Retrieved from Arpa-e: https://arpa-e.energy.gov/sites/default/files/Wittrig_Ammonia_TransportationFuels_Workshop.pdf
- Wlodek, T., Laciak, M., Kurowska, K., & Wegrzyn, L. (2016). Thermodynamic analysis of hydrogen pipeline transportation - Selected aspects. *AGH Drilling, oil, gas*, 379-396.
- Yang, Z., Zhang, J., Kintner-Meyer, M. C., Lu, X., Choi, D., Lemmon, J. P., & Liu, J. (2011). Electrochemical energy storage for green grid. *American Chemical Society*, 3577-3613.
- Zanchi, R., Porter, M., & Miller, N. (2017). *The Dutch wind consortium*. www.rmi.org/BRC_Dutch_casestudy: The Rocky mountain institute.
- Zhang, Y., Wang, L., Wang, N., Duan, L., Zong, Y., You, S., . . . Yang, Y. (2019). Balancing wind-power fluctuation via onsite storage under uncertainty: Power-to-Hydrogen-to-Power versus lithium battery. *Renewable and Sustainable Energy Reviews*, 1-14.
- Zheng, J., Liu, X., Xu, P., Liu, P., Zhao, Y., & Yang, J. (2012). Development of high pressure gaseous hydrogen storage technologies. *International journal of hydrogen energy* 37, 1048-1057.

A. Appendix I – The model

This thesis report was largely based on the outcome of model simulations. The model is too large to show completely. Instead, a selection of images of model components are given in this Appendix. The entire model is available on <https://github.com/SenjaBoom/Power-to-Gas>.

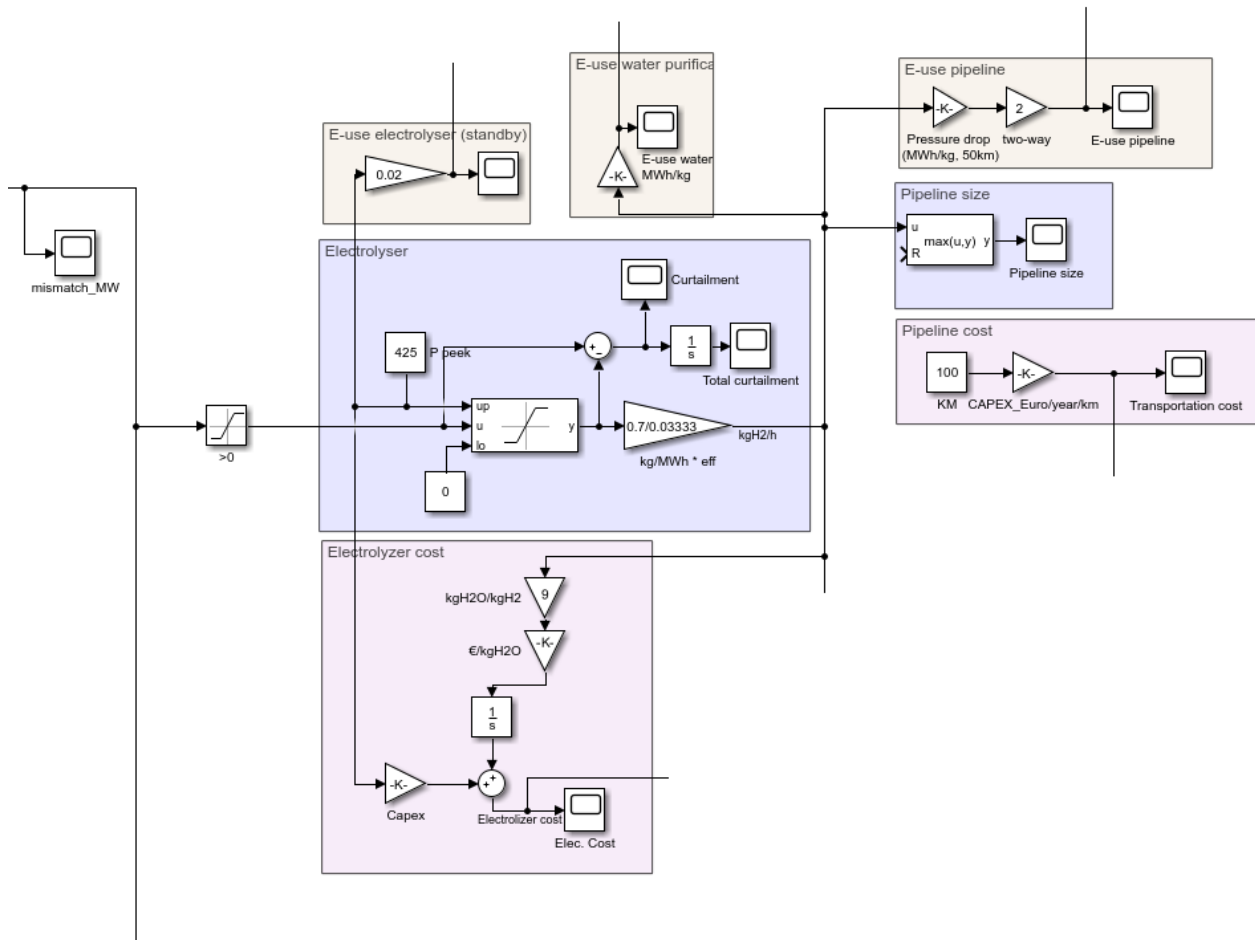
No storage

The basis of the model is the wind generation and electricity demand. Scenario 0 does not contain any storage system. It only contains the predicted wind generation and electricity demand that belong to a 1 GW wind park in 2030. Any surplus of electricity is curtailed, any deficit of electricity is taken from the external grid. The model is shown below.

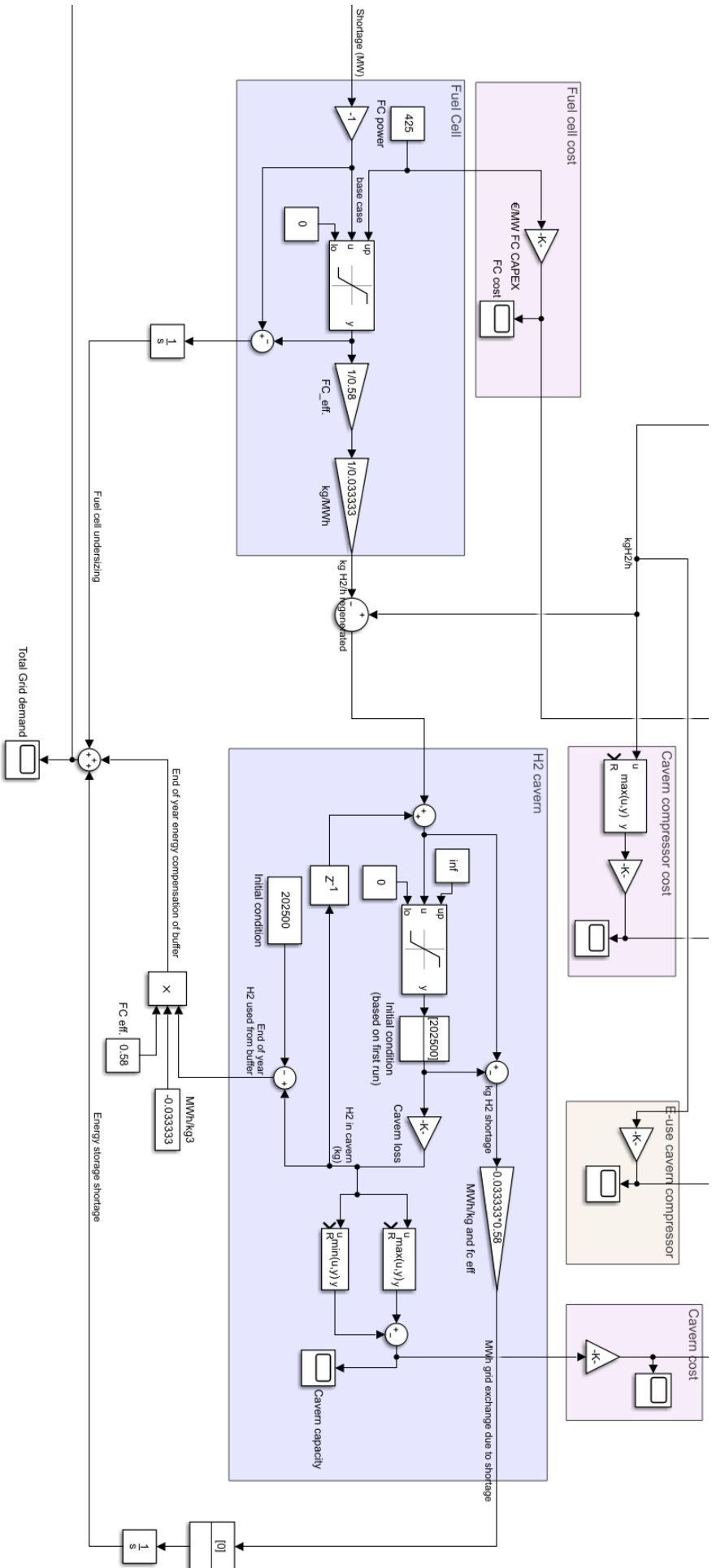


Hydrogen storage

In the second scenario a hydrogen storage system is added. The image below shows the electrolyser and pipeline. Yellow squares indicate calculations of electricity use, the electricity use is fed back and added to the electricity demand with a one-hour delay to prevent algebraic loops. The pink squares indicate cost calculations. The total cost is calculated and used as an output in this report. The image also shows the scaling of the pipeline. It was assumed to not limit the flow of hydrogen, the flow of hydrogen is monitored and the maximum value is taken as the pipeline size.

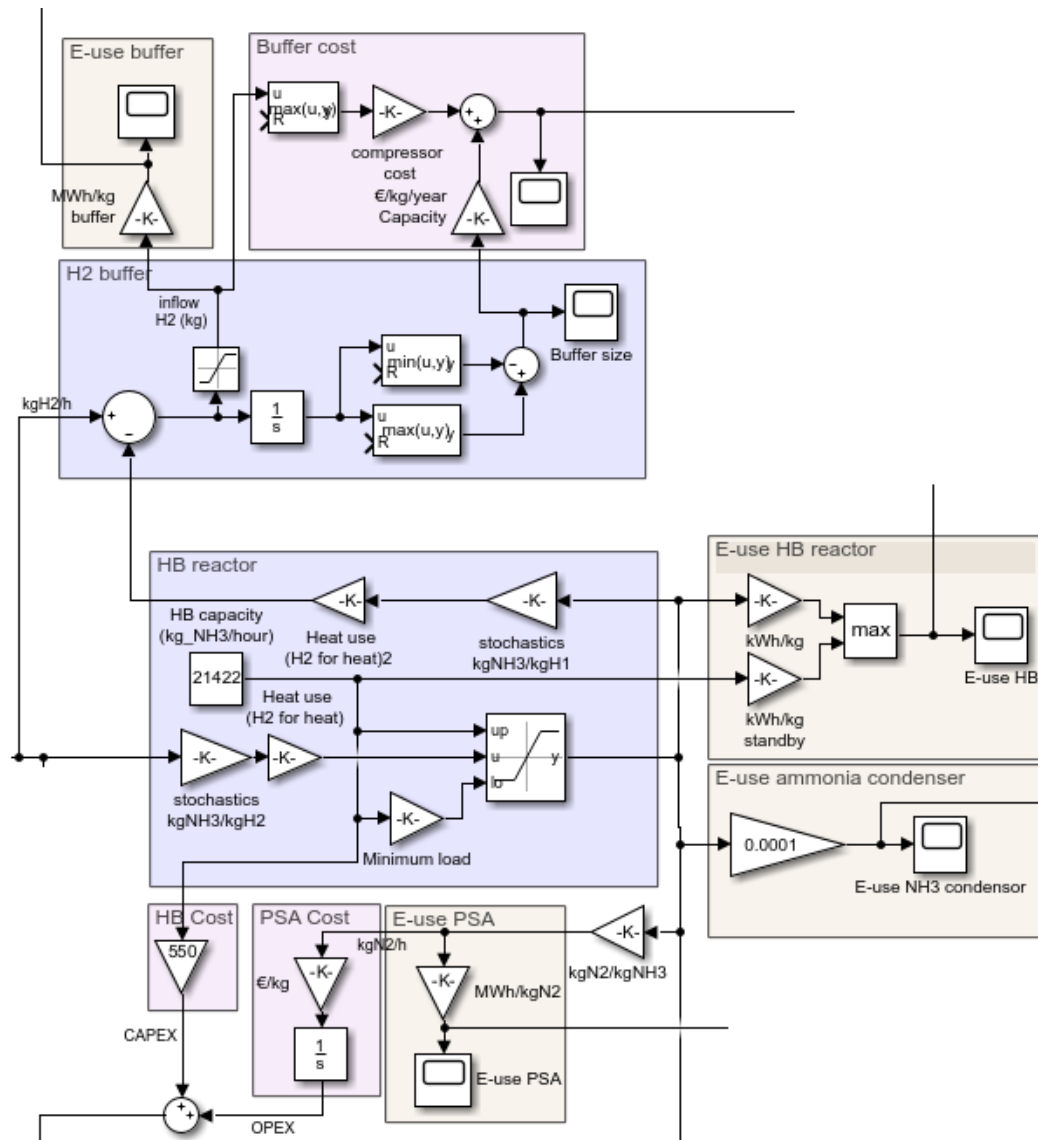


The next page contains an image of the hydrogen fuel cell and hydrogen cavern. Hydrogen produced by the electrolyser comes in from the top and is added to the hydrogen cavern. Any electricity demand is generated by the fuel cell, which consumes hydrogen from the cavern. If the demand is higher than the maximum power of the fuel cell energy/kgH2O must be delivered by the external grid.

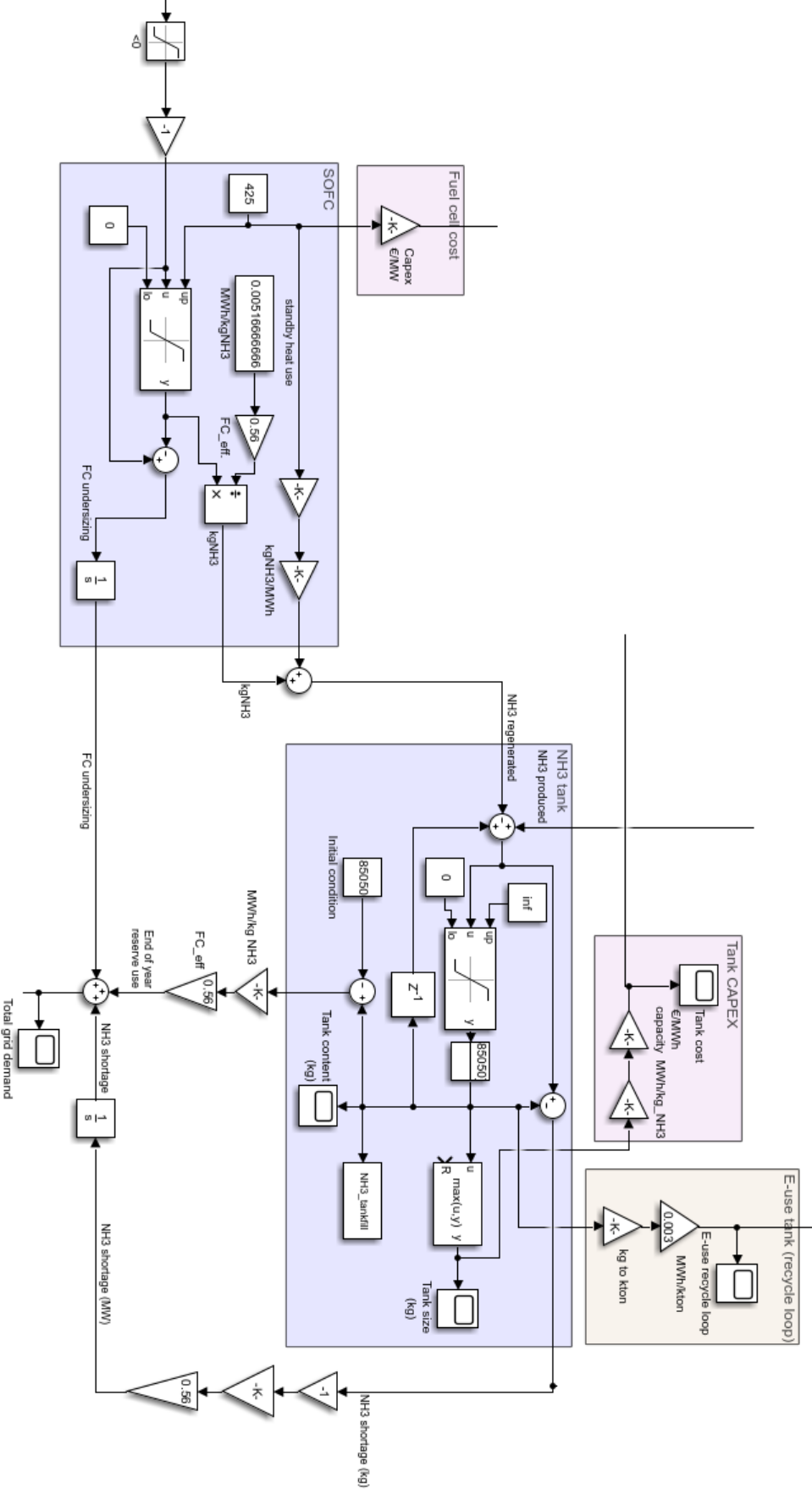


Ammonia storage

In other scenarios the hydrogen storage system is replaced with a hydrogen buffer and ammonia storage system. The image shown below shows the model with a flexible HB reactor and the hydrogen buffer. Hydrogen is either immediately reacted in the HB reactor or is stored in the hydrogen buffer. The size of the hydrogen buffer is unlimited, which means it is calculated as the difference between the maximum and minimum hydrogen content in the buffer. Produced ammonia is transported to the ammonia tank.

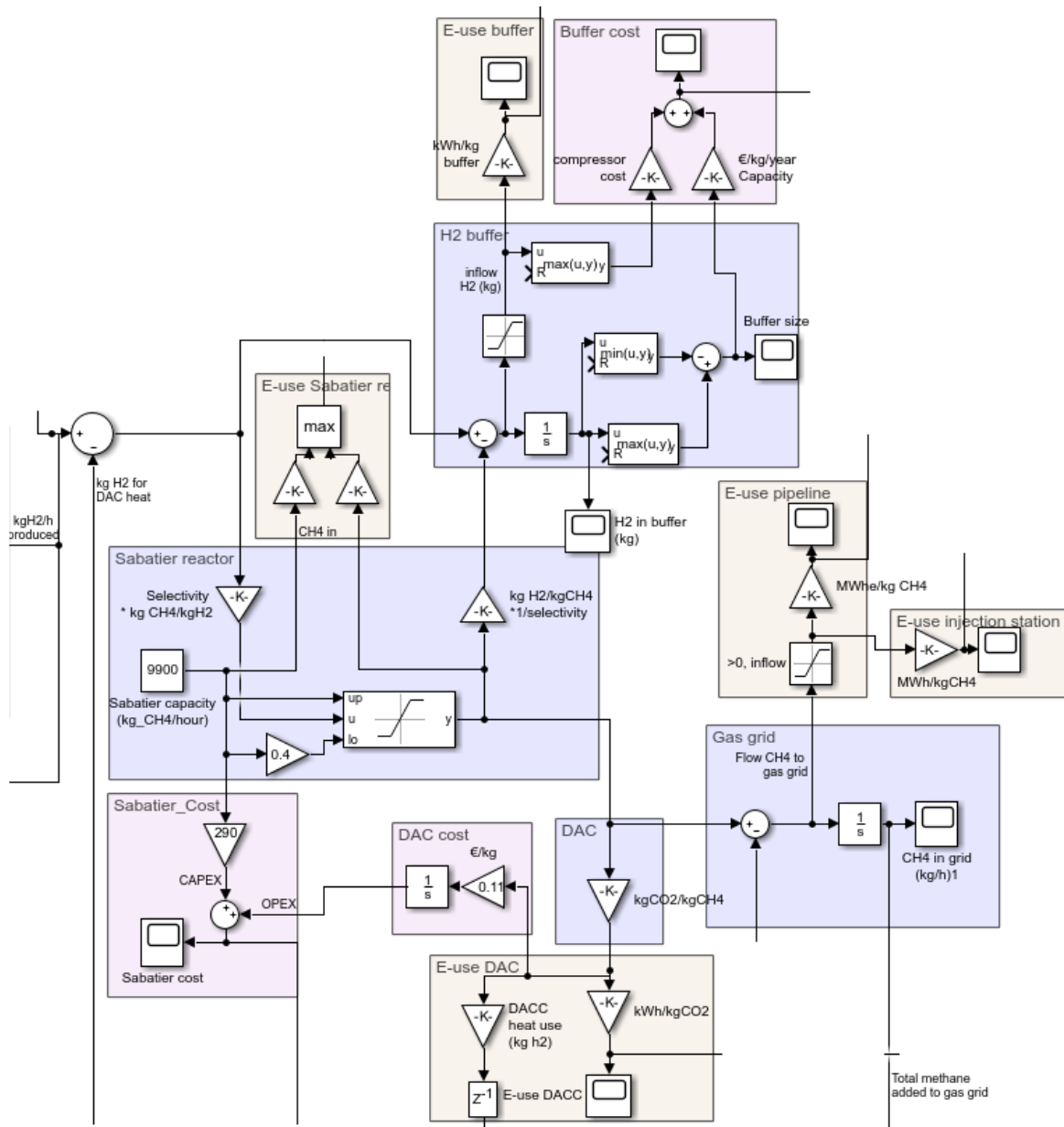


This page shows an image of the ammonia tank and ammonia SOFC.



Methane

The methane and ammonia models are structurally very similar. The image below shows the model of the Sabatier reactor, hydrogen buffer, gas grid and DAC calculations. Produced methane is delivered to the grid, in times of electricity demand, gas is consumed from the grid. At the end of the year the net usage of methane is considered grid exchange.



The final components are the gas turbine and the roundtrip efficiency calculations. Energy demand that is higher than the maximum output of the gas turbine must be delivered by the external grid. The other grid demand component is the gas consumed from the grid. The roundtrip efficiency is calculated as the demand met by the system (total demand-grid demand, E_{out}) divided by the total energy surplus (E_{in}).

